



University
of Glasgow

Canamar Leyva, Alan Leonel (2012) *Seaplane conceptual design and sizing*. MSc(R) thesis.

<http://theses.gla.ac.uk/4030/>

Copyright and moral rights for this thesis are retained by the author

A copy can be downloaded for personal non-commercial research or study, without prior permission or charge

This thesis cannot be reproduced or quoted extensively from without first obtaining permission in writing from the Author

The content must not be changed in any way or sold commercially in any format or medium without the formal permission of the Author

When referring to this work, full bibliographic details including the author, title, awarding institution and date of the thesis must be given



Seaplane Conceptual Design and Sizing

by
Alan Canamar

A thesis submitted to the School of Engineering,
University of Glasgow in
fulfillment of the requirements of
the degree of Master of Science

Aerospace Sciences
Supervisor: L. Smrcek
November 2012

Abstract

Ever since the idea of flying machines that could land and take off from water (seaplanes) was invented in 1910, a huge amount of research was poured into it until it stagnated in 1950. Their performance did not grow according to current aircraft requirements. The idea of designing advance seaplane concepts stopped, and most seaplanes existing these days are approaching their final operating life. The purpose of this research project was to introduce a new seaplane concept design methodology that will suffice the necessities of actual aircraft designers. This concept design replaces old sizing methods proposed with a more efficient methodology based on modern aircraft design methods. The sizing method developed gives the designer a “freedom” in creating an “out of the box” seaplane concept. The optimization method was elaborated in such a manner that the designer can use certain types of aircraft configuration (Conventional, Blended Wing Body, and Flying Wing). The sizing method simplified the design by calculating the most advanced floating device for this seaplane concept. Old seaplane information was blended with modern aircraft and modern ship design information, creating a new preliminary seaplane concept design. Another advantage of this design method is the idea to convert existing landplane into a seaplane by adding the floating device that meets the necessary requirements of the seaplane conversion.

The second part of the research was to address technical solutions to the actual seaplane design. For example, adding a trimaran configuration that increased the hydrodynamic performance and the use of a retractable float system that reduced aerodynamic drag during flight. Final results were elaborated to compare the use of trimaran with other types of floating devices. The final results showed the trimaran concept gave an excellent hydrostatic stability, a greater water speed, and retracting the floats decreased the aerodynamic drag, hence better flight performance.

Aircraft design has been affected by actual economical difficulties showing no radical progress in this field of study. The next purpose of the research was to explore more radical, environmentally efficient, and innovative technologies. With the aid of the proposed sizing methodology for a modern and futuristic seaplane, a new vision was created called: 2050 Visionary Aeronautical Design Concept. Based on this vision the creation of an advance “out of the box” amphibian aircraft was elaborated. The project analyzed technical solutions, and a conceptual design concept for the creation of this 2050 amphibian aircraft. The preliminary design development leads to the creation of an Advance Amphibian Blended Body Wing Aircraft (AABWBA). AABWBA excels in air performance due to the high results generated by the Blended Wing Body (BWB) Aircraft. Adopting modern turbofan engines instead of turboprop engines gave the AABWBA better water takeoff capability, as well as air performance. Modern ideas for 2050 vision are the creation of futuristic seaports in order to increase seaplane traffic, public and commercial awareness, and expand market schemes.

A design analysis was performed to show a model representation of this advance seaplane design. A Computer Aided Design (CAD) model was elaborated to calculate the dimensions, observe the mechanism of the retractable floats, and show the location of the boat hull. With the aid of this CAD model, Finite Element Analysis (FEA) was performed to show the structural strength and impact of the hull and floats when landing on water. Finally, with the aid of this model, a hydrostatic analysis of the seaplane was conducted to show the water stability, and heel turns to observe the performance of the trimaran and the retractable floats when the seaplane is being operated in water.

Acknowledgments

I want to give a special thanks to my supervisor, Dr. Ladislav Smrcek, for all his collaboration, support, and help throughout this project. Also a special gratitude to the University of Glasgow for the support on equipment and facilities provided in order to conduct this MSc Research Project.

I will like to thank the collaboration of Mr. Ludovit Jedlicka, Undergraduate student of VSVU Bratislava (Slovakia) for elaborating the futuristic images of the LET L-410, the Antonov AN-28, and the BAe 146. Also, to Dr. Gerardo Aragon for his knowledge and guidance in the elaboration of the optimization sizing code.

Lovely thanks to my partner and wife, Paulina Gonzalez, for all of her help, patience and trust she gave me during this trip where I came to gain more knowledge and advice from the best educators. For her calming words and knowledgeable guidance throughout this project that always kept me on visualizing the objective of finishing this MSc Research.

Last, thanks to all of my friends and family that gave me advice, guidance, support, and company during this research project.

Table of Contents

| | |
|---|------------|
| Abstract..... | ii |
| Acknowledgments | iii |
| List of Figures..... | vii |
| List of Tables | ix |
| Nomenclature | x |
| 1. Introduction | 1 |
| 1.1. History | 1 |
| 1.1.1. 1903 – 1950 | 1 |
| 1.1.2. 1950 – 1980 | 3 |
| 1.1.3. 1980 – Present | 3 |
| 1.2. Seaplane Aircraft Design | 5 |
| 1.3. Seaplane Traffic and Operations | 6 |
| 1.4. Strengths, Weaknesses, Opportunities, and Threats (SWOT) | 8 |
| 1.4.1. Strengths | 8 |
| 1.4.2. Weaknesses..... | 10 |
| 1.4.3. Opportunities | 10 |
| 1.4.4. Threats | 11 |
| 2. Literature Review..... | 12 |
| 2.1. Aircraft Design | 12 |
| 2.1.1. Examples of Existing Landplane for Seaplane Conversion | 13 |
| 2.2. Water Operation Design..... | 14 |
| 2.2.1. Hydrodynamic Shape Characteristics..... | 14 |
| 2.2.2. Boat Hull Design | 17 |
| 2.2.3. Float Design..... | 17 |
| 2.2.4. Trimaran and Retractable Float System | 18 |
| 3. Advance Seaplane Conceptual Optimization Method | 23 |
| 3.1. Conceptual Design | 23 |
| 3.2. Sizing Code Development and Validation | 24 |
| 3.2.1. Landplane Optimized Testing Source Code (LOTS) | 25 |
| 3.2.2. Floating Device Optimized Testing Source Code (FOTS)..... | 26 |
| 3.2.3. Validation | 28 |
| 3.3. Theory | 29 |

| | |
|--|-----------|
| 3.3.1. Aeronautical Theory | 29 |
| 3.3.2. Naval Architecture Theory | 33 |
| 4. Results | 40 |
| 4.1. Landplane Results | 40 |
| 4.1.1. Geometry | 40 |
| 4.1.2. Empty Weight..... | 41 |
| 4.1.3. Aerodynamic Drag | 41 |
| 4.1.4. Flight Performance | 43 |
| 4.2. Floating Device Results | 47 |
| 4.2.1. Weight Breakdown | 47 |
| 4.2.2. Geometry calculations | 47 |
| 4.2.3. Hydrostatic Stability | 50 |
| 4.2.4. Water Takeoff Requirements..... | 51 |
| 4.2.5. Aerodynamic Drag | 52 |
| 4.2.6. Flight Performance | 54 |
| 4.3. Design Analysis..... | 57 |
| 4.3.1. SOLIDWORKS Computer Aided Design (CAD) Analysis..... | 57 |
| 4.3.2. ORCA 3D | 59 |
| 4.3.3. Software Validation..... | 62 |
| 5. 2050 Visionary Concept: Future Seaplane Transport..... | 63 |
| 5.1. Introduction | 63 |
| 5.2. Review of Literature..... | 63 |
| 5.3. Design Selection..... | 64 |
| 5.3.1. Input Parameters | 64 |
| 5.3.2. Fuselage Thickness..... | 65 |
| 5.3.3. Airfoil | 65 |
| 5.3.4. Wing Sweep (Λ) | 65 |
| 5.4. Preliminary Results | 66 |
| 5.4.1. Geometric Properties (BWB) | 67 |
| 5.4.2. Weight Breakdown | 68 |
| 5.4.3. Control Surfaces | 68 |
| 5.4.4. Trimaran Dimensions | 69 |
| 5.4.5. Hydrostatic Stability | 70 |
| 5.4.6. Water Resistance | 70 |

| | |
|--|-----------|
| 5.4.7. Air Performance | 71 |
| 5.5. Summary | 73 |
| 6. Conclusions and Recommendations | 75 |
| 6.1. Conclusions | 75 |
| 6.2. Recommendations | 76 |
| 6.2.1. Sizing Code Improvements | 76 |
| 6.2.2. Technical Improvements | 76 |
| References..... | 79 |
| Appendix..... | 82 |
| Appendix A. Empirical Equations..... | 82 |
| A.1 Empty Weight Breakdown Equations | 82 |
| A.2 Flat Plate Drag Area Breakdown Equations..... | 83 |
| A.3 Aircraft Flight Performance Equations..... | 85 |
| A.4 Hull geometrical empirical formulas | 88 |
| Appendix B. Artistic impressions of the conversion of current certified aircraft to a seaplane | 89 |
| Appendix C. MATLAB Optimization Source Code | 90 |

List of Figures

| | |
|--|----|
| Fig. 1: Le Canard [2]..... | 2 |
| Fig. 2: The Flying Fish [2]..... | 2 |
| Fig. 3: Navy Curtiss [5] | 2 |
| Fig. 4: Short S-23 Empire [6] | 2 |
| Fig. 5: Sikorsky S-42 [2]..... | 3 |
| Fig. 6: Martin M130 [2] | 3 |
| Fig. 7: Hughes H-4 Hercules “Spruce Goose” [7]..... | 3 |
| Fig. 8: Expeditionary fighting vehicle [8]..... | 4 |
| Fig. 9: <i>Lun</i> -class Ekranoplan [9]..... | 4 |
| Fig. 10: Do.24 ATT [9]..... | 4 |
| Fig. 11: Canadair CL-415 [11]..... | 4 |
| Fig. 12: Beriev Be-103 [12]..... | 5 |
| Fig. 13: Beriev Be-200 [12] | 5 |
| Fig. 14: Average Percentage Growth of Travel in the UK [13]..... | 7 |
| Fig. 15: Seaport in Vancouver Harbor, Canada [15] | 7 |
| Fig. 16: Design Features of a Flying Boat [27] | 14 |
| Fig. 17: Beam Width of a Conventional Boat [36] | 15 |
| Fig. 18: Various Types of Boat Hull Bottoms [41] | 16 |
| Fig. 19: Hydrofoil Example [53] | 18 |
| Fig. 20: Trimaran Example [55] | 19 |
| Fig. 21: Trimaran Stability-Beam Model [56]..... | 19 |
| Fig. 22: Resistance comparison curves [57] | 20 |
| Fig. 23: Trimaran coordinate Axis [56] | 20 |
| Fig. 24: Outrigger stagger and clearance [56] | 21 |
| Fig. 25: Retracting Float Concept [59] | 22 |
| Fig. 26: Example CAD Model with Floats retracted inside Hull | 22 |
| Fig. 27: Heel Overturn Retracting Float System | 22 |
| Fig. 28: Seaplane Design Optimization Method Flow Chart..... | 24 |
| Fig. 29: Flowchart of the LOTS architecture..... | 26 |
| Fig. 30: Flowchart of FOTS architecture | 27 |
| Fig. 31: Input Landplane Characteristics | 27 |
| Fig. 32: Slenderness Ratio | 35 |
| Fig. 33: Wing Tip Floats [42] | 35 |
| Fig. 34: Transverse Metacentric Height [45] | 37 |
| Fig. 35: Wave Making Resistance [67]..... | 38 |
| Fig. 36: Deadrise Angle [67] | 39 |
| Fig. 37: 3-D CAD Model of Conventional Landplane Aircraft..... | 41 |
| Fig. 38: Drag Curves (Landplane) | 42 |
| Fig. 39: Thrust Curves (Landplane)..... | 42 |
| Fig. 40: Landplane Climb Diagram | 44 |
| Fig. 41: Altitude Envelope of Landplane..... | 44 |
| Fig. 42: Payload Range Diagram (Landplane) | 46 |
| Fig. 43: Maneuvering and Gust Envelopes (Landplane) | 46 |
| Fig. 44: Water Landing Load Factor Curve | 49 |

| | |
|---|----|
| Fig. 45: CAD Model of Seaplane with Wing Tip Floats | 49 |
| Fig. 46: CAD Model of Seaplane with Nacelle Support Stabilizers..... | 49 |
| Fig. 47: CAD Model of Seaplane with Trimaran Concept | 50 |
| Fig. 48: CAD Model of Seaplane transverse Metacentre, Centre of Gravity, and Buoyancy | 50 |
| Fig. 49: Righting Moment Graph..... | 51 |
| Fig. 50: Water Resistance Curves and Thrust Available | 52 |
| Fig. 51: Wing Tip Floats Retracted into the Wing Tip | 52 |
| Fig. 52: Nacelle Wing Stabilizers Retracted..... | 53 |
| Fig. 53: Trimaran Outriggers Retracted unto the Boat Hull | 53 |
| Fig. 54: Thrust Curves (Landplane and Trimaran Seaplane)..... | 55 |
| Fig. 55: Altitude Envelope (Landplane and Trimaran Seaplane [Retracted]) | 55 |
| Fig. 56: Payload Range Diagram (Landplane and Trimaran Seaplane [Retracted]) | 56 |
| Fig. 57: Maneuvering and Gust Envelopes (Trimaran Seaplane)..... | 56 |
| Fig. 58: Trimaran Seaplane Fuselage Fixture | 58 |
| Fig. 59: Trimaran Seaplane Load Force at Afterbody Hull | 58 |
| Fig. 60: Trimaran Seaplane Mesh..... | 59 |
| Fig. 61: Trimaran Seaplane Von Mises Stress Analysis..... | 59 |
| Fig. 62: Personal Watercraft Modeled as a NURBS and a T-Spline [69] | 60 |
| Fig. 63: Orca3D Results with Virtual Waterline of Trimaran Seaplane (Longitudinal) | 61 |
| Fig. 64: Orca3D Results with Virtual Waterline of Wing Tip Floats Seaplane (Transverse) | 61 |
| Fig. 65: Trimaran Seaplane at 12° Heel Angle before Overturning | 62 |
| Fig. 66: Trimaran Seaplane at 20° Heel Angle before Overturning | 62 |
| Fig. 67: Example Blended Wing Body Aircraft [70]..... | 64 |
| Fig. 68: Top-down view of BWB showing wing and wing fences..... | 66 |
| Fig. 69: Blended Wing Body Aircraft..... | 66 |
| Fig. 70: Cut view of BWB fuselage..... | 67 |
| Fig. 71: BWB fuel tanks | 68 |
| Fig. 72: Top view of BWB with control surfaces labeled | 69 |
| Fig. 73: CAD Model of AABWBA | 70 |
| Fig. 74: Metacentric Height of AABWBA | 70 |
| Fig. 75: Resistance Curves AABWBA | 71 |
| Fig. 76: Altitude Envelope of BWB and AABWBA | 72 |
| Fig. 77: Payload Range Diagram | 72 |
| Fig. 78: Maneuvering and Gust Envelopes..... | 73 |
| Fig. 79: AABWBA at takeoff from seaport..... | 74 |
| Fig. 80: AABWBA taxiing at seaport..... | 74 |
| Fig. 81: Futuristic CAD Model of Amphibians at a Modern Sea Port | 77 |
| Fig. 82: Futuristic CAD Model of a Turboprop Seaplane and AABWBA..... | 78 |
| Fig. 83: Futuristic CAD Model of AABWBA at taxi..... | 78 |
| Fig. 84: Artistic Impression of LET L-410 [75] | 89 |
| Fig. 85: Artistic Impression of Antonov AN28 [75]..... | 89 |
| Fig. 86: Artistic Impression of BAE 146 [75] | 89 |
| Fig. 87: Artistic Impression of Dornier DO-228 [75]..... | 89 |

List of Tables

| | |
|---|----|
| Table 1: Noise levels for various operations [18] | 9 |
| Table 2: Aircraft Specifications | 13 |
| Table 3: LOTS Comparison Validation | 28 |
| Table 4: FOTS Comparison Validation | 28 |
| Table 5: Spray Coefficient Factors | 35 |
| Table 6: Geometrical Parameters of Landplane..... | 40 |
| Table 7: Empty Weight Breakdown (Landplane) | 41 |
| Table 8: Flat Plate Drag Area Breakdown (Landplane) | 43 |
| Table 9: Endurance and Range (Landplane)..... | 45 |
| Table 10: Weight Component Breakdown | 47 |
| Table 11: Floating Device Dimensions..... | 48 |
| Table 12: Hydrostatic Stability (Seaplane) | 50 |
| Table 13: Flat Plate Drag Area Breakdown Floating Devices..... | 54 |
| Table 14: Flat Plate Drag Area Breakdown Trimaran Seaplane..... | 54 |
| Table 15: Endurance and Range of each Flight Segment | 55 |
| Table 16: Summary of major design values (Landplane and Trimaran Seaplane)..... | 57 |
| Table 17: Blended Wing Body Parameters..... | 66 |
| Table 18: BWB and AABWBA Weight Breakdown | 68 |
| Table 19: Trimaran Dimensions (AABWBA) | 69 |
| Table 20: Flat Plate Drag Area Breakdown Component | 71 |
| Table 21: Summary of major design values (BWB and AABWBA) | 74 |

Nomenclature

| | |
|----------------|---|
| A | = Area of Load Water Plane [m ²] |
| AR | = Aspect Ratio |
| b | = Wing Span [m] |
| BG | = Distance from Center of Buoyancy to Center of Gravity [m] |
| b_h | = Boat Hull Beam [m] |
| BM | = Reduction in Metacentric Height [m] |
| BPR | = Bypass Ratio |
| c | = Mean Wing Chord Length [m] |
| C_D | = Total Drag Coefficient |
| C_{Di} | = Coefficient of Induced Drag |
| C_{Dp} | = Coefficient of Parasite or Viscous Drag |
| C_{Dw} | = Coefficient of Wave or Compressibility Drag |
| C_f | = Friction Coefficient |
| c_{HT} | = Horizontal Tail Volume Coefficient |
| C_L | = Coefficient of Lift |
| c_r | = Wing Root Chord [m] |
| C_{RM} | = Righting Moment Coefficient |
| C_{Rw} | = Coefficient of Water Resistance |
| c_t | = Wing Tip Chord [m] |
| C_v | = Coefficient of Water Viscous Resistance |
| c_{VT} | = Vertical Tail Volume Coefficient |
| C_w | = Coefficient of Water Wave Resistance |
| C_l | = Seaplane Operation Factor |
| C_{Δ_0} | = Static Beam Load Coefficient |
| D | = Total Aerodynamic Drag [N] |
| D_i | = Induce Aerodynamic Drag [N] |
| D_p | = Parasite Aerodynamic Drag [N] |
| D_w | = Wave or Compressibility Drag [N] |
| E | = Endurance [hr] |
| e | = Oswald's efficiency factor |
| EW | = Empty Weight [kg] |
| EW_l | = Empty Weight of Landplane [kg] |
| EW_s | = Empty Weight of Seaplane [kg] |
| F | = Form Factor |
| f | = Flat Plate Drag Area [m ²] |
| FC | = Fuel Consumption [kg/sec] |
| f_{th} | = Throttle Setting |
| g | = Gravitational Acceleration [m/s ²] |
| GM | = Metacentric Height [m] |
| GW | = Total Gross Weight of Aircraft [kg] |
| GW_{est} | = Estimated Gross Weight [kg] |
| I | = Moment of Inertia [m ⁴] |
| K | = Geometrical Form Factor of Floating Device |
| k | = Spray coefficient |

| | |
|-------------|--|
| L | = Lift [N] |
| l | = Distance from the lateral stabilizer to the center of the fuselage [m] |
| l_a | = Afterbody Length of Boat Hull [m] |
| l_f | = Forebody Length of Boat Hull [m] |
| L_h | = Length of Boat Hull [m] |
| L_{HT} | = Horizontal Tail Moment Arm [m] |
| L_{VT} | = Vertical Tail Moment Arm [m] |
| M | = Mach number |
| M_{div} | = Divergence Mach number |
| m_f | = Fuel Mass [kg] |
| M_R | = FAA Righting Moment [N-m] |
| n | = Number of Floats or Stabilizers |
| n_w | = Water Landing Load Factor |
| Q | = Interference Factor |
| q | = Dynamic Pressure [Pa] |
| R | = Range [km] |
| Re | = Reynolds Number |
| RM | = Righting Moment [N-m] |
| R_w | = Water Resistance [N] |
| S | = Planform Wing Area [m^2] |
| S_{HT} | = Horizontal Tail Planform Area [m^2] |
| SLR | = Slenderness Ratio |
| S_{VT} | = Vertical Tail Planform Area [m^2] |
| S_{wet} | = Wetted Wing Area [m^2] |
| t | = Time [sec] |
| T_A | = Available Thrust [N] |
| T_R | = Required Thrust [N] |
| $tsfc$ | = Thrust Specific Fuel Consumption [N-kg/hr] |
| T_0 | = Static Sea Level Thrust [N] |
| U | = Volume [m^3] |
| V | = Velocity [m/s] |
| V_c | = Climb Speed [m/s] |
| V_{so} | = Stall Speed [m/s] |
| V_{TAS} | = True airspeed [m/s] |
| W | = Weight [kg] |
| w | = Density of Water [kg/ m^3] |
| W_{bh} | = Boat Hull Weight [kg] |
| W_f | = Weight of one Float [kg] |
| W_{fi} | = Final Cruise Weight [kg] |
| W_i | = Initial Cruise Weight [kg] |
| W_{WT} | = Wing Stabilizer Weight [kg] |
| β | = Forebody Deadrise Angle [deg] |
| γ | = Heat capacity ratio of air (1.4) |
| θ | = Angle of Heel Inclination [deg] |
| ϑ | = Temperature Ratio |
| λ | = Taper ratio |

| | |
|------------|--|
| ρ | = Density of Air [kg/m ³] |
| Δ_0 | = Weight Water Displacement [kg] |
| Λ | = Wing Sweep at 25% Mean Aerodynamic Chord (MAC) [deg] |

All dimensions are in metric system unless specified

1. Introduction

Since the creation of the world's first successful airplane done by the Wright Brothers in 1903, the idea for improving and exploring the world of aeronautics have been expanding rapidly throughout the 20th century. Aircraft design is the process between many competing factors and constraints accounting for existing designs and market requirements to produce the best aircraft [1]. The expansion in aircraft design allowed a wider perspective into analyzing efficient methods of transportations such as the use of versatile vehicles. There is a design of such versatile vehicles that had existed for decades, amphibious aircraft. Henry Fabre created the first motor seaplane flight in 1910 [2], and since then, much research on seaplane aviation was widely conducted. However, with the concept to improve aircraft designs and the construction of suitable landplane infrastructure, the use of seaplane traffic and operations drastically dropped [3]. Current designs are obsolete, and updates to these vehicles have stagnated. The most important role that seaplanes have today is to conduct fire fighter operations as water bombers; they are also commonly used in the private sector, in which most seaplanes are just small landplanes adapted with floats. The lack of an advance seaplane design has pushed the boundaries into creating a new optimization conceptual design method. The design methodology complies with the necessities of the actual aviation market schemes and will continue to compete in the future, both at a short and long term period.

1.1. History

1.1.1. 1903 – 1950

With the lack of suitable landplane infrastructure and the availability of vast motor boats, the idea of creating a seaplane was born. The first motor seaplane flight was conducted in 1910 by a French engineer Henry Fabre [2] naming this machine 'Le canard' shown in Fig. 1. Since then, much research on seaplane aviation is widely conducted.

These experiments were followed by the aircraft designers Gabriel and Charles Voisin. They adapted a number of Fabre's floats and fitted them into an improved design - the Canard Voisin airplane. The Canard Voisin airplane became the first seaplane to be used in military exercises from a seaplane carrier, *La Foudre* ('the lightning'), in march 1912 [4].

In the United States (US), early development was carried out by Glenn Curtiss who worked in association with Alexander Graham Bell in the Aerial Experiment Association (AEA). His first seaplane, nickname "Hydroaeroplane", took off from the San Diego bay on January 26, 1911. Another model by Curtiss nicknamed as "The Flying Fish" took flight in 1912 shown in Fig. 2. This prototype faced problems at takeoff during its initial run due to suction forces. Curtiss decided to implement the step, separating the forebody from the afterbody becoming the first seaplane to demonstrate the advantages of the step [5]. The first British seaplane flight, by Sydney Sippe, also took place in 1912 [2].

During the periods of the Great War (WWI) (1914-1918), the lack of landplane airfields, and the availability of controlling key water military points made seaplanes an indispensable tool. The Curtiss float planes were the only US designated float planes to see combat in WWI. In 1919, the huge flying boat "Navy-Curtiss" shown in Fig. 3, made the first staged aerial crossing of the Atlantic [5].

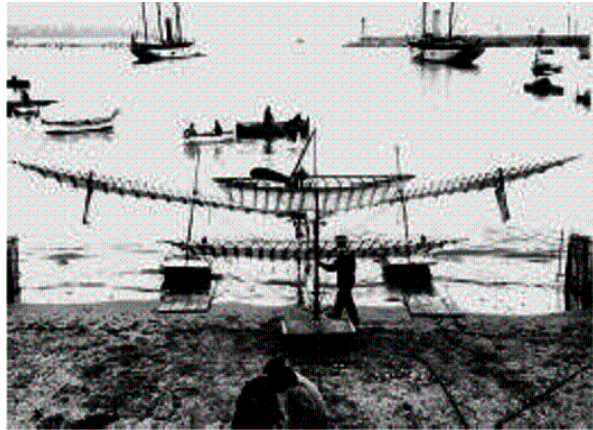


Fig. 1: Le Canard [2]



Fig. 2: The Flying Fish [2]

In the period of post WWI (1918–1939), prospects of the seaplane as a commercial transport vehicle began to fade and the military began to take over. This dream for commercial seaplane transport was hijacked by the military, but some airlines still saw significant promise and potential in seaplanes for long haul travel. Thus, in the late 1930s, forty-two Short Bros' S23 C Empire Flying-Boats shown in Fig. 4 were built at Rochester, England, to be in service during the last days of the British Empire, ending its service in June 1940 [6].

During World War II (WWII) (1939 – 1945), seaplanes continued to play an important role in military aircraft service. In addition to operating with airlines such as Imperial Airways, BOAC, Qantas and TEAL, the big Sunderlands also saw action with Allied air forces. Across the Atlantic, Pan America was building up its transpacific routes with its large and impressive Clipper fleet. The first two trans-Pacific seaplanes were the Sikorsky S-42 and the Martin M130, Fig. 5 and Fig. 6 respectively, but they were superseded by the Boeing B-314 [2]. In 1942, with the loss of many cargo ships in the Atlantic Ocean caused by German U-Boats, the U.S. War Department approved the construction of a transport aircraft that will move the material to Great Britain. The approved aircraft is the largest seaplane ever constructed, the Hughes H-4 Hercules "Spruce Goose", shown in Fig. 7 [7]. However, the H-4 Hercules was completed until 1947, and only one prototype was made.

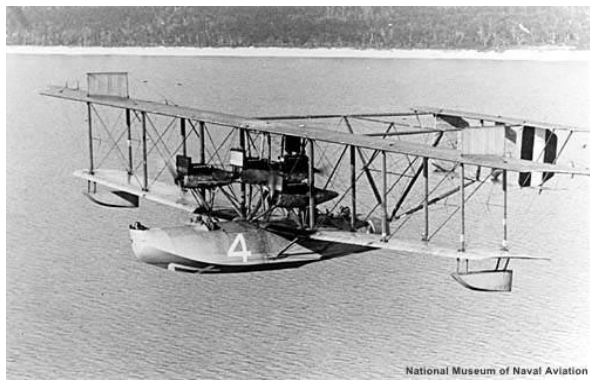


Fig. 3: Navy Curtiss [5]

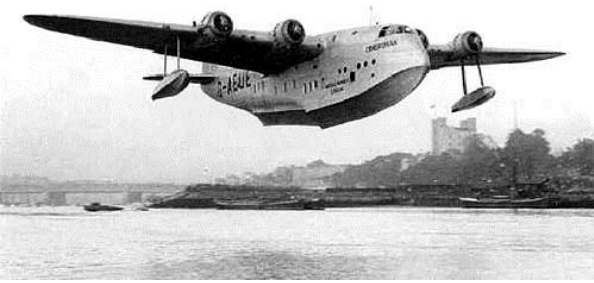


Fig. 4: Short S-23 Empire [6]



Fig. 5: Sikorsky S-42 [2]

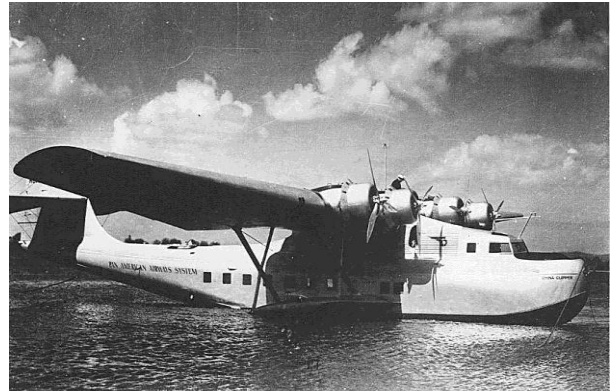


Fig. 6: Martin M130 [2]



Fig. 7: Hughes H-4 Hercules "Spruce Goose" [7]

1.1.2. 1950 – 1980

Sadly, by the end of WWII, the flying boat industry drastically declined with the increase in landplane range and speed, coupled with a world-wide network of airfields; though the US Navy continued to operate some seaplanes. The jet powered seaplane bomber “Martin Seamaster” and the “Martin P5M Marlin” were among a few that were operated by the Navy, whose operation continued till the early 1970’s.

In defiance to the changing trends, in 1948, Aquila Airways was founded to serve destinations that were still inaccessible to land-based aircrafts. This company operated “Short S.25” and “Short S.45” flying boats out of Southampton on routes to a number of remote locations [6]. From 1950 to 1957, Aquila also operated a service from Southampton to Edinburgh and Glasgow. The airline ceased its operations on 30 September 1958. The aerospace industry was preoccupied with the research and development of land planes, the enthusiasm resulting from the expanding spans of commercial air transport, defense and because of certain drawbacks of the obvious aerodynamic compromises that the seaplanes had relative to landplanes.

1.1.3. 1980 – Present

The dormant era of seaplanes continued till the mid 1980’s until the idea resurged as a part of the bigger concept of Advanced Amphibious Vehicles (AAV) [8]. AAV are types of transport vehicles that are able to operate on land as well as on water, an example shown in Fig. 8. The U.S. military designed AAV in order to deploy troops rapidly from an amphibious assault ship

onto land. These military applications revived the idea for designs that could be used by civilian transport. Sporting activities and leisure travel resumed their roles of bolstering seaplanes in the market. Another factor that played hugely to the advantage of the seaplane industry was the introduction of the concept of Wing in Ground effect vehicles (WIG) [9]. The Russian *Ekranoplan*, shown in Fig. 9, for instance was one such vehicle. It was not only designed to minimize drag, but also to work some of the aerodynamic lift forces to its advantage. These vehicles continue to influence yacht and ship designs for high speed cruising and sailing. Presently similar research is being poured into seaplanes in order to improve their performance in high waves and rough weather conditions.

There are a few seaplane companies that excel in some advance designs. Some companies are Dornier and Canadair with the introduction of models like Do.24 ATT [9] and CL-415 [11], Fig. 10 and Fig. 11 respectively. Beriev Aircraft Company is a Russian amphibious aircraft manufacturer with its two most noticeable seaplanes, the Beriev Be-103 Fig. 12 and Beriev Be-200 Fig. 13 [12].

The time table shows the technological improvements of different type of seaplanes that were made throughout the century. Such improvements are to be brought about by paying attention to the obvious drawbacks that the seaplane suffers from despite its improved designs.



Fig. 8: Expeditionary fighting vehicle [8]



Fig. 9: Lun-class Ekranoplan [9]



Fig. 10: Do.24 ATT [9]



Fig. 11: Canadair CL-415 [11]



Fig. 12: Beriev Be-103 [12]



Fig. 13: Beriev Be-200 [12]

1.2. Seaplane Aircraft Design

Designing a seaplane aircraft must gather the knowledge of studying both aircraft and boat technology. The seaplane must meet the buoyancy requirements, have good water takeoff and landing characteristics, an acceptable hydrostatic stability, structural support for both water and air capability, and good aerodynamic characteristics that could affect flight performance.

The initial purpose of this research was the creation of an alternative conceptual design method that created an advance seaplane design. The new conceptual design method adapted old seaplane design concepts that had been gathered during the early stages of the seaplane dream and blended with modern amphibious aircraft design methodology. The advance amphibious aircraft sizing code takes a basic set of inputs and then outputs the aircraft's geometry and performance data. The sizing code allows the designer maximum flexibility when deciding what configuration the aircraft will have. The designer is allowed to choose from four different water operation methods (boat hull, twin floats, wing tip floats, mid-wing stabilizer floats or any combination mentioned), three different aircraft configurations (Blended Wing Body (BWB), Flying Wing, and Conventional configuration), and three engine types (jet, turbofan and propeller engine) that have been included. The code takes the designer's choices on all these configurations and properly analyzes the affect those choices will have on the overall design of the aircraft.

This research proposes modern empirical techniques based on old empirical formulas in order to improve the operation of this advance seaplane design. A proposed idea to improve the hydrodynamic performance was to adapt a trimaran boat hull configuration. The design of a trimaran configuration results by combining a boat hull and twin floats. Few studies on the design of trimaran geometry has been conducted and the known empirical formulas for seaplane design are well adapted to conventional floats and boat hulls, but not for a trimaran concept. Therefore, a theoretical sizing technique was proposed combining conventional flying boat theory to obtain trimaran calculations.

Finally, preliminary results were elaborated with the aid of the sizing code in order to analyze the performance done by the trimaran concept compared with other water operation devices. A drag breakdown was elaborated to demonstrate the decrease in aerodynamic drag due to the assistance of the retractable float system. A design analysis in structures and hydrostatic stability was conducted. Structural analysis was conducted using SOLIDWORKS. The longitudinal and lateral water stability of the design was tested using Orca3D. The design analysis was useful in determining whether the sizing code and theoretical calculations were adequate and comply with

the conceptual design requirements. Together, this information is useful in determining ways to improve the sizing code and optimization techniques used to make an efficient preliminary design of a seaplane.

1.3. Seaplane Traffic and Operations

Over the last years global economy has expanded widely with the involvement of vast national economies. This has derived an expansion in telecommunications, computing technology, and transportation vehicles. For this case, transportation has been one of the keys of this global economy expansion, specifically aircraft vehicles. Relying on airplane transportation will carry people faster and safer to farther places. This is the same case in United Kingdom (UK). Fig. 14 shows a graph of the average percentage growth of travel in the UK from 1996 to 2006 [13]. The graph shows the rapid increase in air transportation compared to railways, or motor land vehicles (cars, buses, etc). However, this is not the case for seaplanes.

Some factors that contributed for the decline in seaplane operations could be derived from an economical point of view, rather than a technical issue. Seaplanes have to face with aviation regulations as well as water regulations when operating in water. Some of these regulations are not well established in Europe, especially in the United Kingdom. Water and air maneuvering contributes an additional drawback for seaplane operations. As explained by an experienced seaplane pilot, the greatest difficulty for the new seaplane operator is to convince the authorities that there should be no rigid rule as to the exact landing and maneuvering areas for safe seaplane operations [14]. In his paper, Lightening explains the future of landing sites and passenger terminals, in which he highlights all negative and positive points that seaplanes face today. He states that the best way to convince the authorities is by demonstrating that seaplanes can operate safely in busy boating areas, the aircraft has the necessary safe water maneuverability, and stopping capabilities. He also highlights that in order for a seaplane operation to be successful a careful attention must be made to the geographic relief, weather conditions, availability of fuel, and good market research. Finally, it is explained that a Landing Site Manual (LSM) should be created the same way as any other airport manual is created, in which seaplanes could operate with their own manual instructions.

An important factor that will help increase seaplane traffic and operations is the establishment of convenient, modern and advanced seaplane facilities. Suitable seaports will require funding either by government or private entities, but they are not confident to invest since seaplanes are not a major investment in the transportation sector [13]. Since seaplane traffic cannot compete with major airline companies, seaplanes can complement in adding more routes into remote areas where landplanes are inaccessible [15]. Therefore the necessity of planned and developed infrastructure must be made.

In Europe, one project in particular, was created to attack and solve the struggles that seaplanes and amphibians face today, called FUSETRA (Future Seaplane Traffic) [16]. An online survey has been created and made accessible to operators worldwide to investigate the common points of interest they think about seaplanes [17]. The following topics have been identified as subjects of interest:

- General Information about Seaplane Operators
- Operational Issues
- Pilots, Regulations and Certification
- Infrastructure and Aircraft
- General issues and comments on the future development of the seaplane transport system.

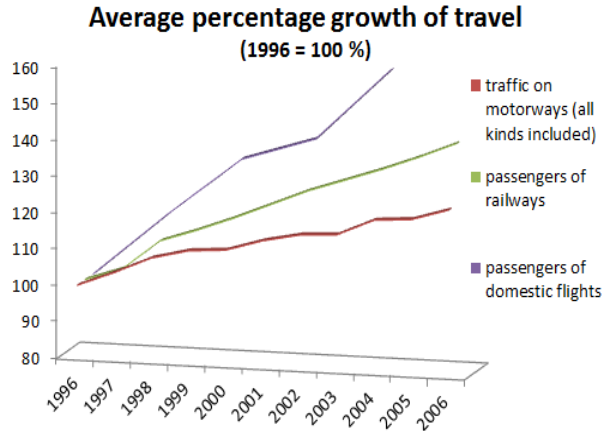


Fig. 14: Average Percentage Growth of Travel in the UK [13]

In North America, especially in Canada, the large number of bodies of water and the remoteness of many important locations has produced an active seaplane traffic. An example is a seaplane seaport in Vancouver Harbour, Canada shown in Fig. 15. In a concept for the near future, seaplane facilities are not required to be complex structures where huge amount of investment must be made. In a simple case, the use of simple mooring buoys and boat, small beaching ramp, pier or floating docks might fulfill the prerequisites for a seaplane operation facility.

The current obstacles of social issues, regulations, operations and infrastructure are not in particularly the only issues confronted. In summary, these were some of the circumstances of the decline in seaplane operations [16]:

1. Landing on water runways became less ostentatious compared to the increase in the number and length of land based runways during WWII.
2. WWII left a large amount of landplanes unused and concrete runways on ex-military bases. Thus, upcoming airlines could purchase this landplanes cheaply from the military.
3. The speed and range of land based aircraft had increased, due to an advance in engine design and performance.
4. The commercial competitiveness of flying boats diminished, especially since their design compromised aerodynamic efficiency and speed to accomplish the feat of waterborne takeoff and landing.
5. Anti-Submarine warfare and Search and Rescue operations could be easily handled by modern helicopter designs, which give an advantage to operate on smaller ships.



Fig. 15: Seaport in Vancouver Harbor, Canada [15]

1.4. Strengths, Weaknesses, Opportunities, and Threats (SWOT)

The aim of this SWOT analysis is to recognize the key internal and external factors that are important to seaplane operations [18]. The SWOT analysis may be then split into two main categories as follow:

- Internal factors: strengths and weaknesses internal to this particular type of transportation.
- External factors: opportunities and threats presented by the external environment.

Strengths and weaknesses of seaplane operations are here analyzed under the light of the “European Aeronautics: a vision for 2020” document [19], where the concept of sustainability is introduced and made the kernel of the aviation future. EU vision 2020 is not a deadline, but a sensible reflection on what should lie ahead for Europe in the near future in order to win global leadership in aeronautics. In vision 2020 aeronautics must satisfy constantly rising demands for lower costs, better service quality, the highest safety and environmental standards and an air transport system that is seamlessly integrated with other transport network.

Skies have to be always safer and the most advance automated systems have to be integrated to eliminate accidents. Aircraft need to be cleaner and quieter and the environment sustainable with the contribution of the aeronautic sector. The definition of sustainability states that “sustainability is the concept to endure”. It depends on the wellbeing of the natural world as whole and the responsible use of natural resources. One EU (European Union) main objective, in this regard, is to halve, by 2020, carbon dioxide (CO_2) emission, perceived noise pollution, and reduced nitrogen oxide (NO_x) emission by 80% from 2000 levels. In conclusion it can be said that if a generation ago the imperatives were: higher, further and faster, then, according to the vision 2020 guidelines, these have become: more affordable, safer, cleaner and quieter.

1.4.1. Strengths

One of the major deterrents facing the seaplane market today is the opposition by environmental authorities on the perceived impact of seaplane. The main argument is based on the noise impact of seaplane landing, taxiing and taking off, which is known to exceed the ambient noise level. Additionally, there is a belief that noise, landing and take-off all impact on wildlife. A current example of this is the on-going dispute between Loch Lomond Seaplanes and Trossachs National Park. Moreover, as mentioned before, also worldwide the greatest obstacle facing seaplanes is considered to be the opposition of environmental authorities. In Europe this was also agreed by 20% of operators [17].

Only few studies have been completed to assess the seaplane environmental impact anywhere in the world and in many cases these are independent studies carried out by private seaplane operators [20]. The most inclusive and unbiased is probably an investigation conducted by US Army corps of Engineers (USACE) [21] and Cronin Millar Consulting Engineers to Harbor Air Ireland [22], and the outcomes were: No Impact on Air, Water, Soil, Wildlife, Fisheries, and Hydrology.

It is true that carbon emission generated from seaplane exceed the emission produced by boats. However, consideration should be given to the fact that the number of boat movements within any given area greatly outweighs seaplane movements in this area. Additionally, it should be considered that the next propulsion generation (which is already tested) will have much lower noise and carbon emission levels. Attention should also be drawn to the fact that seaplanes do not discharge sewage or oily bilge water and are not treated with toxic anti-fouling paints unlike boats. Seaplane exhaust are emitted into the air, much above the water giving low water impact, and currently used seaplane fuel does not contain the flammable and volatile compound MBTE

(Methyl Tertiary-Butyl Ether), which is found in boats. Moreover, seaplane propellers are located away from the water, giving no disturbance on sediments or marine life, and they are near negligible polluters in regard of foul water and waste from chemical toilets. Evidently, a further study validated that floatplanes generate no more than a three inch wake without any shoreline erosion effects [22].

Seaplanes have relatively low impact on noise pollution too. The majority of noise is generated during takeoff when high engine power is required to make the seaplane airborne. The following Table 1 lists typical noise levels for various operations at typical distances from the sound source and, once again, highlights the minimal impact seaplanes produce.

Attention should be also paid to the fact that the figure quoted is representative of the seaplane taking off, a short period of daytime-only occurrence which, compared to taxiing and landing, requires the highest throttle power.

Table 1: Noise levels for various operations [18]

| Noise | dBA | Example |
|----------------------|-----------|---|
| Military jet | 120+ | |
| Jet ski | 110 | e.g. watersports on lake |
| Chainsaw | 100-104 | e.g. tree felling/ forestry/ logging |
| Grass Cutting | 88-100 | Golf courses |
| Tractors | 95 | e.g. general operations |
| All terrain vehicles | 85 | |
| Speedboat | 65-95 | e.g. watersports on lake |
| Seaplane | 75 | on take-off only @ 300m (20 sec) |
| Inside car – 30 mph | 68-73 | |
| Normal conversation | 65 | |

In conclusion it may be said that seaplanes do not have negative effect on hydrodynamics, hydrology, water quality, air quality, wildlife fisheries and birds or noise pollution when compared to existing background activities on lakes and seaports. Air travel does not develop in a vacuum: its size, shape and success will be determined by society as a whole. Nowadays there are specific aspects of air transport that can be better or only satisfied by seaplane/amphibian operations. The most noticeable strengths in this regard are [18]:

- Very versatile type of transportation.
- Point to point connections.
- Connections to very difficult to reach places.
- Safe and efficient surveillance in otherwise inaccessible destinations.
- Monitoring of wildlife and management of national parks.
- Very good safety records with few incidents during takeoff, landing operations or related to collisions with boats.
- Sightseeing tours/tourism.
- Ability to conduct rescue operations over large bodies of water, water bombers.
- Avoid the ever congested airfield, holding patterns and control sequences.
- No need for runway infrastructures, “unprepared” landing strip, smaller landing fees than landplanes.
- Access from 40% (flying boats) to 70% (amphibian plane) more of the earth’s surface area than a conventional land plane.

1.4.2. Weaknesses

Seaplanes today are “endangered species” and although they possess undoubted potential, the lack of ability to unlock this potential is due to numerous problems. These are of a various nature and involve different aspects of seaplane/amphibian’s environment. Certainly, the design aspect is a major impediment on seaplane advancement and is linked to many other areas. In fact, as with the introduction of new efficient commercial aircraft designs, the use of the seaplane declined, no new advanced designs have been made, and most extant seaplanes existing these days are approaching the end of their operating life. This situation has resulted in a scarcity of modern and cost-efficient seaplanes. The lack of innovative designs and use of today’s technology then force seaplanes to VFR (Visual Flight Rules) and make them not suitable in adverse weather conditions or rough waters. In addition, some environmental issues could, in the near future, change what is currently a strength factor into a weakness. As stated before, vision 2020 aims to reduce polluting emissions by 50% for CO₂ (Carbon dioxide) and by 80% regarding NO_x (Nitrogen oxide). Alternative fuels and new generation engines, together with better aerodynamic performances, must be considered in order to keep these values as low as possible and match the suggested targets by the year 2020.

Finally, but equally important, the limited amount of seaplane bases and missing standard infrastructure equipment is surely a weak point that limits the seaplane market. It means that refueling and regular maintenance are factors which need serious consideration.

1.4.3. Opportunities

There is huge room for improvements in seaplane operations and many opportunities that can be exploited in such market. While demand is difficult to forecast without a detailed market research and an overview of current trends, something that is not available to fledgling industries, it can be presumed that demand should arise if the industry can offer a different service from large commercial airlines, either in terms of savings, convenience or novelty. Following is a list of the main features that may be considered as reliable new opportunities for seaplane:

- Easy usability among places with lots of islands and area/s with (many) resource/s of water.
- Faster service compared to ferries when connecting mainland-islands or island-island (e.g. Greece, UK, Ireland, etc) and the possibility to fly directly from major inland cities catering also specific groups of commuters in their daily journeys [23].
- Unconventional experience from transport (especially for tourists).
- Transport with quick dispatching.
- To shorten travel times avoiding the use of a combination of other means of transportation (e.g. Malta-south coast of Sicily) or considerable time savings that can be made where travel by any land based means is significantly time consuming.
- Avionics systems (lighten the burdens on the pilot, help making correct decisions and reduce human error, night flight). In fact, seaplanes are limited to daytime VFR. Then the way to eliminate this disadvantage is by adding advance cockpit technology, or the used of advance gear such as GPS (Global Positioning System), radar, laser altimeters, gyros, advance sensors, among other gear.
- Larger seaplanes with better range, more seats and less affected by weather/water conditions.
- Efficient, safe, comfortable infrastructures [24] (seaports, docking facilities, accessibility...).
- Air freight services: cargos travel by air because it is more competitive.

- Modifications of existing planes with innovative new design. Based on the market research and the technological review, the creation of a new seaplane design will require time, manufacturing costs, regulation and certification, and social acceptance.
- Investments in new technology, materials and new seaplanes/amphibians advance design. When new advance design is involved, it should be consulted with operators, due to future equipment plans, and maritime authority regulations should be considered in advance of the design process. However, it may be expected that new solutions that lower drag when airborne, maintenance times and costs, and enhance competitiveness in cost/seat/miles ratio will be always looked forward by operators.
- Add value to the air transport market by opening up more locations to air travel and in doing so make it more convenient, while reducing the congestion on airfields and offering significant time savings to passengers.

1.4.4. Threats

For seaplanes to really take off there are a number of barriers that must first be overcome. This paragraph highlights the major threats that seaplane operation is facing today and the fundamental issues that need to be addressed [14]:

- Possibly difficult accessibility of airport (to replace automobile and railway means of transport is very hard in this case because of difficult approach of airports).
- Public perception of light aircraft safety may impact on the acceptability of seaplane transportation. However, it should be noted that in the UK there has not been a single reported accident according to their Air Accidents Investigation Branch (AAIB) [25], though this is in part due to the fact that there have been historically very few seaplane operated in the UK [26].
- Acceptance from population and environmental activists.
- Fly time limitations. Alleviation on this regulation is needed so as to better meet the requirements of seaplane operations thus making them more financially sustainable without any subsequent of flight safety standards.
- Lack of a minimum level of training and acceptability of Dock Operating Crew so as to be multifunctional with regard to, assisting in the arrival and departure of aircraft on pontoons or piers, passenger handling, as well as manning the requirements of Rescue and Fire Fighting activities.
- Certification process for new seaplanes.
- General regulations: government regulation and control includes both aviation authority regulations and naval authority regulations. Nowadays there is not a set of unified regulations throughout Europe and these can also be sometimes in conflict.
- Corrosion resistance.
- Seaplanes are still too much depended on the weather conditions.

2. Literature Review

2.1. Aircraft Design

The complexity of aircraft design makes it possible for many proposed methods to be utilized in order to size an aircraft model. “Sizing” refers to the general size of the aircraft, focusing on the airplane weight, geometry and other parameters needed to fulfill its required mission objectives. Raymer [27] has published a detailed breakdown of the steps involved in the conceptual design of an aircraft. It is explained in detail the processes involved in taking initial requirements for the aircraft and sizing the aircraft from those requirements. He proposes two types of sizing processes, Class I and Class II. The Class I sizing process, does a progressive build-up of the takeoff weight of the aircraft which includes the weight of the crew, payload, fuel and empty-weight of the aircraft. Based on an empirical ratio of the takeoff weight to the empty weight of the aircraft, an empty-weight estimation is performed. The ratio depends on the type of aircraft being designed. The Class II sizing process uses a different method of calculating the empty weight of the aircraft, in which the individual component weights are calculated based on statistically weight equations.

The weight process follows a series of steps. First estimates of fuel-fractions (takeoff, climb, descent, landing, cruise, and reserves) during different portions of the mission are made. Then the empty weight calculations can proceed. Finally, an iterative approach is used to calculate an estimated takeoff weight using the estimated fuel-fractions and empty weight equation. An initial takeoff weight guess is made, followed by the empty weight calculation and an estimate of fuel fractions, which leads to an estimated takeoff gross weight. Then, the initial guess is compared to the calculated takeoff gross weight. If the results do not match, a value between the two is used as a next guess and the process is iterated until convergence is obtained.

Using the initial guess weight, the next step in the sizing process explained by Raymer is to create the geometry of the aircraft. This includes the selection of an airfoil shape, main wing and tail geometries, engine and fuselage sizing. Airfoil selection is based on its lift, drag, stall, and pitching moment characteristics, and available thickness to accommodate ribs and fuel. The main wing geometry consists of determining the necessary platform area, S , of the wing based on its gross takeoff weight and lift coefficient. The parameters to determine the wing geometry could be done by its aspect ratio, taper ratio and sweep and twist angle. The horizontal and vertical tails are designed using the “tail volume coefficient” method. Engine sizing is performed using historical thrust-to-weight ratios (T/W) for jet-engine aircraft or power-to-weight ratios for propeller-powered aircraft. The T/W value is then used to calculate the required lift to drag ratio during different mission segments. Finally, initial sizing of the fuselage is based on historical data trend. Raymer’s conceptual design method is based solely on gross takeoff weight but has shown to have very good correlation to most existing aircraft.

However, as explained before, this research project was mainly focused on the study of the water operation of the seaplane, rather than the aircraft design. A proposed aircraft design study had been introduced in order to understand the whole seaplane conceptual design elaborated in this project. In the end, the seaplane designer can choose whatever design method that is most suitable and comfortable to elaborate the advance aircraft configuration. This idea can expand the seaplane designer into converting an existing certified aircraft, i.e. converting an existing landplane into a seaplane by adding a floating device. The seaplane conversion is cheap to repair due that it can share all the parts of its landplanes counterparts, except for the floating devices used.

2.1.1. Examples of Existing Landplane for Seaplane Conversion

Some examples of landplanes that were taken into account are the following. All aircraft specifications are shown in Table 2:

1) Antonov AN-28

The Antonov AN-28 is a high wing aircraft with a 2-engined Turboprop and it is used as short-range airliner. It uses a conventional design and has a notable feature that will not stall due to its automatic slots [11]. FAR 23 requirements.

2) LET-410

The LET-410 is a high wing, twin turboprop engine used mainly as a short-range transport aircraft [28]. FAR 23 requirements.

3) Dornier Do 228

Dornier Do 228 has a high wing configuration, with 2 turboprop engines. The Do 228 is used mainly as a transport aircraft carrying between 15-19 passengers [29]. FAR 23 requirements.

4) Britten Norman BN-2

The BN-2 Islander is a British light, regional airliner and cargo aircraft. It has a high wing configuration with 2 piston propeller engines; however, the BN-2T Turbine Islander is designed with 2 turboprop engines [30]. FAR 23 requirements.

5) BAe 146

The BAe 146 is a British, high wing, 4 turbofan engine aircraft used mainly as a cargo and mid-size passenger airplane. This aircraft has a very quiet operation and has the characteristic of Short Takeoff and Landing capability (STOL) [31]. FAR 25 requirements.

6) Antonov AN-72

The Antonov AN-72 was design with many advanced features intended to maximize short takeoff and landing (STOL). It has two turbofan engines that are located above and forward of the high mounted wing. It has a combined triple slotted flaps and other high lift features to reduce runaway distance [32]. FAR 25 requirements.

Table 2: Aircraft Specifications

| Aircraft | MTOW (kg) | Length (m) | Height (m) | Max Speed (km/h) | Range (km) | Passenger | Power Plant |
|---------------------------|-----------|------------|------------|------------------|------------|-----------|---------------|
| Antonov AN-28 | 6,100 | 12.98 | 4.6 | 355 | 510 | 18 | 2 Turboprop |
| LET-410 | 6,600 | 14.42 | 5.83 | 380 | 1,380 | 19 | 2 Turboprop |
| Dornier 228 | 6,600 | 16.56 | 4.86 | 433 | 1,111 | 19 | 2 Turboprop |
| Britten Norman BN2 | 6,600 | 10.86 | 4.18 | 273 | 1,400 | 9 | 2 Piston Prop |
| BAe 146 | 42,184 | 28.6 | 8.59 | 801 | 2,909 | 80 | 4 Turbofan |
| Antonov AN-72 | 34,500 | 28.07 | 8.65 | 700 | 4,325 | 52 | 2 Turbofan |

In order to obtain an efficient design, the seaplane complies with special characteristics that are shown and compared from the above description of each aircraft and the information from the table. They all have a high wing configuration; use both turboprop or turbofan engines, that gives the aircrafts Short Takeoff and Landing (STOL) capability. Therefore, locating the advantages and disadvantages of these designs makes it a proposed goal of this research by elaborating advance versions of seaplanes that outstands the compared seaplanes explained in the history subsection of the Introduction chapter.

2.2. Water Operation Design

A seaplane is not only to be optimized for aerodynamic, but also for superior hydrodynamic performance. The drawbacks of a traditional seaplane are [33]:

1. Higher aerodynamic cruise drag due to additional structures.
2. Hydrodynamic drag while planning due to large wetted surface area.
3. Stability issues resulting from limits on dimensions and weight of floating gears.
4. Hindrance from water spray, requiring specially designed shapes to divert the spray away.
5. Low performance in high waves and cross winds, making smooth cruising in rough weather difficult.
6. Even maneuverability in water could be a deciding criterion, especially where narrow water strips pose a problem.

Most of the points stated above recall problems associated with the water performance of the seaplane. The design calls for an extensive investigation in the water operation of a seaplane, improving the design in such a way that won't affect other parameters. The extended research covered an analysis of the old designs looking into the advantages and disadvantages. The design accounted and implemented the advantages of the old designs, and suggestions for the disadvantages were researched, until a suitable idea was established.

Let us first recall that the study of the water operation design of a seaplane is focused mainly on naval architecture terminology, such as beam, step height, fore body, after body, trim angle, keel angle, stern post angle, etc. A brief explanation of these terms is given.

2.2.1. Hydrodynamic Shape Characteristics

Seaplane hulls and floats share the same shape characteristics that will affect the hydrodynamic as well as the aerodynamic design. Thus, some of the parameters that largely affect the hydrodynamic characteristics of the seaplane are shown in Fig. 16.

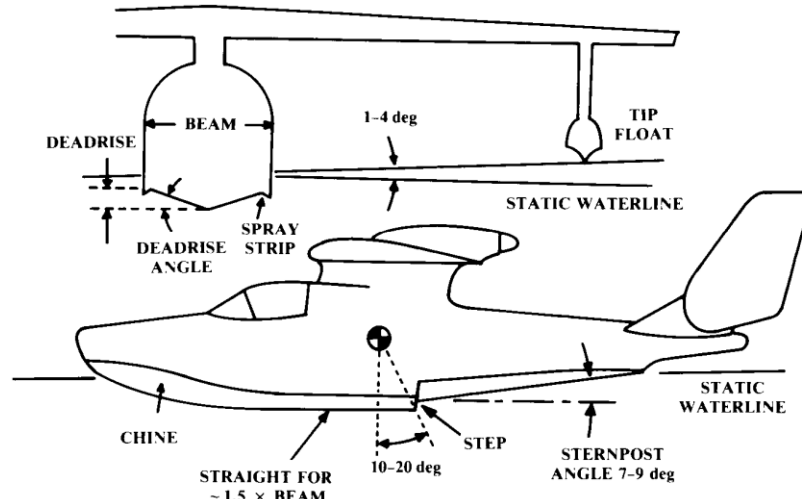


Fig. 16: Design Features of a Flying Boat [27]

2.2.1.1. Beam

Based on the literature review, generally the beam is established as the design reference parameter of seaplane floats and hull [35]. The beam is the widest section of the float as shown in Fig. 17.

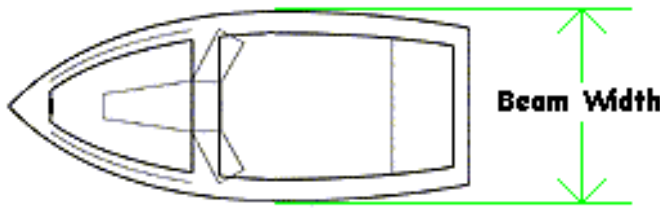


Fig. 17: Beam Width of a Conventional Boat [36]

The beam is determined by the buoyancy requirement and the width required for accommodation of payload. Loading of a hull is expressed in terms of beam load coefficient C_{Δ_0} which is based upon the beam as a characteristic dimension and has the following effect on performance [37]:

- Load to resistance ratio reduces at hump speed with increasing C_{Δ_0} , but increases near getaway speed.
- Both the upper and lower trim limits of stability are increased.
- Maneuverability decreases and spray increases.

2.2.1.2. Length to Beam ratio

The length to beam ratio of a flying boat hull or float is a ratio that affects the drag (either aerodynamic or hydrodynamic) and resistance of the aircraft. Choosing a slender hull offers benefits in terms of drag and structural weight. A slender hull is found to carry more weight with the same resistance than a short or wider hull. As the beam width of the hull increases, the aerodynamic drag increases. Beam width is related to the cross sectional area and hence the aerodynamic drag [38]. The length to beam ratio is directly linked to structural weight. The structural weight tends to increase with the product of length and beam.

For length to beam ratios between 9 and 10, no gain in hydrodynamic characteristics is obtained. Hulls with length to beam ratios between 6.3 and 9, the stability range of center of gravity locations are the same [37].

2.2.1.3. Forebody and Afterbody Length

A seaplane can be divided into forebody and afterbody depending upon the location of the step. The location of the step however has to be optimized, assuming the aspect ratio to be constant, so as to derive favorable hydrodynamic characteristics. Another assumption made is that the center of gravity remains or fixed relative to the step in order to eliminate inherent changes in trim.

2.2.1.4. Deadrise Angle

Deadrise is the angle of the bottom of the hull in a cross-section view of a boat. Angles of deadrise ranging from 20 degrees to 30 degrees probably represent the best overall performance suggested by World War II designs. Tank tests on the effect of deadrise angles were done on hulls of the Sunderland III [39]:

- Increasing the deadrise in the range of 15 to 30 degrees has little effect on hump resistance.
- Resistance increases at speeds exceeding the hump speed.
- The positive trimming moment at planning speed increases.
- The lower trim limit of stability increases with deadrise angle.
- Impact loads are considerably reduced.

Another study indicated that landing stability is improved by increasing the deadrise from 20 to 25 degrees [40]. Further studies confirm the most noticeably effect of deadrise angle is on impact loads which goes down with increasing deadrise angle [38].

However, increasing the dead rise angle at step makes the hull bottom a less efficient planning device. The hull will ride more deeply in water and hence will experience increased frictional drag an effect more pronounced in the planning range.

2.2.1.5. Hull Bottom

Fig. 18 shows a variety of different bottom shapes for a boat hull or float aircraft. The bottom chosen will always be a compromise between quick takeoff and seaworthiness. According to Brimm [41], the flatter the bottom, the quicker an aircraft will takeoff in calm seas. But, in rougher seas, the flatter bottom will cause severe pounding due to wave slam, which will likely make the aircraft takeoff slower than if it had a sharp bottom, which cuts through waves instead of going over them. This tendency to slam in rough water makes having a flat bottom hull a poor choice for an amphibious aircraft that is to operate in the littoral zone.

The double concave is desirable because it combines the advantages of the sharp and blunt "Vee". It has a sharp edge for entry into the water and cutting through waves yet still has a comparatively flat surface on which to plane. Another benefit of the double concave is that it deflects spray down and away from the fuselage and wings of the aircraft, which decreases loads and reduces the threat of water spray into the engines. The best overall compromise is the double scalloped bottom. Not only does it share the advantages of the double concave, but as the aircraft increases speed and begins to plane, it begins to rise up out of the water, and is supported on successively lower scallops, reducing the water resistance as the speed increases. The forebody of the boat hull was chosen to have a double scalloped bottom, for its combination of reduced drag and spray characteristics as well as its ability to cut through the water, while the afterbody was designed to be a double concave because of its behavior during planning.

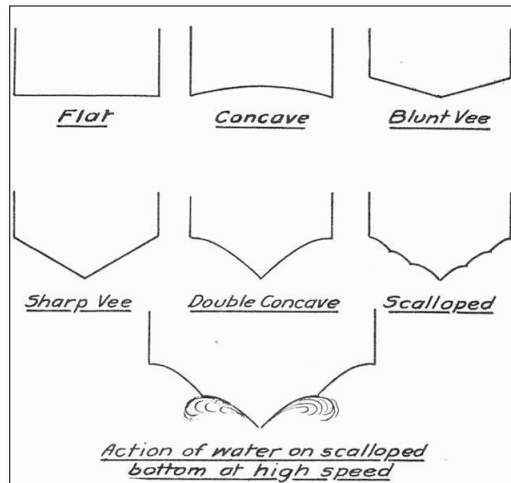


Fig. 18: Various Types of Boat Hull Bottoms [41]

2.2.1.6. Step

When water moves over the convex surface of the bottom of a seaplane, it creates suction in a normal direction to the surface. This means that as an amphibious aircraft accelerates through the water, the downward suction would increase with increasing speed. Takeoff performance would be greatly hampered by this. To prevent this from happening, a sharp step is placed into the hull

to separate the water from the skin of the seaplane. The step is “ventilated,” in that an air pocket generally forms behind it. As the speed of the aircraft increases, more air is drawn into this pocket and begins to extend back toward the stern, eventually completely separating the aft end of the hull from the water, which is called planning. The location of the step can vary, but is generally placed approximately 1/16 of the length of the hull behind the center of buoyancy. It is recommended that the depth of the step be approximately 5-8% of the breadth of the hull [42].

2.2.2. Boat Hull Design

Most seaplane designs are elaborated into two water operation configurations, twin floats or boat hull with wing tip stabilizers [43]. Boat hull seaplanes have less longitudinally stability problems than twin floats due to the large fore and afterbody of the hull, reducing the tendency to pitch at speed. However, boat hull seaplanes experience issues with transverse stability [44]. This is due sometimes to the fact that the metacenter is below the center of gravity, creating a lower metacentric height [45]. Wing tip floats can counteract heel turn, keeping the vessel stable. As the weight of the aircraft increases, the center of gravity with respect to the metacenter moves down, making the seaplane sufficiently stable.

A noticeable drawback that boat hull encounter is the increase in aerodynamic drag due mainly because of the odd shape hulls have. Studies on the effects of varying the length-beam ratio of the hull have been conducted in order to reduce this aerodynamic drag [46]. It was found through wind tunnel tests that the minimum drag coefficient was reduced by 29% for a length-beam ratio increase from 6 to 15, while the hydrodynamics of the hull have not been affected. Some other studies [47] performed the use of a retractable planning flap in place of a fixed step on a hull or float. The step is the abrupt break in the bottom line between the forebody and the afterbody of the hull. The step causes the water to separate from the hull, which leads to a reduction in suction, assists in getting to plane, and improves longitudinal control. Performance improvements of eight percent in water resistance and two to three percent in total air drag were noted because of the adjustment to the depth of the retractable step during and after takeoff.

Other tests have been conducted on the effects of waves on the takeoff resistance of the hull [48]. Factors that increase the resistance of the seaplane at takeoff can be associated with the increase in drag due to the larger wetted length to beam ratio, and unusual trim conditions due to uncontrollable pitching and heaving of the seaplane. Tests were run on a boat-hulled seaplane with a length to beam ratio of 15 and a wing loading of 120 lb/ft². Results showed that the maximum takeoff resistance increase occurred at around 70 percent of takeoff speed. In 6 ft waves, the takeoff resistance of the aircraft increased 65 percent over nominal values during calm seas.

Essentially, the seaplane hull must meet the following requirements in order to satisfy an efficient water performance [49]:

1. Must be buoyant.
2. Attain static and dynamic stability.
3. Must allow for hydrodynamic lift through water and in do so must counter the suction force between water and hull.
4. Must avoid or minimize hydrodynamic resistances associated with planning and taxiing.

2.2.3. Float Design

Float design, in general, features the same characteristics boat hulls have. A difference between floats and boat hull is the longitudinally stability. For longitudinally stability, floats have a tendency to be unstable if the nose pitched downwards at approximately one third of its

takeoff speed. The region of greatest curvature, which is generally towards the front of the float, shows suction over the bottom that causes the longitudinal instability. Though, if the float could be longitudinally stable by restoring the moment, it would still be susceptible to instability caused due to insufficient damping, which results in oscillations known as porpoising [50].

Porpoising is a dynamic instability of the seaplane and may occur when the seaplane is moving across the water while on the step during takeoff or landing [51]. It occurs when the angle between the float or hull, and the water surface exceeds the upper or lower limit of the seaplane's pitch angle. There are two types of porpoising. One type can be counteracted by applying a steady load to the horizontal tail surface, which causes the aircraft to pass to another trim angle, "getting through" the porpoising as quickly as possible. The second type can only be counteracted through an alternative application of upward and downward loads on the tail surfaces, although even this is not always successful.

2.2.4. Trimaran and Retractable Float System

Many proposed ideas were analyzed for possible technical solutions that aim to reduce costs on research, manufacturing and operation of the advance seaplane design. Some water operation ideas that were considered were the use of retractable floats, inflatable floats, advance navigational aid instruments, hydrofoils, water thrusters, folded wings, advance composite materials, reversed thrusters, multihulls, among many more ideas.

Inflatable floats will give the advantage of reducing aerodynamic drag; however the main concern of inflatable floats will be stability and control of the seaplane during water operations. Water thrusters can be used to aid the seaplane maneuvering in water when taxiing in the seaport, but water thrusters may increase payload weight and they will become useless once the seaplane is in the air. Retractable wings can be used when the seaplane is operating on water to reduce clearance space and have a better access to seaports and maintenance hubs. Navigation aid instruments will be useful for a seaplane to operate in many types of weather conditions. Hydrofoil, shown in Fig. 19, is a foil that operates on water. A hydrofoil is a wing-like structure mounted on the bottom or side of a boat hull and its purpose is to lift the boat out of the water in order to reduce hull water resistance [52].

After analyzing all of the proposed ideas, the complexity and high costs of some of these narrow the search for technical solutions that will meet the requirements of this futuristic seaplane concept. It was decided that the use of trimaran hull and the use of retractable floats will give the seaplane an exceptional performance.



Fig. 19: Hydrofoil Example [53]

2.2.4.1. Trimaran

Multihulls have become an alternative boat design for their speed, stability, large capacity and resistance to high waves. Moreover, the drag in case of multihulls is also dependent upon the wave interference between the hulls. Approximately, a 20% increase in drag is observed compared to hulls at infinite spacing [54]. Trimaran is a type of multihull boat consisted of one main hull and two smaller outer hulls attached to the main hull with lateral struts as shown in Fig. 20 [55].

The trimaran possesses some advantages over other types of boat hull designs [56]:

- Low wave resistance at high speed due to its slender ship hulls.
- Superior stability attributable to suitable layout of the side floats. A trimaran can keep a high speed under high sea conditions.
- The wave interference between the main hull and the outriggers can produce a beneficial wave interference optimizing the speed and engine power required correlation
- In case of an emergency the all float structure remains floating even when the hull or the outriggers are severely damaged.

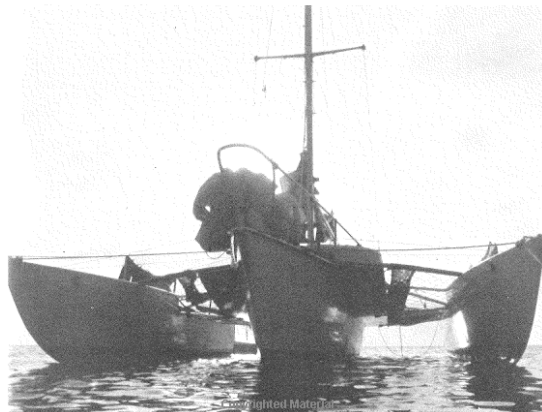


Fig. 20: Trimaran Example [55]

Trimarans are superior in terms of stability because the arrangement of the hulls is such that individual centers of buoyancies have a righting moment about the centre of gravity that helps in stabilizing the vessel as shown in Fig. 21. This gives the boat, and the seaplane, more roll stability, better water maneuverability for docking and better water performance at high waves.

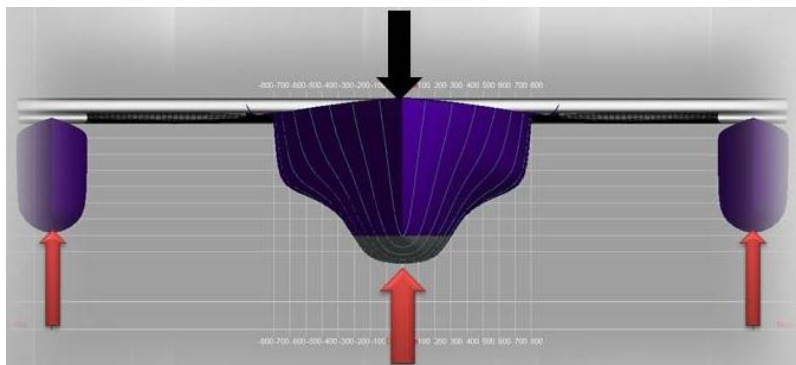


Fig. 21: Trimaran Stability-Beam Model [56]

Another important aspect to analyze is wave performance. Seaplanes must have the ability to perform in any weather and water conditions. When a wave passes through a conventional float,

it reaches the bow producing a lift force which pushes the stern down; as the wave passes through the body of the float, the center of buoyancy changes along with the wave. When the wave reaches the stern, the lift force pushes the bow; at high speeds, during rough water conditions, a dangerous pitch effect could cause the bow to be submerged and capsize violently. For the outriggers, when the peak of the wave moves towards stern, the lack of buoyancy on this section to the shape, negates the lift force which produces the pitching effect, therefore the outriggers are capable to operate in a wider range of rough water conditions than the conventional floats. Past studies conducted on trimaran shows that wave resistance of trimarans is significantly lower compared to an equivalent catamaran as shown in Fig. 22 [57]. For this instance, in theory, trimaran has superior seagoing performance.

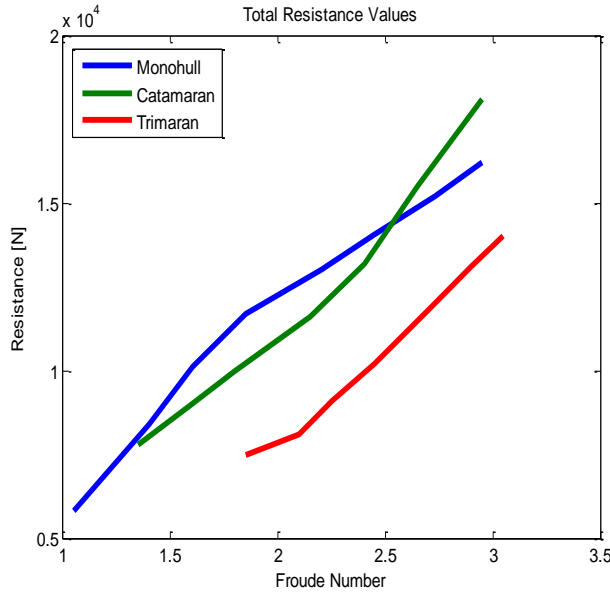


Fig. 22: Resistance comparison curves [57]

2.2.4.2. Outrigger Design

The total resistance of the trimaran can be reduced by the design of the outrigger form and position. For an ideal trimaran design, an outrigger is half the length of the main hull and has 4% of the displacement of the main hull [58]. The positions of the outriggers with respect to the main hull are quantified in terms of the longitudinal displacement of the centre line of the outrigger from then centerline of the hull (known as clearance) and the lateral displacement of the outrigger with respect to the main hull (known as stagger), shown in the following figures.

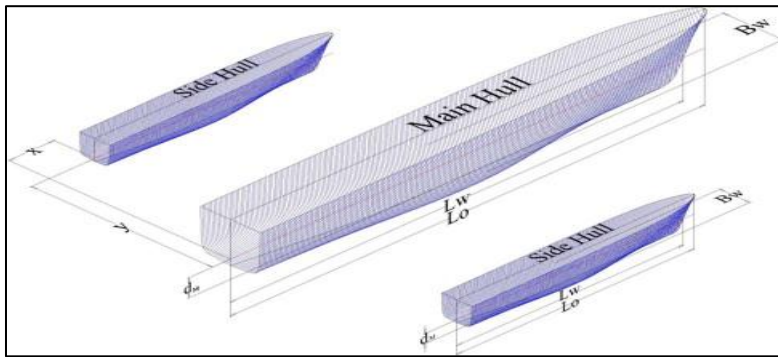


Fig. 23: Trimaran coordinate Axis [56]

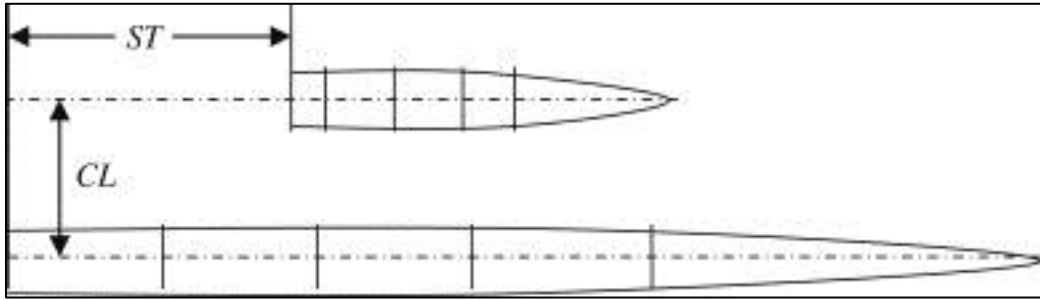


Fig. 24: Outrigger stagger and clearance [56]

Assuming that the mid latitude of the main hull is the origin of the coordinate system, positive stagger is the distance of the mid latitude of the outrigger in the direction of the stern. Clearance is the departure of the centerline of the outrigger from the centerline of the main hull in the vertical direction.

The stagger ‘x’ and the clearance ‘y’ are rendered dimensionless by representing them as a ratio to the total length of the main hull. The following results performed by Begovic [58] of tank tests done for a series 64 trimaran hull with different stagger and clearance. The first series of tests involved testing the model for a stagger ‘ x/L ’ = -0.0625 and for clearances of 0.10, 0.11 and 0.12 respectively. The second series involved testing the model for a clearance ‘ y/L ’ = 0.1 and staggers of 0.25, 0, -0.0625 and -0.125 respectively.

For the tested clearance 0.10, minimum resistance was obtained for a stagger of - 0.125 in the Froude number range of 0.7 to 1.0, probably due resulting from a larger lift effect. However this layout is fairly unrealistic for large scale trimarans. Therefore, the results of the two practical values of stagger (the values of 0 and -0.0625) were considered. It was also observed that resistance dropped further with the clearance due to changes in the interference phenomenon.

2.2.4.3. Retractable Float System

One concern of using trimaran will be the exposed floats at flight. One solution is to retract the floats or either mount them inside the fuselage or hull, which in theory reduces aerodynamic drag.

Tigerfish Aviation developed the use of retractable pontoons called Retractable Amphibious Pontoon Technology (RAPT) [59]. Adapting the same concept idea, the floats will form a single component embodied to the hull and fuselage when retracted, as shown in Fig. 25. This will reduce the drag form interference factor added by the floats and boat hull [60], hence decreasing the aerodynamic drag. However, retracting the floats into this position will not reduce entirely the aerodynamic drag caused by the floats. A final solution is to place the floats inside the boat hull, as shown in Fig. 26. The floats will be retracted inside the boat hull, the same way the landing gear is retracted inside the fuselage. The only drawback will be the added structural support required, compromising an increase in weight of the strutting.

For this design, another advantage of the retracting float system was to keep the seaplane stable. The retracting system can be automated in order to control the seaplane on unexpected heel turns. If the seaplane tilts to a side, the automated retracting system will be configured to maintain a position in the water in which one float will move upwards towards the waterline while the other float will move downwards, maintaining both floats at the waterline. Fig. 27 shows the mechanism of the retracting system in the water.

Last, another advantage of the floats will be as an extra storage compartment. Since the floats do not account for the total displacement of the seaplane, extra fuel or payload could be stored inside the floats, increasing the performance of the seaplane.

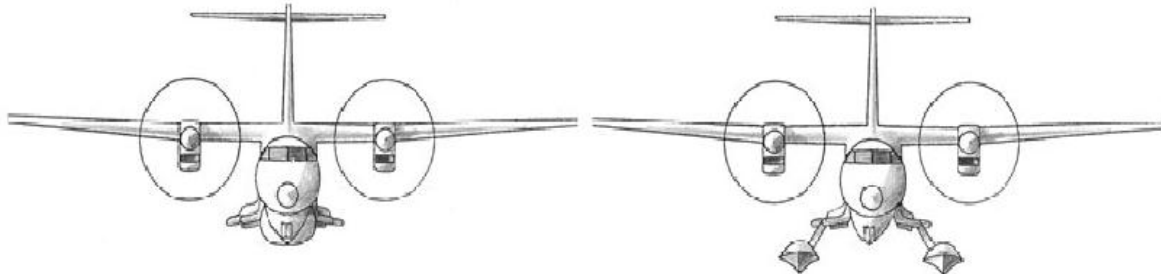


Fig. 25: Retracting Float Concept [59]

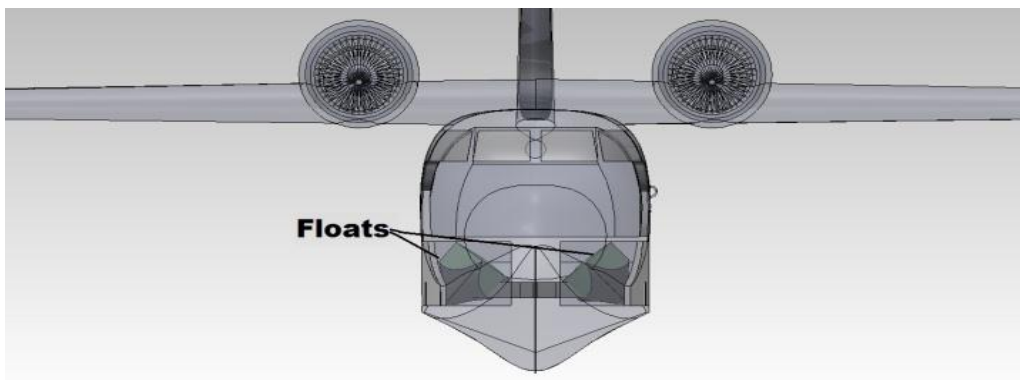


Fig. 26: Example CAD Model with Floats retracted inside Hull

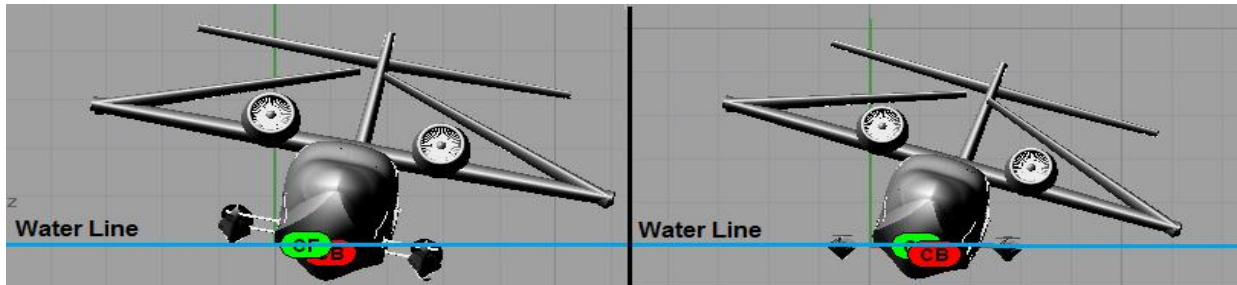


Fig. 27: Heel Overturn Retracting Float System

3. Advance Seaplane Conceptual Optimization Method

3.1. Conceptual Design

The first step of this research was the creation of an advanced seaplane conceptual design method. Many old seaplane publications approached the conceptual design by developing the water operation requirements (i.e. the boat hull or floats) before the air requirements [35], [42], [44]. With the hull sized, the fuselage of the aircraft was built around the hull dimensions, and the rest of the aircraft components (wings, empennage, etc.) were then added. In other words, seaplane design had to comply with water requirements before fulfilling air requirements. The design must perform an acceptable hydrostatic stability, with outstanding aerodynamic and hydrodynamic properties, and a strong structure supporting water loads. This gives the seaplane designer a disadvantage in having an open mind on the manner on how to elaborate an advance seaplane design with an “out of the box” aircraft configuration.

Nonetheless, the idea to create a modern conceptual design that will allow the designer to create a futuristic seaplane, made it possible for this research to analyze the proposed method. The advance seaplane design method was elaborated by gathering studied seaplane information, adapting the advantages of the old seaplane features, and attacking the disadvantages in order to modify them by creating the modern conceptual seaplane design.

To generalize, the proposed design sizes each of the seaplane segments (“boat” and “aircraft”) in a separate manner. There are three main advantages of adapting this conceptual design:

1. The “aircraft” segment can be design in a separate manner, using whatever optimization method the designer will like to choose. The “boat” optimization design method was elaborated in such a manner that will adapt which ever aircraft configuration and will then design the desire water operation device design parameters. Therefore,
2. The conversion of an existing landplane structure into a seaplane configuration will be elaborated into this design method.
3. Simplification of this method will expand the complexity of creating an advance seaplane “boat” segment by studying a more reliable hull design and running separate trial tests.

Since the design of an aircraft has to comply with many requirements such as airworthiness, stability, structural strength, etc., only certain requirements of the seaplane were analyzed for simplicity of this research. Air stability, structural strength, and engine modeling were not analyzed in this research. For this instance, to recognize which aspects to study, the research attacks the most noticeable disadvantages common seaplane designs have today. This way, seaplanes will have excellent air performance as well as water performance to compete in the global aeronautical industry. Then, the main goals that should be attained to acquire the desire design were focused on the following:

1. The seaplane should acquire an outstanding hydrostatic stability in order to excel during water taxing operations, hence the trimaran concept.
2. The advance design will have the capability to operate in rough, high wave waters, giving the seaplane more water options in which to operate.
3. The increase in aerodynamic drag caused by the extra components should not compromise the flight performance of the seaplane, hence the retracting float system.
4. Water Performance should be comparable to that of a speed boat.
5. Air Performance must obtain related performance as that to its landplane design.

Then, in order to attain the necessary criteria explained, the advance design follows the proposed flow chart shown in Fig. 28.

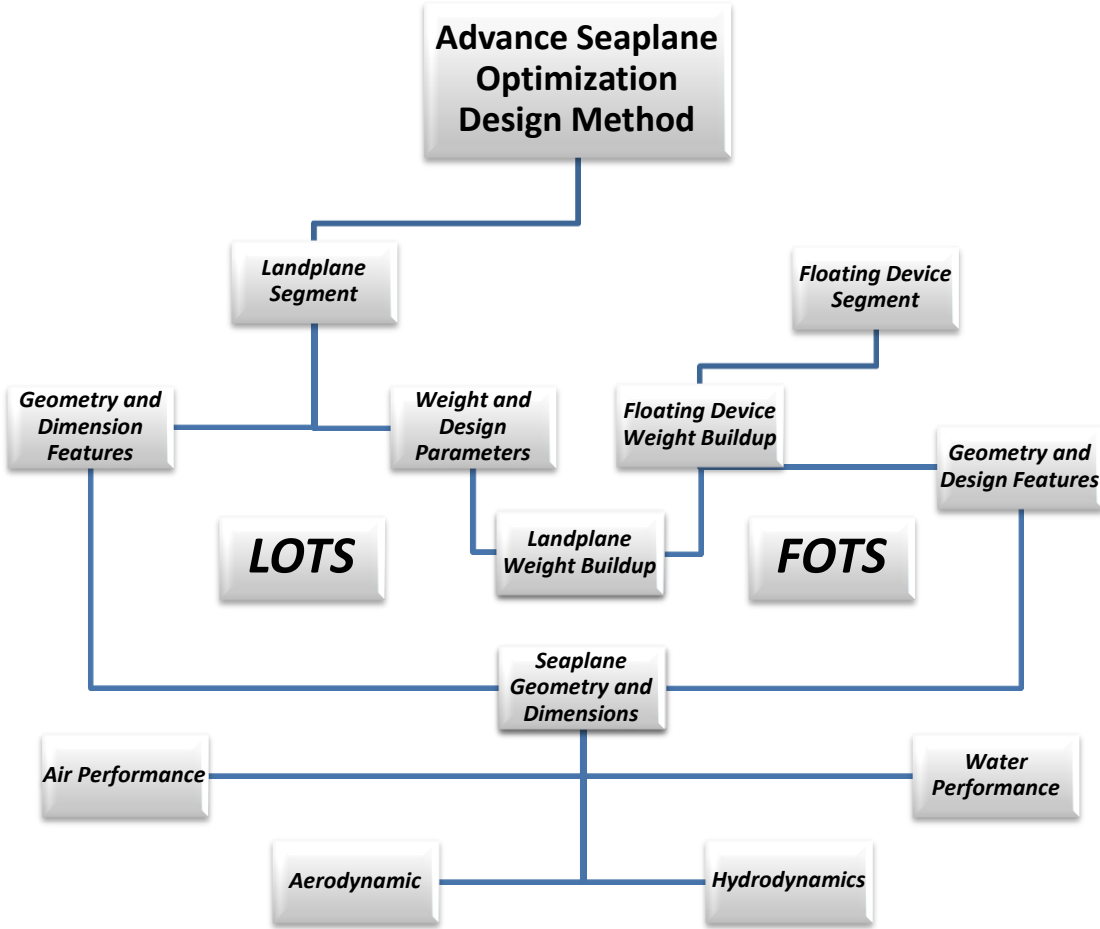


Fig. 28: Seaplane Design Optimization Method Flow Chart

The design architecture of this seaplane design shows two divisions. One design segment is elaborated towards the landplane segment, while the other towards the floating device segment.

The first step towards this design methodology is the elaboration of the landplane aircraft. The optimization code sizes the geometry and the weight parameters based on initial inputs given by the designer which are define by the specific mission profile the aircraft must obtain. The method calculates the weight of each component until a total gross weight of the landplane is obtained. The next step of the methodology is to calculate the weight parameters and geometry features of the floating device. With the obtained total gross weight and the geometry features of the landplane, elaboration of the floating device is then calculated. The method optimizes the geometry of the floating device based on the inputs of the landplane, and calculates the added weight to the aircraft. Finally, with the weights and geometrical features of both the landplane and the floating device done, the design methodology blends the results to form the seaplane, finalizing the calculations for water and air performance of the seaplane. An extended explanation of the elaboration of the sizing codes and the empirical calculations is given in the following sections.

3.2. Sizing Code Development and Validation

A sizing mathematical code was developed in order to run specific theoretical calculations that are necessary to size the optimum seaplane design. The sizing code is set up to work with a

number of different aircraft configurations which would then add the desired floating device (boat hull, twin floats, wing tip floats, trimaran) to transform the landplane aircraft into an amphibious configuration. To increase the usefulness of the sizing code, as well as to obtain a more feasible final preliminary design, any combination of the various water operations methods may be used, which allows for testing as many configurations as possible.

The seaplane optimization code works in two separate optimization codes. The first code called the Landplane Optimized Testing Source Code or LOTS, sizes the characteristics of the landplane aircraft chosen. The second code, called the Floating Device Optimized Testing Source Code or FOTS, sizes the floating device chosen by the seaplane designer, based on the characteristics given by the landplane.

3.2.1. Landplane Optimized Testing Source Code (LOTS)

Using Raymer's Class II sizing process design method the following Landplane Optimized Testing Source Code (LOTS) was elaborated. The LOTS code was written using the Mathwork's MATLAB programming language and compiler. Separate functions were written to accomplish various tasks, which are all then compiled into pre-processing, computation and post-processing codes. The following image (Fig. 29) shows the proposed flowchart of the LOTS architecture. To begin the optimization sizing code, selection of desired input parameters must be made by the designer depending on the mission requirements the aircraft must perform. These parameters are wing aspect ratio (AR), Wing Loading (W/S), taper ratio (λ), and tail volume coefficients. Then, an initial guess for GW is made and aircraft geometry, such as wing span and wing area, are calculated. Using these values, weights of individual components are calculated and summed together to get a GW . The two GW s are compared and iterated until convergence. Depending on the mission requirements, then the mission code is run, which calls upon the various other cruise codes, in order to get a weight of the fuel required for the mission. Once this is obtained, new aircraft geometries are calculated and both the weights and mission codes are run until a GW is converged. Then, the drag code is ran which calculates a more accurate at plat drag based on the current aircraft geometry and weight. Once this value is obtained, the drag code is iterated with the weights and mission code until a common GW and equivalent at plate drag value is obtained. Once these values are converged, the program calls upon the final process in order to determine if this aircraft meets the mission requirements. If the requirements are met, then the data is saved as a comma separated value file. If the requirements are not met, then the values are deleted and new values for AR and/or W/S are run.

As explained before, LOTS is able to size three different aircraft configurations, conventional, BWB, and Flying Wing. Let us recall that this research project does not emphasize the work of the optimizer source code, so a depth explanation is not elaborated. Principle algorithms and numerical iteration methods are run throughout the code in order to size the landplane geometry and flying characteristics. As stated, the designer may be eligible to use any computation device or code to elaborate the desire aircraft design.

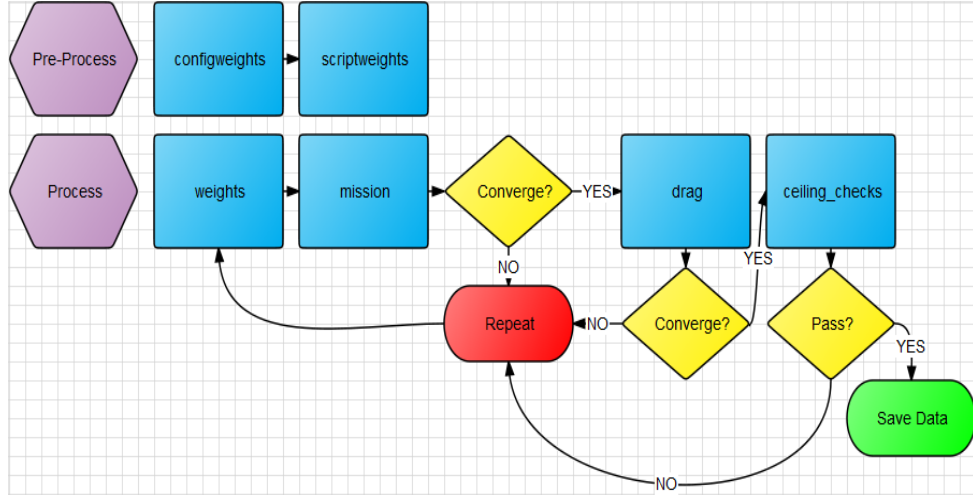


Fig. 29: Flowchart of the LOTS architecture

3.2.2. Floating Device Optimized Testing Source Code (FOTS)

The Floating Device Optimized Testing Source Code (FOTS) functions similarly as the LOTS sizing code. The proposed flowchart architecture of the FOTS code is shown in Fig. 30.

The FOTS sizing code will start by entering the output characteristics of the landplane sized by the LOTS code. Fig. 31 shows the input characteristics of the landplane necessary to calculate the floating device characteristics. Based on the input gross weight of the landplane, the FOTS code calculates the buoyancy required which is necessary to size the dimensions of the floating device. The designer chooses either a boat hull with mid wing stabilizers, boat hull with wing tip floats, twin floats, or boat hull with twin floats (trimaran). The designer then chooses a slenderness ratio and a spray coefficient depending on the characteristics of the seaplane desired by the designer. With the buoyancy calculated, and the slenderness ratio and spray coefficient chosen, the code sizes the dimensions of the main hull. The code then checks if the length of the fuselage is less or equal to the length of the boat hull. If this is the case, the code continues to size the rest of the floating device. If this is not the case, the code selects new slenderness ratio and spray coefficient until it converges to the desire hull length value. With the hull and the rest of the floating device sized (stabilizers) the code checks for hydrostatic stability requirements. If the hydrostatic stability is not met, the code runs new values of slenderness ratio and spray coefficients running the geometric loop again. When hydrostatic stability is satisfied, water takeoff is calculated based on the thrust available (T_A) of the landplane. If the water takeoff is not satisfied, either a new T_A is needed from the LOTS code, resizing the whole landplane parameters, and starting the sizing methodology, or the FOTS code changes the geometry of the floating device which will be resized until convergence. When all requirements are met, the seaplane features are given, and geometry and performance characteristics are then output. With this data obtained, a picture showing the basic geometry is drawn.

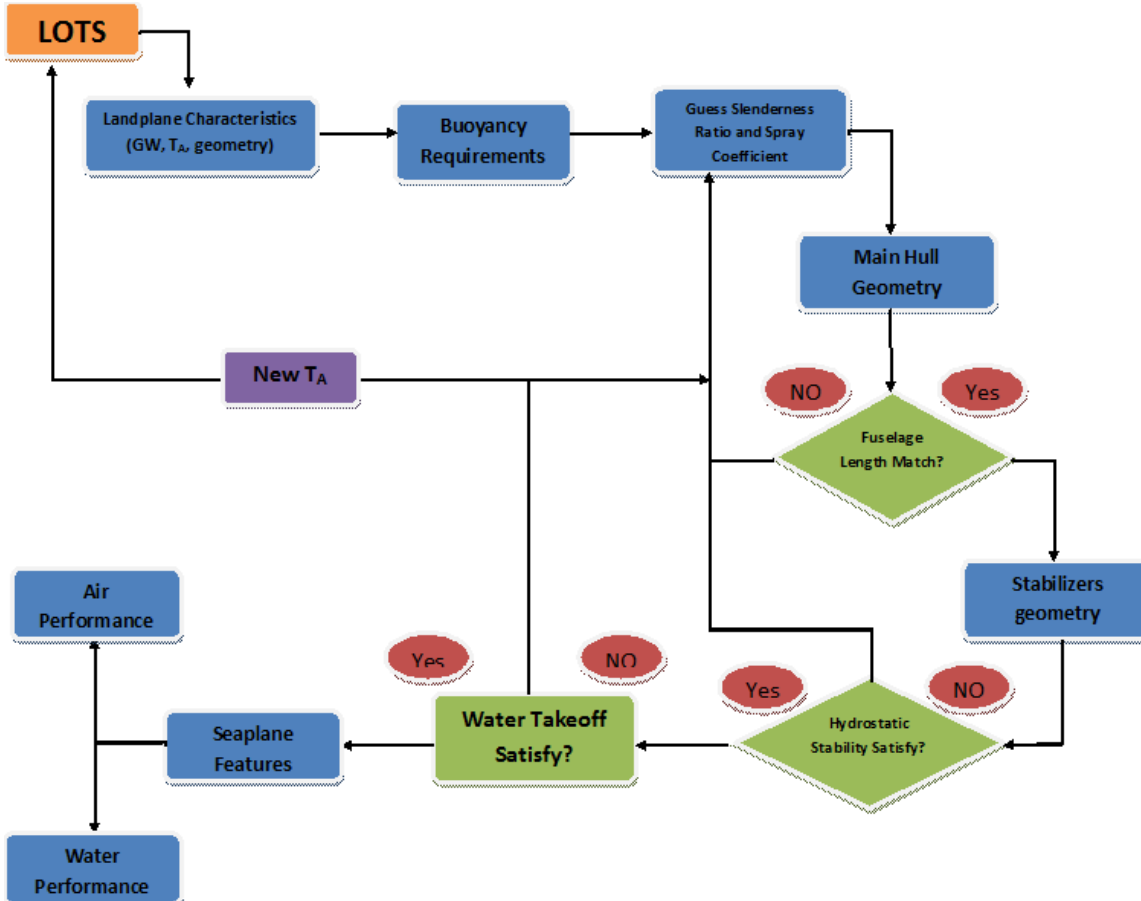


Fig. 30: Flowchart of FOTS architecture

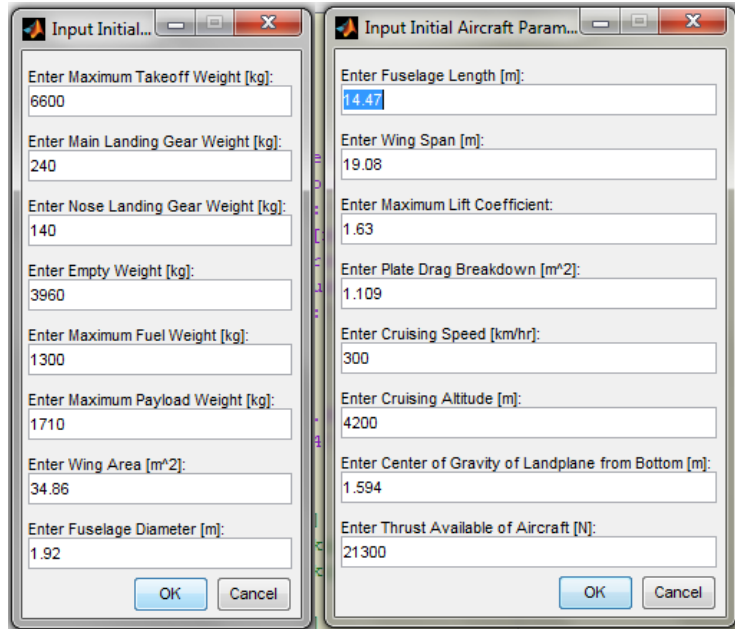


Fig. 31: Input Landplane Characteristics

3.2.3. Validation

In order to validate the functionality of the sizing code and to ensure that the sizing algorithms used in the code are working properly over a range of aircraft types, geometry of an aircraft was run through the code to determine how the coded algorithms predicted the takeoff weight and performance parameters. First, validation of the LOTS sizing code was done by comparing data from the LET L-140 [28]. For simplicity, the validation assumed no floating device was added; therefore the FOTS sizing code calculated the air performance of the landplane. The following comparison data obtained from the sizing code is shown in Table 3.

Table 3: LOTS Comparison Validation

| Parameters | Typical | Let L-410 | % Error |
|----------------------------------|---------|-----------|---------|
| Gross Weight [kg] | 6,600 | 6,670 | 1.05% |
| Empty Weight [kg] | 3,900 | 4,020 | 2.99% |
| Max Fuel [kg] | 1,300 | 1,370 | 5.11% |
| Fuselage Length [m] | 14.47 | 14.43 | 0.28% |
| Wing Area [m²] | 34.86 | 34.9 | 0.11% |
| Wing Span [m] | 19.08 | 19.7 | 3.15% |
| Max Speed [km/hr] | 392 | 390 | 0.51% |
| Rate of Climb [m/s] | 6.6 | 7 | 5.71% |
| Service Ceiling [km] | 7.27 | 7.4 | 1.76% |
| Thrust Available [N] | 25,500 | 25,000 | 2.00% |

Now validation of the FOTS sizing code was done by comparing the performance of the Canadair CL-215 amphibian aircraft [11]. In this case, the LOTS sizing code sized the aircraft without the floating device. Then the FOTS sizing code adds the boat hull and stabilizer floats, and finally the performance was calculated. This validation is only an approximation on the functionality of the sizing codes and not necessarily sizes the aircraft from the original sample. Table 4 shows the comparison data of the Canadair CL-215.

Table 4: FOTS Comparison Validation

| Input | Typical | Canadair | % Error |
|----------------------------------|---------|----------|---------|
| Gross Weight [kg] | 17,000 | 17,100 | 0.58% |
| Empty Weight [kg] | 12,000 | 12,200 | 1.64% |
| Max Fuel [kg] | 3,800 | 3,800 | 0.00% |
| Fuselage Length [m] | 21.2 | 19.82 | 6.96% |
| Wing Area [m²] | 98.52 | 100.3 | 1.77% |
| Wing Span [m] | 26.5 | 28.6 | 7.34% |
| Max Speed [km/hr] | 396 | 360 | 10.00% |
| Rate of Climb [m/s] | 9.2 | 8.1 | 13.58% |
| Service Ceiling [km] | 5.2 | 4.5 | 15.56% |
| Thrust Available [N] | 67,000 | 67,500 | 0.74% |

The data obtained shows the functionality of the advance seaplane sizing code. The LOTS code has a percent of error of less than 5% over most of the parameters compared, proving a good functionality of the algorithms. On the other hand, the FOTS code shows a percent error of

less than 15% in some parameters. The reason for increase in percent error is the newly air performance calculation done when the floating device is added to the landplane. As explained, the sizing methodology proposed differs from the conventional seaplane conceptual designs.

3.3. Theory

The seaplane conceptual design and the sizing code followed a proposed aircraft design theory in order to size the optimum advance amphibian aircraft. Basic aircraft design theory proposed by Raymer was used [27]. Water performance theory was elaborated with the aid of many proposed publications [35],[38],[42],[44],[45] and finally adapting the use of the trimaran design blended with conventional flying boat theory [57].

3.3.1. Aeronautical Theory

Since the study of aircraft design has been elaborated for many years, this field of study has been corrected and improved in order to find suitable empirical equations that will size the desire aircraft design. As explained previously, the seaplane designer can use the optimization process desired and in this case, the theoretical calculations necessary to size the landplane aircraft. For the purpose of this research, only a brief explanation of landplane aircraft theory is given. The sizing theory of the landplane aircraft follows the flowchart architecture shown from Fig. 29.

3.3.1.1. Geometry Calculations

The first step of the LOTS code is to size the major components of the aircraft based on the initial parameters (GW , AR , W/S , λ , etc.). The required platform area of the main wing, S , can be calculated using the estimated gross takeoff weight and wing loading.

$$S = \frac{GWest}{W/S} \quad (1)$$

The total wing span of the main wing can be found using eq. (2)

$$b = \sqrt{S \cdot AR} \quad (2)$$

The root and tip chord lengths are calculated using the following expressions:

$$c_r = \frac{2S}{b(1 + \lambda)} \quad (3)$$

$$c_t = c_r \lambda \quad (4)$$

The platform areas for the vertical and horizontal tails are calculated using the following equations from Raymer [27].

$$S_{VT} = \frac{c_{VT} b S}{L_{VT}} \quad (5)$$

$$S_{HT} = \frac{c_{HT} c S}{L_{HT}} \quad (6)$$

3.3.1.2. Weights

The first step in calculating the weight of an aircraft is to identify the “Design takeoff gross weight (GW)” [27]. Takeoff gross weight can be divided into payload weight, fuel weight, and empty weight as shown from the following equation.

$$GW = W_{payload} + W_{fuel} + EW \quad (7)$$

Payload weight and fuel weight would be determined depending on the mission requirements of the aircraft, such as amount of passengers or cargo, the range or endurance, among other characteristics.

3.3.1.2.1. Empty Weight

With the geometry of the aircraft found, an empty weight breakdown of each component of the aircraft is calculated. Empty Weight breakdown is elaborated using the statistical equations proposed by Raymer [61] and shown in Appendix A.1. All equations and multiplicative factors are taken for a general aviation aircraft, unless specified.

3.3.1.2.2. Fuel Weight

Total fuel weight is broken down into each of the required segments the aircraft needs to perform in order to attain its mission, take-off, climb, cruise, descent, and landing, as well accounting for taxi operations and reserves. Then the equation for fuel weight is:

$$W_{fuel} = m_{fL} + m_{fTAXI} + m_{fTO} + m_{fC} + m_{fD} + m_{fLN} + m_{fH} \quad (8)$$

Where L is level flight, $Taxi$ is fuel at taxi segment, TO stands for take-off, C is climb, D is for descent, LN is for landing, and H is for holding fuel or fuel reserve. To calculate the mass of the fuel for each segment the following equation is used:

$$m_{fi} = t_i FC_i \quad (9)$$

Fuel consumption (FC) depends on the available thrust and thrust specific fuel consumption which is explained in more detail in the engine modeling section.

3.3.1.3. Aerodynamic Drag

Drag forces results from a combination of pressure and shear forces. Alternatively, the drag forces are broken down into induced drag and wave drag which is the drag due to pressure forces and viscous or parasite drag which accounts for the shear forces.

$$D = D_i + D_w + D_p \quad (10)$$

3.3.1.3.1. Induced Drag

The vortices caused by the wing in generating lift also cause the effective angle of attack of the wing to be lowered. This phenomenon slightly reduces lift but causes a noticeable increase in drag. The drag that is created by this phenomenon is known as induced drag. Induced drag greatly depends on the lift distribution of the wing, with an elliptical wing loading being the most efficient with the lowest amount of induced drag [60].

The total induced drag coefficient is then found using the equation,

$$C_{DI} = \frac{C_L^2}{\pi \cdot AR \cdot e} \quad (11)$$

To relate a given wing distribution to an elliptical wing distribution, the Oswald efficiency factor (e) is calculated from Raymer [60].

$$\text{Straight Wing} \quad e = 1.78(1 - 0.045AR^{0.68}) - 0.64 \quad (12)$$

$$\text{Swept Wing} \quad e = 4.61(1 - 0.045AR^{0.68})(\cos\Lambda)^{0.15} - 3.1 \quad (13)$$

3.3.1.3.2. Wave Drag

In high subsonic flight, regions on the wing can experience air speeds of over Mach 1. This will in turn cause shock waves to form which cause adverse pressure distributions that increase the drag of the wing. This is known as wave drag. Wave drag is calculated by finding the Mach number at which the wing experiences supersonic flows, also known as divergence Mach number (M_{div}). M_{div} is greatly influenced by wing sweep (Λ), C_L and wing thickness ratio (t/c). Higher Λ increases M_{div} , while a larger C_L and t/c decreases M_{div} . According to [63], a plane with a Λ of 35° and a t/c of 10%, the minimum M_{div} number is 0.79. Wave drag is calculated using the method provided by [63].

$$M_{div} = (-0.25C_L) + 0.91 \quad (14)$$

$$C_{D_w} = 0.002e^{21.652(M - M_{div})} \quad (15)$$

3.3.1.3.3. Parasite Drag

Surface tension effects create a force opposing the relative motion of aircraft as particles of air move over the exposed surfaces, or wetted area. This is known as friction or parasitic drag and is the major contribution to drag in low speed flight. A useful measure of the parasite drag is the equivalent flat plate-drag area (f). Therefore, the total parasite drag (D_P) is [27], [68]:

$$D_P = f \frac{1}{2} \rho V^2 \quad (16)$$

Each exterior component of the airplane is considered separately, and the total (f) of each component is finally sum together. The equivalent flat plate drag area can be computed from the following expression:

$$f_i = C_{fi} F_i Q_i S_{wet_i} \quad (17)$$

Where (C_f) is coefficient of friction, (F) is form factor, (Q) is interference factor and (S_{wet}) is the wetted area of the component. These variables are calculated using the equations from Appendix A.2.

Miscellaneous component flat plate area is an additional 5% increase to the flat plate drag to take into account of sensors, joints, and other surface disturbances. The total parasitic drag coefficient is then found using,

$$C_{D_P} = \frac{f}{S} \quad (18)$$

3.3.1.4. Air Performance

“Performance” is a term used to describe the ability of an airplane to accomplish certain things that make it useful for certain purposes. For example, the ability of the airplane to land

and take off in a very short distance is an important factor to the pilot who operates in and out of short, unimproved airfields. The ability to carry heavy loads, fly at high altitudes at fast speeds, or travel long distances is essential performance for operators of airline and executive type airplanes. The chief elements of performance are the takeoff and landing distance, rate of climb, ceiling, payload, range, speed, manoeuvrability, stability, and fuel economy. For simplicity and the complexity of the subjects, manoeuvrability and stability are concepts that were not widely researched. Then, basic fundamental equations for calculating the performance of the aircraft were done with the aid from several handouts [28]. Some of the key equations for the calculation of the performance are shown in this section while the rest are in Appendix A.3.

One of the most important graphs in aircraft performance is thrust as a function of velocity. A comparison of the required thrust and power calculations are given by using the following equations:

$$T_R = \frac{C_D}{C_L} GWg \quad (19)$$

Some important speed performance parameters are stall speed (V_{S0}), climb speed (V_c), which are calculated by the following:

$$V_{S0} = \sqrt{\frac{2GWg}{C_{Lmax}\rho_0 S_{wing}}} \quad (20)$$

$$V_c = \frac{(T_A - T_R)V_{TAS}}{GWg} \quad (21)$$

Last, other important parameters useful in the performance of an aircraft are endurance and range. Using Breguet Range equation, endurance and range are calculated:

$$E = \frac{1}{g \cdot tsfc} \frac{L}{D} \ln \left(\frac{W_i}{W_{fi}} \right) \quad (22)$$

$$R = V \cdot E \quad (23)$$

3.3.1.5. Engine Modeling

To calculate the weight of the fuel for each flight segment of the aircraft, it is necessary to calculate the amount of fuel consumption the engines produced. Then, from the following:

$$FC_i = T_A \cdot tsfc_i \quad (24)$$

i represents the flight segment (takeoff, descent, etc.) An equation for the fuel flow can be found based upon the thrust of the engine. The referred fuel flow is the engine fuel flow normalized by the pressure and temperature ratios and the engine thrust is normalized by the pressure ratio. Therefore, the equation for fuel flow ($tsfc$) is:

$$tsfc = f_{th}(0.34 + 0.19M)\sqrt{\vartheta} \quad (25)$$

Engines have different ratings in which the engine can be operating depending on the flight segment; maximum contingency, maximum take-off, maximum continuous, and idle. At take-off the engines operate at maximum take-off, at climb and level flight engines are operating at

maximum continuous rating, and for descent and landing engines operate at idle rating. $tsfc$ depends on the thrust of the engine and its throttle setting. At idle, turbojet and turbofan engines are not efficient since they are designed to be operated at higher temperatures and air flows, so the $tsfc$ is increased by a factor of 1.378 [27]. The available engine thrust at altitudes varies with the speed of the aircraft; and, the pressure ratio and is calculated from [72]:

$$Turboprop \quad T_A = T_0 e^{(-0.0099V)} \quad (26)$$

$$TurboJet \quad T_A = T_0 \left[1 + \frac{\gamma - 1}{2} M^2 \right]^{\gamma/(\gamma-1)} (1 - \sqrt{90.25}M) \quad (27)$$

$$TurboFan \quad T_A = T_0 \left[1 + \frac{\gamma - 1}{2} M^2 \right]^{\gamma/(\gamma-1)} (1 - \sqrt{90.25}M)(1 - (0.1 \cdot BPR \cdot M)) \quad (28)$$

3.3.2. Naval Architecture Theory

The design method of an amphibious aircraft implemented uses a wide variety of methods in order to compare and maximize the desire results fulfill from the 5 points in the conceptual design section. Since this amphibian aircraft must excel in both hydrostatic and hydrodynamic, it was first calculated the use of a conventional boat hull with stabilizers and compare with a more advance design method that could exceed the water characteristics.

3.3.2.1. Geometry Calculations

The primary functions of any floating device is to give the amphibious aircraft buoyancy, and to provide longitudinal and transverse stability on the water and when underway to takeoff speeds. The float or hull must provide reasonable resistance while in the water so that the aircraft is capable of taking-off with the power it has available. It must also be designed in such a way so as to hold landing impact pressures to reasonable levels. All of these factors can drastically change the form of the floating device.

First, in order to find the necessary calculations for the geometry of the floating device, fundamentals of Archimedes Principle must be understood. The volume (V) required for the seaplane to stay afloat on water is calculated based on the displacement weight (Δ_0), as shown in eq. (29).

$$U = \frac{\Delta_0}{w} \quad (29)$$

Calculation of the total volume of the floating device should take into account an extra 100% of the total displacement, which represents the “reserve of buoyancy” [44]. Based on the literature review, generally the beam is established as the design reference parameter of seaplane floats and hull [35].

From fluid dynamics, Tomaszewski came with an empirical formula on how to calculate the beam (b) of a hull based on a beam load coefficient (C_{Δ_0}) [35]:

$$b_h = \sqrt[3]{\frac{\Delta_0}{C_{\Delta_0} w}} \quad (30)$$

However, this empirical formula is well adapted to conventional floats and boat hulls, but not for an advance floating device concept such as a trimaran. A new approach was then manipulated

in order to find suitable formulas for the design process of the floating device. The key characteristic connection between length and beam of a boat hull is the slenderness ratio (*SLR*) shown in eq. (31).

$$SLR = \frac{L_h}{b_h} \quad (31)$$

The slenderness ratio takes values depending upon the functional utility of the vessel in question.

An important component of designing a hull or float is the forebody length. The size of the forebody represents compromising between flight requirements and seaworthiness at low speeds on water. If the length and the beam are too great, the structural weight and the aerodynamic drag limits the performance of the whole seaplane. On the other hand, if the length and the beam are too short, the spray characteristics become a limitation in gross weight and increase the hazards of operation in rough water [65]. The forebody length (l_f) in terms of a beam for a given beam load coefficient (C_{Δ_0}) is [35]:

$$l_f = b_h \sqrt{\frac{C_{\Delta_0}}{k}} \quad (32)$$

From hydrodynamic point of view, the afterbody (l_a) assists getting over the hump and to provide buoyancy at rest. A relation between the length of the forebody and the afterbody is shown in eq. (33) [38]:

$$l_a = (110\% - 115\%)l_f \quad (33)$$

Since the total length (L) of the hull or float is as follows:

$$L_h = l_f + l_a \quad (34)$$

Rearranging eq. (32) to static beam load coefficient (C_{Δ_0}) as a function of forebody length (l_f) the following was obtained:

$$C_{\Delta_0} = k \left(\frac{l_f}{b_h} \right)^2 \quad (35)$$

Choosing 111% of forebody to afterbody length from eq. (33) and plugging l_a to eq. (34), the total length is now:

$$L_h = 2.11l_f \quad (36)$$

Substituting eq. (36) to eq. (31) and rearranging:

$$\frac{l_f}{b_h} = \frac{SLR}{2.11} \quad (37)$$

Plugging eq. (37) to eq. (35), and substituting the result to eq. (30), the final empirical equation for calculating beam was obtained:

$$b_h = \sqrt[3]{\frac{\Delta_0}{k \cdot w} \left(\frac{SLR}{2.11} \right)^2} \quad (38)$$

The only two unknown variables are spray coefficient (k) and slenderness ratio (SLR). Spray coefficient can be selected depending on the mission characteristics shown in Table 5.

Table 5: Spray Coefficient Factors

| | |
|--------------|----------------------------|
| $k = 0.0525$ | Very Light Spray |
| $k = 0.0675$ | Satisfactory Spray |
| $k = 0.0825$ | Heavy but acceptable Spray |
| $k = 0.0975$ | Excessive Spray |

The standard values of slenderness ratio are shown in Fig. 32.

| | | |
|-----|----------|---------------------------|
| SLR | 8-10: 1 | For slow cruising vessels |
| | 12-14: 1 | For performance cruisers |
| | 20: 1 | For extreme racers |

Fig. 32: Slenderness Ratio

Selecting the appropriate spray coefficient (k) and slenderness ratio (SLR), the beam of the hull (b) can be calculated from eq. (38). With the slenderness ratio (SLR) selected and the beam hull calculated, the total length of the boat hull (L) is calculated using eq. (31). However, there is a constraint in calculating the hull length. The hull length should not exceed the length of the landplane fuselage. The afterbody and forebody of the hull are calculated using equations (34) and (36), respectively. With the dimension of the beam hull, other characteristics of the hull can be calculated (Bow Height, Forebody Deadrise Angle, Step Height, etc.). Empirical formulas for the calculation of these characteristics are shown in Appendix A.4.

Most amphibious aircraft that use a boat hull as their primary water operation method must augment their transverse stability through auxiliary means. A method used to increase the transverse stability of a boat plane without the drastic measure of greatly increasing the beam is the used outboard wing-tip floats mounted on either side of the fuselage (Fig. 33) or even in the mid section of the wing.

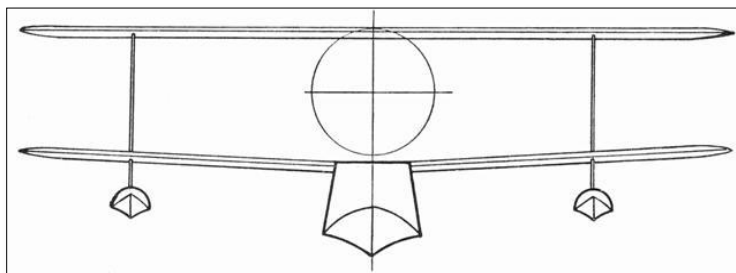


Fig. 33: Wing Tip Floats [42]

The Federal Aviation Administration [66] has specified a required buoyancy for any lateral stabilizing floats by mandating that the righting moment provided by a float when fully submerged be greater than [42],

$$M_R = C_{RM} \cdot GW(GM + \sqrt[3]{GW})\sin\theta \quad (39)$$

C_{RM} is the righting moment coefficient ($C_{RM} = 0.75$), and θ is the angle of heel required to completely submerge a lateral float. Based on the literature review [66], the angle of heel should not exceed 7° .

The buoyancy required is found by dividing the righting moment by the distance from the center of gravity of the lateral stabilizing float to the center of the fuselage.

$$\Delta_{stabs} = \frac{M_R}{l} \quad (40)$$

Then, the breadth or beam of the stabilizing floats, b_{stabs} , is calculated using eq. (41)

$$b_{stabs} = \sqrt[3]{\frac{\Delta_{stabs}}{2}} \quad (41)$$

where Δ_{stabs} is the displacement of one stabilizing float. The ratios for the length and depth to the breadth are given by Langley [42], with the length being 4 times the breadth and the depth being 0.5 times the breadth.

The second part of the research focused on the study of the advance seaplane design. Then a trimaran configuration was introduced to compare the effects it produces to the design. In order to maximize the efficiency of the trimaran concept, the outriggers (floats) should be half the length of the main hull [36]. Therefore, with slenderness ratio (SLR) selected, the beam of the outriggers can be calculated from eq. (31). The same approach as the main hull applies to calculate the rest of the outrigger characteristics.

3.3.2.2. Weights

Using the initial Gross Weight (GW) of the aircraft, the weight of the boat hull and floats is calculated using Langley's experimental testing. Calculation of Float Weight (W_f) was elaborated using a comparative curve of area and streamline forms [64], in which the following equation was derived:

$$W_f = 0.0365GW + 43.5 \quad (42)$$

Langley calculates the weight of the boat hull (W_{bh}) and wing-tip floats based on statistics using materials from 1935. The empirical relationships [64] are shown as follows:

$$W_{bh} = 0.12GW \quad (43)$$

$$W_{WT} = 0.012GW \quad (44)$$

With the introduction of new materials such as composites, the weight parameters of the floating device components could be reduced. Most composite materials have a density of around 1.60 g/m^3 , as compared to most aluminum alloys 2.8 g/m^3 . Since Langley based his equations of weight [(42) and (43)] from aluminum materials, then it can be assumed that these equations can be reduced by 50%. The added weight of the boat hull and floats will

increase the empty weight of the aircraft, reducing payload weight. The new empty weight of the seaplane (EW_s) is calculated as follows:

$$EW_s = EW_l + nW_f + W_{bh} + nW_{WT} \quad (45)$$

3.3.2.3. Hydrostatic Stability

As explained before, amphibian aircraft use auxiliary devices to maintain hydrostatic stability. To properly understand the reason for this lack of transverse stability, it is necessary to explain the concept of the transverse metacenter. The transverse metacentric height (GM) is the distance between the center of gravity (CG) and the transverse metacenter (M).

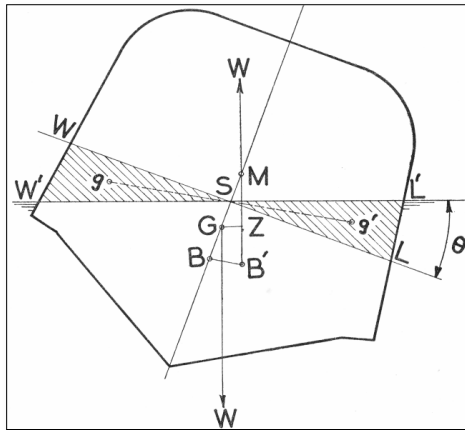


Fig. 34: Transverse Metacentric Height [45]

Fig. 34 shows the center of gravity of the hull is located at point G . The center of buoyancy is located at point B . If the metacenter is above the center of gravity, the aircraft is stable. If the metacenter coincides with the CG , the aircraft is in neutral stability. If the metacenter is below the CG , the aircraft is unstable. The derived formula for the reduction in metacentric height (BM) on water is [45]:

$$BM = \frac{I}{U} \quad (46)$$

To calculate the metacentric height (GM), the following expression is used [67]:

$$GM = BM - BG \quad (47)$$

BG is the distance between the Center of Buoyancy CB and the CG . Location of the CG and CB was elaborated with the aid of the SOLIDWORKS mass properties analysis. The metacentric height is an approximation of the vessel stability for small angle (0-15 degrees) of heel. Beyond that, the stability of the vessel is dominated by what is known as the righting moment (RM):

$$RM = \Delta_0 GM sin\theta \quad (48)$$

3.3.2.4. Water Resistance

In order to attain a desirable water performance the seaplane must be able to outstand in its water operation, especially at takeoff. The thrust available generated by the engines must overcome the water resistance caused by the floating device.

To calculate the water resistance (R_w) the following equation is used:

$$R_w = \frac{1}{2} C_{R_w} w A V^2 \quad (49)$$

where C_{R_w} is the coefficient of water resistance. The coefficient of water resistance is divided into coefficient of viscous resistance and wave coefficient expressed as follows:

$$C_{R_w} = C_v + C_w \quad (50)$$

Viscous resistance (C_v) is the resistance caused by the friction between the fluid and the object, in this case the floating device, in which factors such as velocity, geometry, and dynamic viscosity are taken into account. It is a function of Reynolds Number and is equated as followed:

$$C_v = (1 + K) C_{fv} \quad (51)$$

and

$$C_{fv} = \frac{0.075}{(\log(Re) - 2)^2} \quad (52)$$

Wave coefficient (C_w) is the resistance of water to the movement of the body across the formation of waves as shown in Fig. 35 and is obtained from water tank tests. Wave coefficient is a function of Froude Number. For simplicity, it was assumed to use a wave coefficient 60% of the total value obtained for the viscous resistance [67].

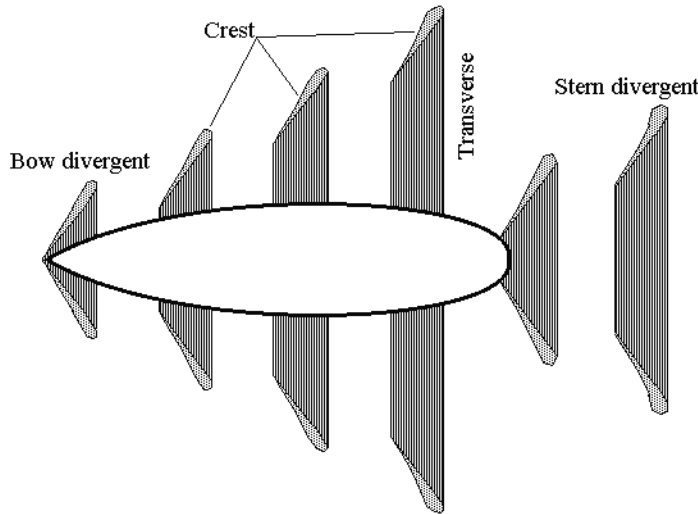


Fig. 35: Wave Making Resistance [67]

3.3.2.5. Water Landing Requirements

FAR 23 and FAR 25 requires the following load factors using empirical formula [66]:

$$n_w = \frac{C_1 V_{s0}^2}{\tan(\beta)^{\frac{2}{3}} G W^{\frac{1}{3}}} \quad (53)$$

The load factors required by FAR 23 and FAR 25 should not exceed 2. β is the deadrise angle. Example image of deadrise angle is shown below:

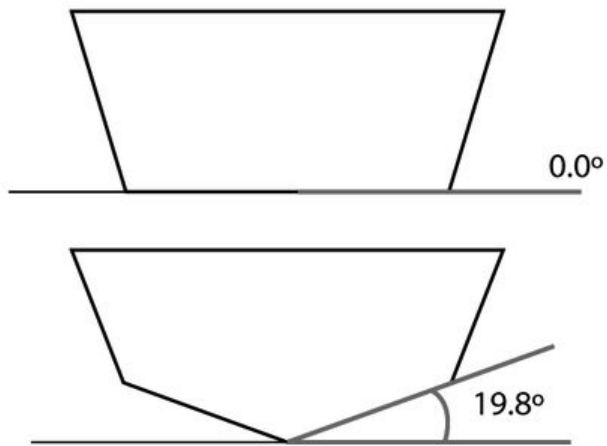


Fig. 36: Deadrise Angle [67]

4. Results

4.1. Landplane Results

One of the main problems seaplanes have during its water operation manoeuvres is the corrosion of the components (wing, stabilizers, etc.) caused by the excess in spray. For this instance, the conventional design elaborates a seaplane with a landplane structure that uses a high wing profile, with the engines mounted on the wing, instead of using nacelles and a T-tail configuration to avoid water spray. A high wing configuration gives the aircraft a greater visibility, no ground effect, it uses light structure, it has a greater wing and propeller clearance, and it is convenient for boarding.

In order to meet desire results, a mission profile is first set in order to size the amphibian aircraft. The mission profile complies with a mid-range size, subsonic aircraft, payload capability of around 1,400 kg for passenger capacity, or to carry water for used as water bomber, a range of around 1,000 km, and engines with Short Takeoff or Landing (STOL) capability. The use of Short Takeoff and landing gives the aircraft more options where to land, especially in bodies of water that are short such as lakes or ponds. Using the LOTS code and the equations from the theory section, the following landplane was sized.

4.1.1. Geometry

The geometry of the aircraft was calculated using eqs. (1) - (6), and the guessed GW , AR , and W/S . The following table shows the principle geometrical results of the landplane aircraft obtained. Some parameters were chosen for simplicity of the model. Extensive research on the selection of wing thickness, taper ratio, and other aspects must be paid much attention. A CAD (Computer Aided Design) Model of the typical landplane aircraft was created in SOLIDWORKS with the dimensions obtained from Table 6 shown in Fig. 37.

Table 6: Geometrical Parameters of Landplane

| Parameters | |
|------------------------------------|-------|
| Gross Weight [kg] | 6,600 |
| Wing Loading [kg/ m ²] | 190 |
| Aspect Ratio | 10.4 |
| Wing Area [m ²] | 34.86 |
| Wing Span [m] | 19.08 |
| C_{Lmax} | 1.63 |
| Fuselage Length [m] | 14.47 |
| Fuselage Diameter [m] | 1.92 |
| Taper Ratio | 0.44 |
| Wing Root Chord [m] | 1.12 |
| Horizontal Tail Span [m] | 1.8 |
| Vertical Tail Span [m] | 3.31 |

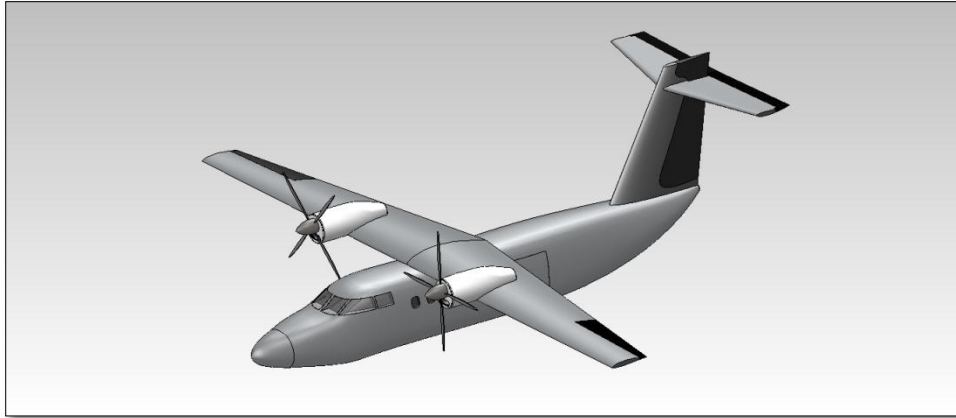


Fig. 37: 3-D CAD Model of Conventional Landplane Aircraft

4.1.2. Empty Weight

The next step is calculating the weight of the aircraft. Elaboration of the empty weight breakdown is done using the equations from Appendix A.1, the following table showing the weight of each calculated component was elaborated (Table 7).

Table 7: Empty Weight Breakdown (Landplane)

| Component | Weight [kg] |
|------------------------------|--------------------|
| Wing | 840 |
| Fuselage | 1350 |
| Horizontal Stabilizer | 270 |
| Vertical Stabilizer | 320 |
| MLG | 190 |
| NLG | 50 |
| Engines | 625 |
| Fuel System | 40 |
| Equipment | 215 |
| Total | 3900 |

4.1.3. Aerodynamic Drag

From eq. (10), drag is broke into induce, parasite and wave drag. The induced drag was calculated using eq. (11). A flat plate drag area breakdown of each of the aircraft components (fuselage, wing, etc.) was elaborated to calculate the parasite drag of the aircraft using eq. (18). A detailed explanation of flat plate drag area is shown in Appendix A.2. The effects of wave or compressibility drag are neglected since the aircraft is travelling at low subsonic speed ($M < 0.5$). With the following stated, a graph shown in Fig. 38 is created to show the drag curves. It is seen the minimum drag is 4,841 N at a speed of 72 m/s, which is the efficient speed.

Engine modeling is a key characteristic not only to obtain desired air performance but to calculate the thrust power necessary for water takeoff. The LOTS code has the option of choosing a Turboprop, Turbofan, or Turbojet engines. In order to decide which type of engine to choose, first thrust curves were elaborated to observe the trend between the available thrust of each engine with the thrust required of the landplane. It was decided to use a total of 25,500 N of Static Sea Level Thrust that meets the mission profile. The thrust required and thrust available

curves were plotted (using eqs. (19), (26), (27) and (28)) in order to decide which type of engine to choose.

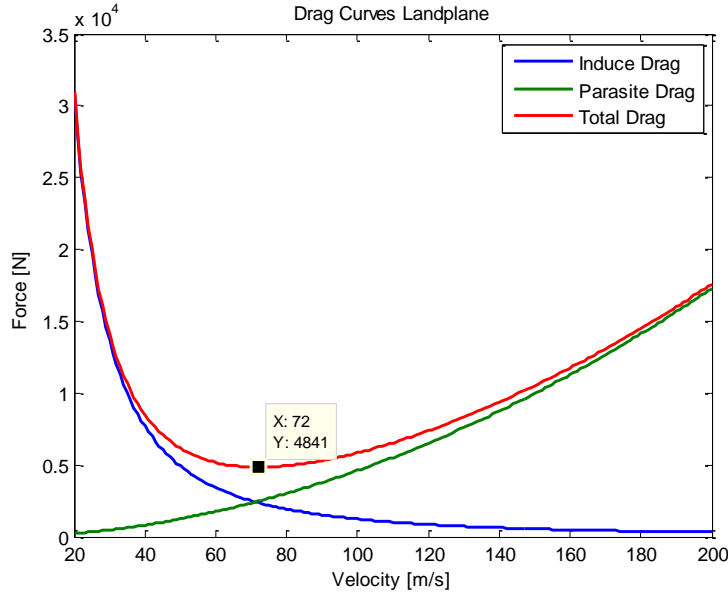


Fig. 38: Drag Curves (Landplane)

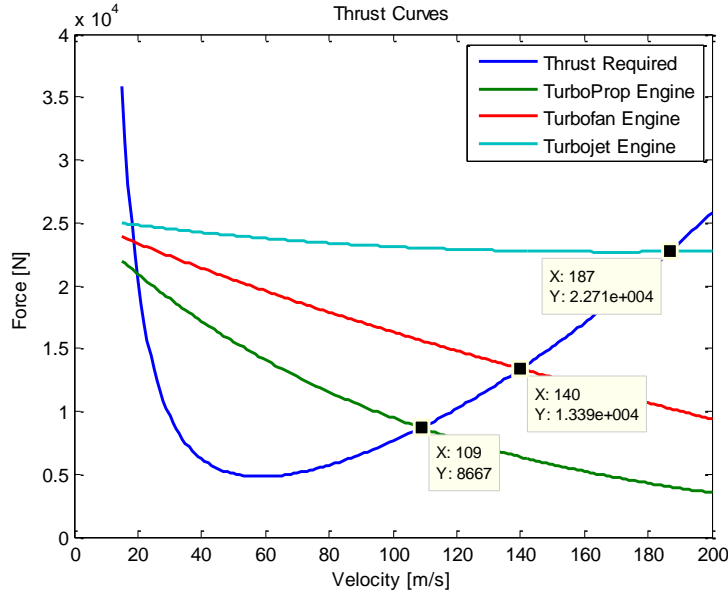


Fig. 39: Thrust Curves (Landplane)

At first, it was thought to use a turbofan engine. The initial thrust available was not powerful to overpass the water resistance making water takeoff difficult. In the end, with the use of high lift devices to increase C_{Lmax} , and using 2 turboprop engines instead, made it possible for the aircraft to meet the required mission profile of both air and water performance, succeeding in every requirement satisfactory. The point where the two curves meet shows the maximum speed of the aircraft at sea level. Fig. 39 shows a maximum speed of 140 m/s with a force of 13,390 N, for the turbofan engine with Bypass Ratio (*BPR*) of 10, while the turboprop has a maximum speed of 109 m/s with a force of 8,667 N.

Using eq. (20) and the C_{Lmax} provided, the Stall speed of the aircraft at sea level is 43.13 m/s.

The maximum coefficient of drag was calculated by assuming the landplane was cruising 90% of the maximum speed at a cruising altitude of 4,200 m. Table 8 shows the flat plate drag breakdown of the landplane to obtain parasite drag. Calculations of induced drag as well as compressibility drag (which is neglected) are also shown.

Table 8: Flat Plate Drag Area Breakdown (Landplane)

| Flat Plate Drag Area [m²] | Aircraft |
|---|-----------------|
| <i>Fuselage</i> | 0.152 |
| <i>Wing</i> | 0.323 |
| <i>Horizontal Tail</i> | 0.079 |
| <i>Vertical Tail</i> | 0.056 |
| <i>Engines</i> | 0.101 |
| <i>Upsweep</i> | 0.389 |
| <i>Total</i> | 1.154 |
| Drag | |
| C_{dp} | 0.033 |
| C_{di} | 0.0095 |
| C_{dw} | 5.3e-008 |
| C_d | 0.043 |

4.1.4. Flight Performance

The air performance of the aircraft must be analyzed in order to observe if the landplane meets the requirements stated in the mission profile. The flight performance of the aircraft was calculated with the obtained maximum speed (109 m/s). A cruise speed 90% of the total maximum speed was assumed to calculate the flight performance of the landplane aircraft in order to obtain an efficient mission in which compromising the excess caused by the increase in drag due to the maximum speed.

The climb speed (V_c) of the aircraft was calculated using eq. (21). It was found the aircraft has a maximum V_c of 6.6 m/s at sea level and a V_c of 2.8 m/s at cruising altitude of 4,200 m. Assuming a linear relation between V_c and altitude (H), a curve of V_c vs. H was plotted in order to obtain the service and absolute ceilings of the aircraft shown in Fig. 40.

The absolute ceiling of the aircraft is shown to be 6,721 m at a V_c of 0.5 m/s. The service ceiling is 7,273 m at $V_c = 0$ m/s. With the service ceiling, the maximum speed, and stall speed of the aircraft, an altitude envelope was created, Fig. 41. An altitude envelope generally shows the relation between speed at level flight and altitude although other variables are also possible. It takes more effort to make than an extra power calculation, but in turn provides much more information such as ideal flight altitude. The plot typically looks something like an upside-down U and is commonly referred to as a doghouse plot due to its resemblance to a doghouse.

The outer edges of the diagram, the envelope, show the possible conditions that the aircraft can reach in straight and level flight. For instance, this aircraft can fly at altitudes up to about 7,000m, at which point some external influence means it can no longer climb. The aircraft can also fly at up to Mach 0.32 at sea level, but no faster. This outer surface of the curve represents the zero-extra-power condition. All of the area under the curve represents conditions that the plane can normally fly at, for instance, this aircraft can fly at Mach 0.45 at 7,000 m, and doing so

would require something less than full power. Flying outside the envelope is possible, since it represents the straight-and-level condition only. For instance diving the aircraft allows higher speeds, using gravity as a source of additional power.

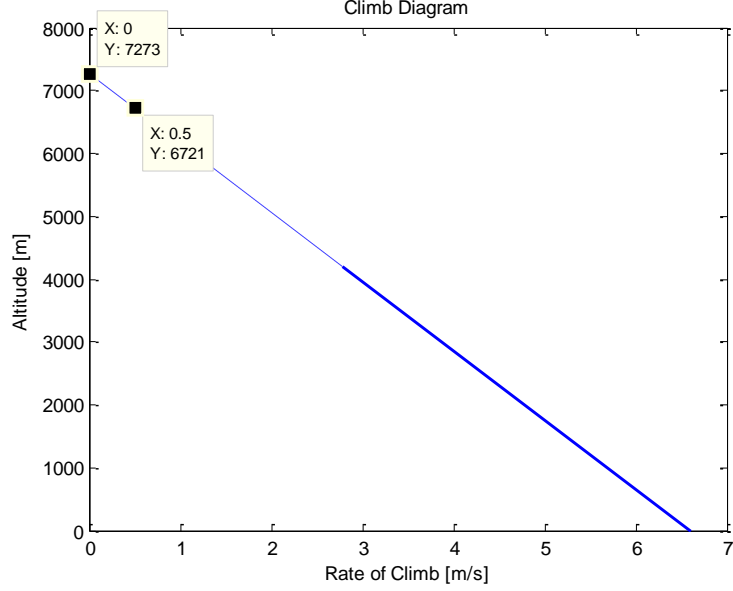


Fig. 40: Landplane Climb Diagram

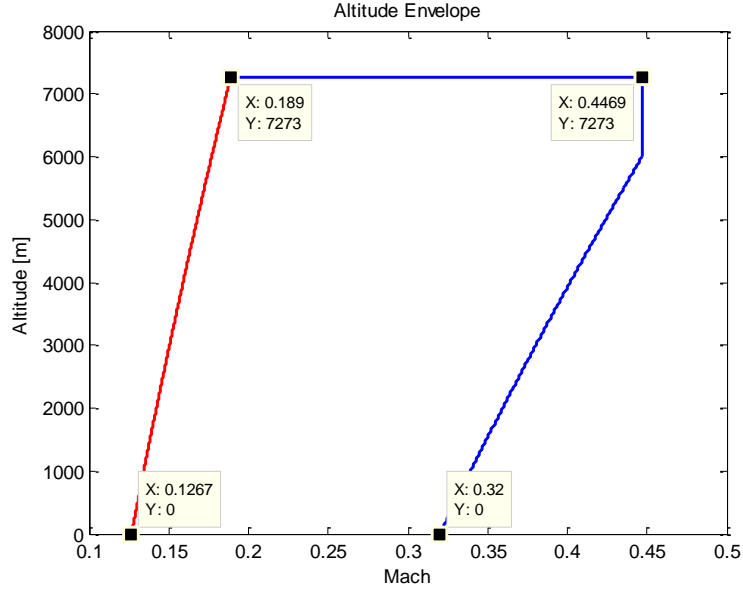


Fig. 41: Altitude Envelope of Landplane

Next, calculations of the range and endurance of the aircraft were performed. The aircraft must be able to have a range of around 1,000 km. To calculate the range and endurance, every segment of the mission (takeoff, climb, cruise, descent, and landing) was calculated.

Several assumptions are taken into consideration to calculate each flight segment. The landplane is designed with high lift devices (flaps), then it is assumed an increase in C_L at takeoff, hence an increase in C_D . The landplane takes off at $1.2 \cdot V_{S0}$ and a friction coefficient of 0.03 was considered for dry concrete. Last, an increase in drag due to the landing gear extended

was also considered. For descent, a descent angle of 3° was used. Finally, for landing the same assumptions for takeoff are taken into consideration. The same increase in C_D due to landing gear extended was considered. The increase in C_L and C_D due to high lift devices was used, however higher values due to full configuration were assumed. The same friction coefficient for dry concrete was used; however a new friction coefficient was introduced when the aircraft applied the brakes. Finally, the aircraft was designed with spoilers in order to decrease C_L , where C_D was also assumed to increase.

The elaboration of the mass fuel breakdown was elaborated based on the performance of the aircraft and the thrust available produced. The two turboprop engines producing a total of 25,500 N of static sea level thrust were enough to meet the mission profile. Calculation of the mass fuel weight was elaborated using eqs. (8) and (9). Since the amount of fuel needed for each flight segment depends on the amount of time and fuel consumption, eqs. (24) and (25) were used to calculate the amount of fuel consumption and selecting the appropriate throttle settling for each flight segment. Last, using the empirical equation of thrust available for a turboprop engine was elaborated using eq. (26).

With the assumptions considered, the amount of distance, time and fuel were calculated for each segment and are shown in Table 9. The cruise endurance and range of the aircraft were calculated using eqs. (22) and (23). The complete equations for calculating the mission segments are shown in Appendix A.3.

Table 9: Endurance and Range (Landplane)

| | Endurance [hr] | Range [km] | Fuel [kg] |
|-----------------|----------------|------------|-----------|
| Takeoff | 0.005 | 0.5 | 14 |
| Climb | 0.18 | 62.4 | 57 |
| Cruising | 2.81 | 992.3 | 1100 |
| Descent | 0.28 | 80 | 41 |
| Landing | 0.007 | 0.8 | 3 |
| Total | 3.28 | 1136 | 1215 |

The total fuel weight of the mission was 1,215 kg. Considering 75 kg for reserves and 10 kg for taxi manoeuvres, the total required mass of fuel is 1,300 kg. The estimated initial Gross Weight (GW_{est}) enter into the LOTS code was 6,600 kg, then the total payload for maximum fuel and using eq. (7) was 1,400 kg. The total payload the aircraft accounts for crew weight, avionics, cargo or passengers, etc. To account the aircraft is able to carry more payload than what was calculated (1,400 kg), it is assumed the aircraft has a capability to carry a maximum of 1,700 kg, for that instance reducing fuel weight to 1,000 kg.

A tradeoff between payload and range of the aircraft can be illustrated in a payload-range diagram. There are 3 factors to consider in a payload-range diagram. The top horizontal line shows the maximum payload that the aircraft is structurally permitted to carry. The vertical line represents the total range of the aircraft. Finally, the diagonal line after the range at maximum payload point shows how reducing the payload allows increasing the fuel (and range) when taking off with the maximum take-off weight. This diagonal line represents the tradeoff between maximum fuel and maximum payload. Smaller the diagonal line, smaller the tradeoff, therefore obtaining more productivity weight between payload and fuel. The payload-range diagram for this aircraft is shown in Fig. 42.

Finally, Fig. 43 shows the manoeuvring envelope of the landplane. The maximum positive load factor is 4.4 and the maximum negative load factor for dives is -1.76. These values are

obtained from FAR 23/25 for a utility aircraft. Fig. 43 also shows the gust envelope. The gust speeds are obtained from Raymer [27] and the maximum gust speed is a function of altitude only. As can be seen from the figure, the gust loads do not exceed the manoeuvring loads.

Since the LOTS code complies with all the mission requirements, final aircraft parameters and performance are given ending the iteration.

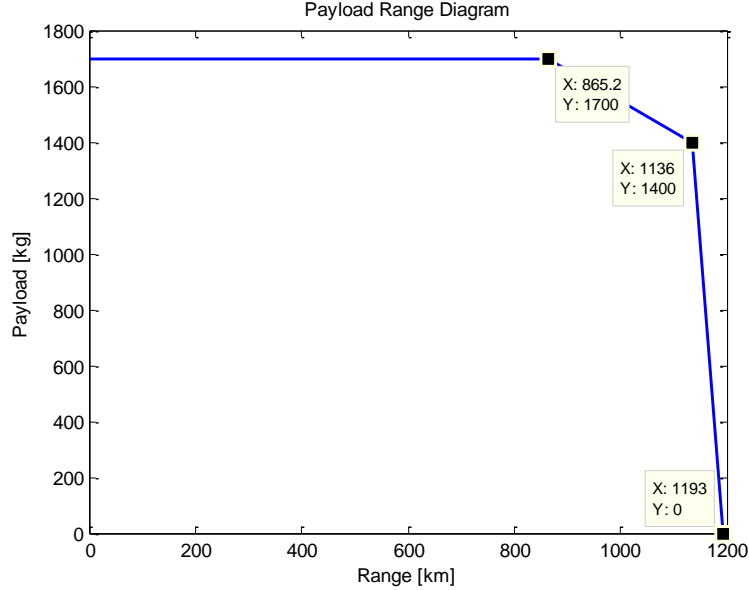


Fig. 42: Payload Range Diagram (Landplane)

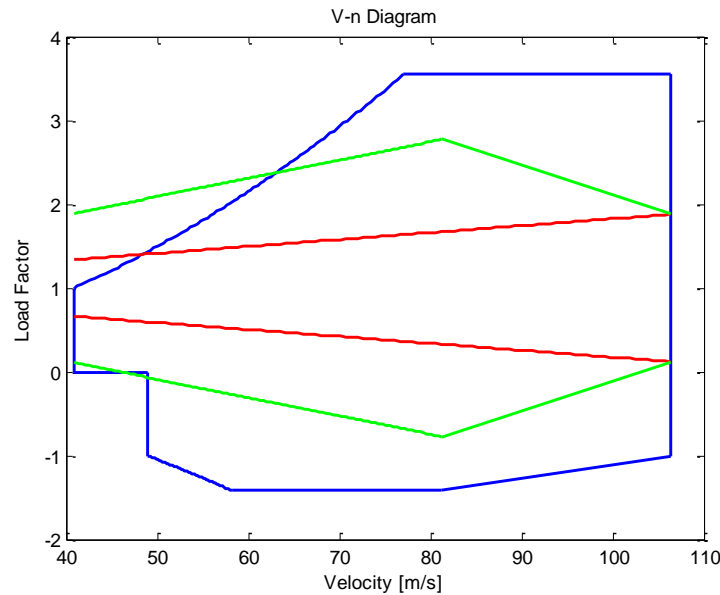


Fig. 43: Maneuvering and Gust Envelopes (Landplane)

4.2. Floating Device Results

After elaborating the landplane aircraft, the next step in the design is the elaboration of the floating device. The advance optimization code calls the FOTS code to iterate and optimize the most efficient floating device the seaplane should use. As explained, the FOTS code can elaborate a boat hull with wing tip floats, mid wing stabilizers, or side floats creating a trimaran configuration. The proposed solution is the integration of a trimaran design to the floating device. Therefore, in order to prove the advantage of the trimaran over other configurations, the results of the 3 design configurations are compared and analyzed.

4.2.1. Weight Breakdown

First, based on the FOTS code, the first step of the sizing iteration is the calculation of the weight components of the floating device. Based on eqs. (42) - (44), the following weights for the floating devices are found.

It is seen in Table 10, the weight increase of the seaplane with a trimaran configuration, mid wing stabilizers and wing tip stabilizers. For the trimaran, using maximum fuel, the payload decreased 400 kg. Comparing with wing tip floats, the payload weight reduced 300 kg, in which the difference is not excessive. In the end, the trimaran configuration shows larger empty weight compared to the other configurations. The reason is in the size of the stabilizers, in this case the outriggers. This increase in size depends on the hydrostatic and hydrodynamic performance of the seaplane, which is explained further in detail. The lost payload capacity of the trimaran can be recovered by the outriggers in which extra storage for fuel or luggage could be used.

Table 10: Weight Component Breakdown

| Weights [kg] | Landplane | Seaplane Trimaran | Seaplane Mid Wing | Seaplane Wing Tip |
|------------------------|-----------|-------------------|-------------------|-------------------|
| Boat Hull | 0 | 220 | 220 | 220 |
| Outriggers | 0 | 130 | 0 | 0 |
| Mid Stabilizers | 0 | 0 | 70 | 0 |
| Wing Tip Floats | 0 | 0 | 0 | 50 |
| Strutting | 0 | 50 | 60 | 30 |
| Empty Weight | 3,900 | 4,300 | 4,250 | 4,200 |
| Max Fuel | 1,300 | 1,300 | 1,300 | 1,300 |
| Payload | 1,400 | 1,000 | 1,050 | 1,100 |
| Gross Weight | 6,600 | 6,600 | 6,600 | 6,600 |

4.2.2. Geometry calculations

The next calculation done by the FOTS code is sizing the geometry of the floating device. Using the equations from the subsection of the geometry calculations from the theory section, sizing of the main hull, outrigger, mid wing stabilizer and wing tip stabilizer was elaborated. Table 11 shows the dimensions of each of the floating devices.

When the FOTS code is sizing the main boat hull of the aircraft, it checks if the length of the hull does not exceed the length of the fuselage, in this case 14.47 [m]. Finding a suitable Slenderness Ratio (*SLR*) is vital to attain the desire design. In first instance, the first guessed *SLR* used was of 12 to obtain a performance cruiser seaplane. Then, a suitable Spray Coefficient (*k*) equal 0.0825 to have heavy but acceptable spray was used. The FOTS code decided the most optimum *SLR* for the main hull was 7 with a *k* of 0.0975. One of the big issues the FOTS code

encountered to attain the desired sizing was to not exceed the fuselage length. If using a $SLR=12$, $k=0.0825$ and not exceeding the 14.47 [m] of fuselage length, the beam of the hull became excessively large, showing a bad aspect to the seaplane. In the end, the beam of the hull was 2.03 [m], which does not exceed the diameter of the fuselage, making an aesthetic design. To counteract the excess in spray, chines are placed at the edges of the hull to reduce this complication. In the end, the SLR and k used for the outriggers (14 and 0.08, respectively) are satisfactory to attain the desired design.

Some of the dimensions are calculated using the equations stated; however, the angles (afterbody, and keel) were selected based on the literature review [36], the aspect of the stabilizers, and other aspects that increased the optimization of the design. The forebody deadrise angle is obtained using eq. (53), from the FAR requirements. Then based on FAR requirements [66], the following curve was plotted to identify the desired forebody deadrise angle that meets the landing requirements shown in Fig. 44. To obtain a slender trimaran, the forebody deadrise angle of the main hull used was 30° , with a load factor of 1.716. For the outrigger, an angle of 45° was used, with a load factor of 1.19.

As explained before, the weight of the outriggers is larger compared to the stabilizers or wing tip float. The size of the stabilizers depends on the righting moment from eq. (39), and the clearance distance; With greater clearance distance, smaller stabilizers.

With the dimensions of the main hull, the outriggers, the stabilizers and the wing tip floats calculated, the new floating device was added to the landplane aircraft to create the seaplane. Fig. 45, Fig. 46 and Fig. 47 show the 3 different configurations of the seaplane.

Table 11: Floating Device Dimensions

| | Main Hull | Outrigger | Stabilizer | Wing Tip |
|----------------------------------|------------|------------|------------|------------|
| Slenderness Ratio | 7 | 14 | - | - |
| Spray Coefficient | 0.0975 | 0.08 | - | - |
| Beam [m] | 2.03 | 0.51 | 0.95 | 0.65 |
| Length [m] | 14.47 | 7.13 | 3.82 | 2.60 |
| Forebody [m] | 6.99 | 3.38 | 1.81 | 1.23 |
| Afterbody [m] | 7.48 | 3.75 | 2.01 | 1.37 |
| Bow Height [m] | 1.32 | 0.53 | 0.48 | 0.32 |
| Step Height [m] | 0.18 | 0.05 | 0.09 | 0.06 |
| Forebody Angle | 30° | 45° | 15° | 15° |
| Afterbody Angle | 22° | 40° | 20° | 15° |
| Keel Angle | 7° | 7° | 7° | 7° |
| Volume [m^3] | 17.43 | 1.51 | 1.74 | 0.55 |
| Clearance [m] | - | 1.74 | 3.00 | 9.54 |
| Stagger [m] | - | -0.90 | 2.25 | 2.25 |

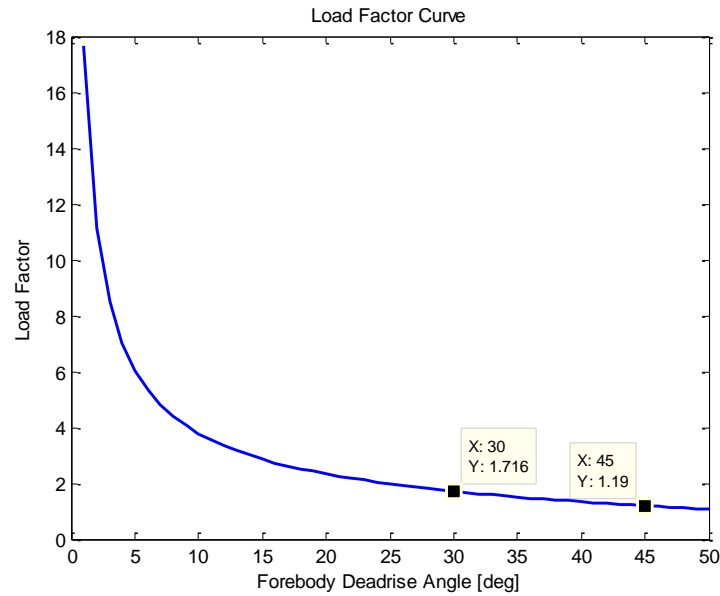


Fig. 44: Water Landing Load Factor Curve

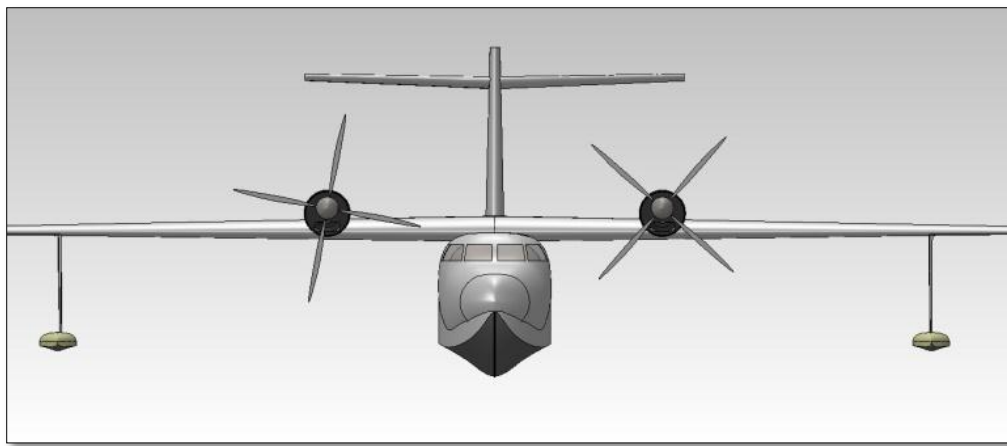


Fig. 45: CAD Model of Seaplane with Wing Tip Floats

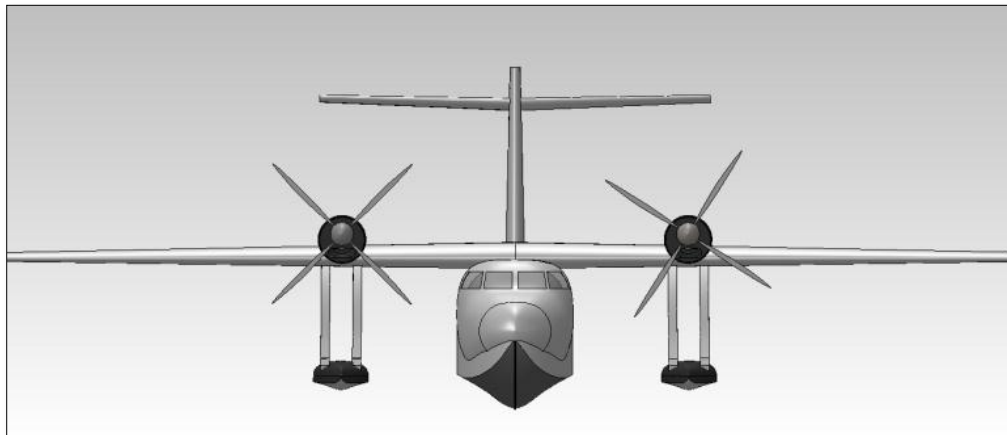


Fig. 46: CAD Model of Seaplane with Nacelle Support Stabilizers

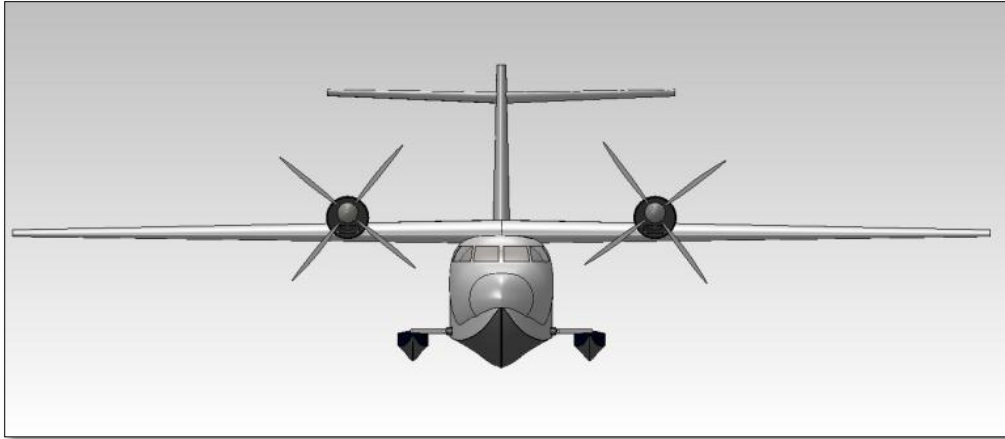


Fig. 47: CAD Model of Seaplane with Trimaran Concept

4.2.3. Hydrostatic Stability

The next goal of the FOTS sizing code is to meet the hydrostatic stability. Using the approach from eqs. (46) - (48) in the theory section, the following hydrostatic results were obtained. The center of gravity, center of buoyancy, metacentre and metacentric height are shown in Table 12. Using the approach from eq. (47), the metacentric height was calculated; The center of gravity was found using SOLIDWORKS mass properties analysis; the center of buoyancy was calculated by dividing the volume displacement over the water line area.

To show an example of the location of the metacentre (GM), center of buoyancy (CB), and the centre of gravity (CG), a model of a seaplane was elaborated shown in Fig. 48.

Using eq. (48), the data obtained from Table 12 and the required displacement of each component, the following plot was graphed showing the Righting Moment (RM) as a function of heel angle θ , in Fig. 49.

Table 12: Hydrostatic Stability (Seaplane)

| <i>Distance from Keel [m]</i> | Trimaran | Stabilizer | Wing Tip Float |
|-------------------------------|-----------------|-------------------|-----------------------|
| Draft Line | 0.48 | 0.48 | 0.53 |
| Center of Bouyancy | 0.45 | 0.45 | 0.51 |
| Center of Gravity | 1.75 | 1.84 | 1.84 |
| Metacentre | 1.61 | 4.13 | 17.93 |
| Metacentric Height | 0.32 | 2.75 | 16.60 |

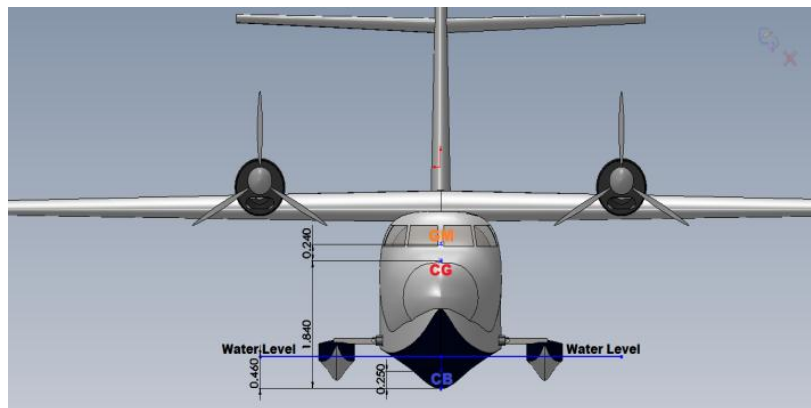


Fig. 48: CAD Model of Seaplane transverse Metacentre, Centre of Gravity, and Buoyancy

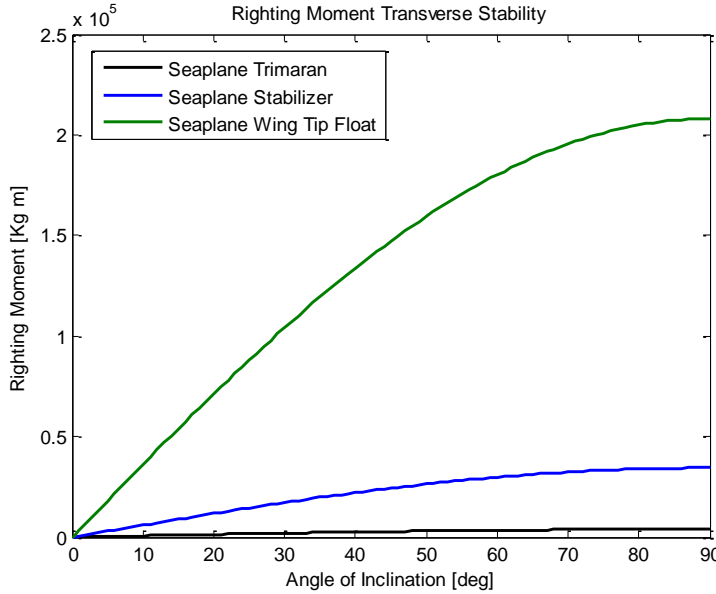


Fig. 49: Righting Moment Graph

Table 12 shows the trimaran as the most unstable method with the lowest metacentric height. Still, if the metacentric height remains positive, the vessel is statically stable. The method used to increase stability is the use of the retracted float system, and folding the wings. Most likely, for longitudinal stability, the seaplane tends to be very stable, especially as it gains speed, as compared to the same phenomena that occurs when riding a bike [44].

A hydrostatic analysis was performed in ORCA 3D to compare the results obtained from the FOTS code. Based on ORCA 3D, the maximum heel angle of the trimaran seaplane before overturning was calculated to be 12° . Using the retracted float system, the heel angle increased to 18° and with folded wings increased to 20° , proving the use of the retracted float system.

4.2.4. Water Takeoff Requirements

Next step is to compare the hydrodynamic characteristics of the seaplane by calculating the water resistance of the 3 different floating devices. To calculate the water resistance eq. (49) was used. Plotting water resistance (R_w) as a function of velocity, the following graph was obtained.

Fig. 50 shows the water resistance curves of the 3 floating device methods, and the available thrust generated by the engines. For comparison, thrust available curves of the turboprop, turbofan and turbojet were shown.

The curve starts at 0 speed, until reaching lift off speed, in the case of this seaplane lift off speed is around 45 m/s. Water resistance curve starts to increase due to wave propagations and water drag interference. The curve then forms a hump at its maximum peak. This peak is the point where the amphibian starts to separate from the water, therefore, if the engines do not generate enough thrust, the aircraft is not able to take off from water. The water resistance of the trimaran is less compared to the other devices shown. Clearly from the graph, the water resistance of the trimaran is lower than the thrust available curve of either of the engines and therefore, be able to takeoff. From the graph, resistance of mid wing stabilizers exceeds the thrust power of the turboprop engine. The coefficient of wave interference is larger for the mid wing stabilizer, than the trimaran or wing tip floats. As the body cruises through water, the body

creates waves along its path as shown in Fig. 35. Since seaplanes use lateral stabilizers and a main hull, the stabilizers as well as the hull create wave patterns along its way. The point where these two propagated waves collide generates a phenomena that increases the viscous drag of the seaplane. To reduce this point, the stabilizers must have a low clearance distance or very high as in the case of the trimaran and wing tip floats.

As explained before, at first instance, using turboprop engines with a sea level thrust of 25,500 N, did not generate enough thrust to overcome the water resistance. It was then assumed the aircraft uses high lift devices that increase the $C_{L_{max}}$ from 1.63 to 2.08.

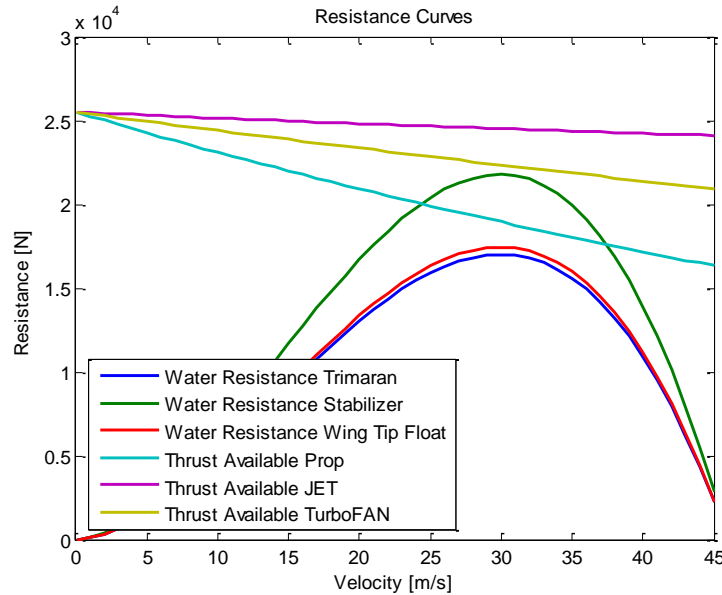


Fig. 50: Water Resistance Curves and Thrust Available

4.2.5. Aerodynamic Drag

Now it is essential to think on techniques to reduce the aerodynamic drag caused by the outriggers, stabilizers, or wing tip floats in order to increase the flight performance of the seaplane. A useful technique is to retract the floats into a position where the floats create a single body shape, either to the wing or the fuselage. The following images show how the floats were being retracted.

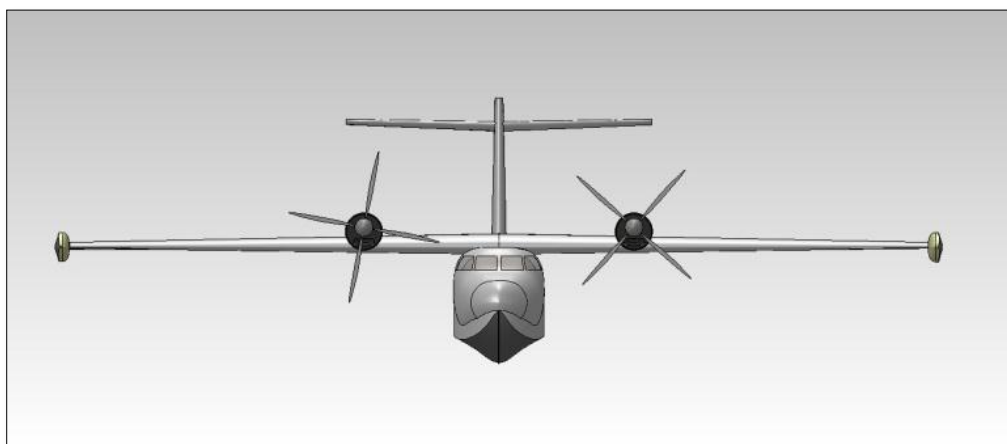


Fig. 51: Wing Tip Floats Retracted into the Wing Tip

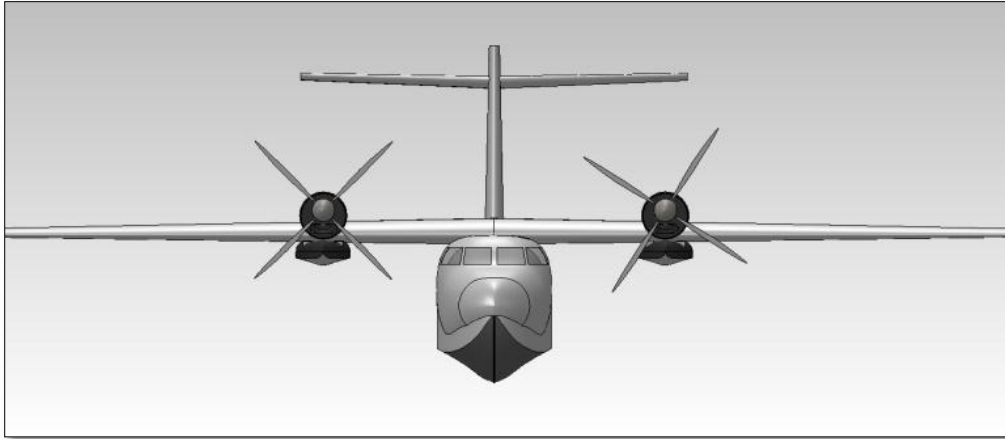


Fig. 52: Nacelle Wing Stabilizers Retracted

The strutting on the wing tip floats and stabilizers compromises some the wing structural support, and requires a complex retracting system with strong and heavy material required. This also compromises an excess in weight, reducing the useful weight the aircraft is able to carry. In the case of the trimaran, the strutting is placed through the boat hull, in which the boat hull and the entire fuselage are built as a single component of the aircraft, reducing the need for strong material used for the strutting. The outriggers are retracted into the boat hull, creating a “smoother” body that results for less aerodynamic drag, as shown in Fig. 53 [59].

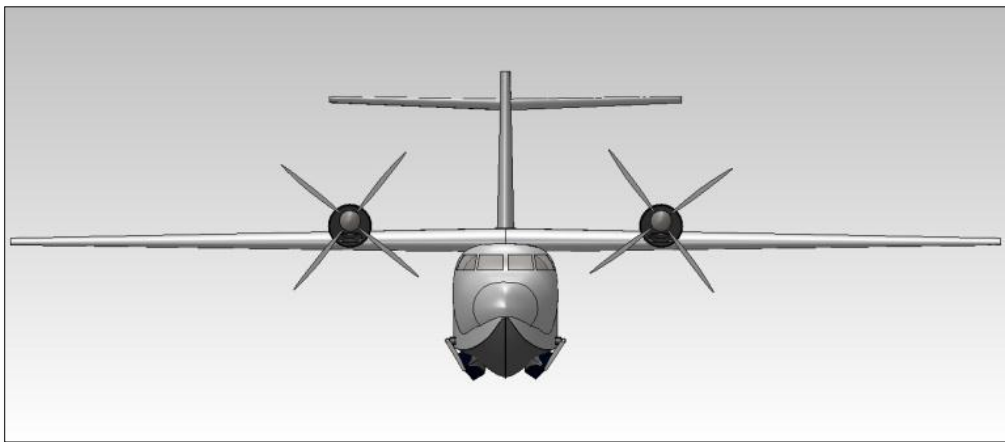


Fig. 53: Trimaran Outriggers Retracted unto the Boat Hull

The same approach to calculate the coefficient of drag for the landplane was applied to the floating device. It is explained when an odd shape component is being calculated, an increase in drag form interference factor must be added to the actual value [60]. It is also explained: “The form factor is a measure of how “streamlined” the component is; it is a function of the component thickness-to-length ratio” [68]. In this case, the form interference factor (F) of a flying boat hull must increase by a 50%, and for floats from 75%-300%, depending on the shape. In the end, the boat hull is designed as a smooth, slender body. Then, it was assumed that the interference factor for the boat hull had an increase of 10%, rather than 50% increased, due to the perfect aerodynamic shape mounted of the hull with respect to the fuselage. A comparison of the decrease in parasite drag for the floating devices in retracted position, and extended position is

elaborated theoretically in Table 13. Calculation of the parasite drag was done with a flat plate drag area breakdown of each of the 3 configurations for comparison.

As expected, the greatest increase in drag are the mid wing stabilizers. Wing Tip floats show the least increased in drag due to its small size compared to the other stabilizers, and the retractable system assembles the tip floats as wing tip tanks.

Table 13: Flat Plate Drag Area Breakdown Floating Devices

| Flat Plate Drag Area [m²] | Trimaran | | Mid Wing Stabilizers | | Wing Tip Floats | |
|---|-----------------|------------------|-----------------------------|------------------|------------------------|------------------|
| | Extended | Retracted | Extended | Retracted | Extended | Retracted |
| <i>Boat Hull</i> | 0.127 | 0.105 | 0.127 | 0.105 | 0.127 | 0.105 |
| <i>Stabilizer</i> | 0.075 | 0.051 | 0.09 | 0.072 | 0.044 | 0.034 |
| <i>Strutting</i> | 0.005 | 0.002 | 0.009 | 0.003 | 0.004 | 0.001 |
| <i>Total</i> | 0.185 | 0.158 | 0.204 | 0.18 | 0.153 | 0.14 |
| C _{dp} | 0.0059 | 0.0045 | 0.0065 | 0.0052 | 0.0050 | 0.0040 |

A comparison of the increase in parasite drag, with the landplane aircraft is made to show the increment in percent and the advantage of using the retractable system. Table 14 shows the values of the increase in parasite drag of the trimaran seaplane.

Another solution in solving the increase of drag is by retracting the floats inside the boat hull as explained earlier and shown in Fig. 26. There is nearly a 3% decreased in parasite drag compared to the floats in the retracted position.

Table 14: Flat Plate Drag Area Breakdown Trimaran Seaplane

| | Landplane | Seaplane [Extended] | Seaplane [Retracted] | Seaplane [No Floats] |
|----------------------------------|------------------|--------------------------------|---------------------------------|---------------------------------|
| Drag Area [m²] | 1.154 | 1.361 | 1.312 | 1.269 |
| C _{dp} | 0.033 | 0.039 | 0.038 | 0.036 |
| C _{dp} Increment | - | 0.006 | 0.005 | 0.003 |
| Drag Increase | - | 12.24% | 9.63% | 6.63% |

4.2.6. Flight Performance

With the increase in drag, new calculations of the flight performance for the seaplane were performed. Comparison of the landplane performance and the trimaran seaplane is made. The required thrust increases if the coefficient of drag increases (C_{Dp}), hence compromising the flight performance of the seaplane. Therefore, the maximum speed of the seaplane must decrease as shown in Fig. 54.

The maximum speed of the seaplane with floats extended at sea level decreased to 103 m/s. The thrust required increased due to the increase in coefficient of drag, therefore the rate of climb of the seaplane decreased. The seaplane with extended floats has a lower rate of climb, as compared to seaplane with retracted floats. The seaplane takes longer and more distance to climb the desire altitude, i.e. the absolute and service ceilings decrease as shown from Fig. 55.

The calculations of each of the flight segments for the trimaran seaplane take into consideration the same assumptions described for the landplane. The only difference is takeoff and landing in which the seaplane does not apply brakes; instead water resistance comes into action. For water takeoff, high lift devices increase the C_{Lmax}. Also, the increase in C_d due to the floating device is then added. At takeoff and landing, the C_d increase with the outriggers

extended is first used. At climb, cruise and descent, the outriggers are retracted, decreasing C_d . Table 15 shows a comparison of the endurance and range of the landplane, the seaplane with outriggers in retracted position, and seaplane with outriggers in extended position. As shown, there is an increase of around 100 km of the trimaran seaplane with the outriggers retracted, compared to the outriggers in the extended position.

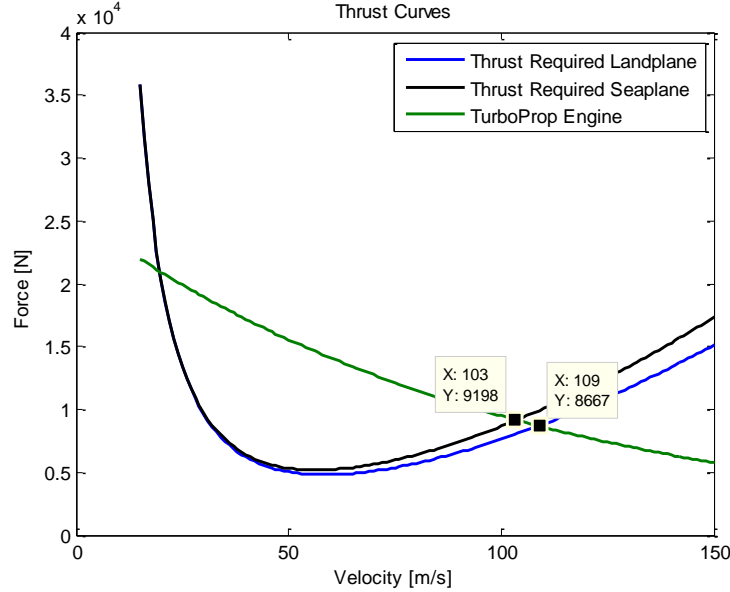


Fig. 54: Thrust Curves (Landplane and Trimaran Seaplane)

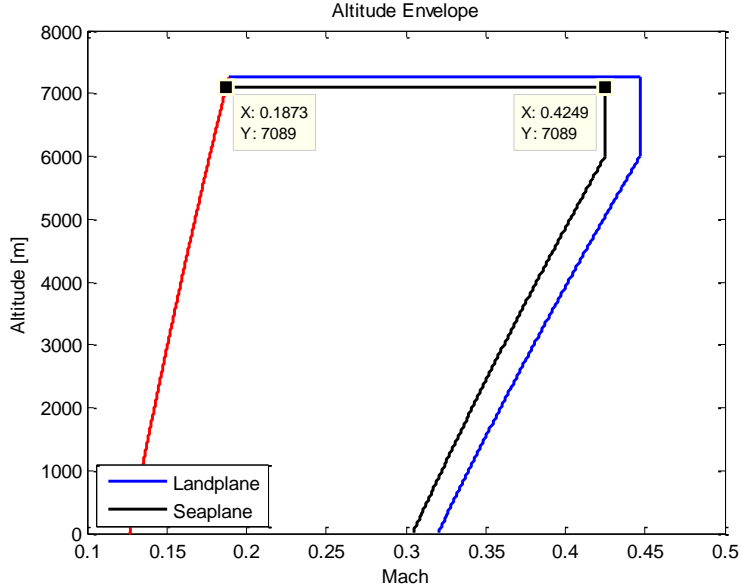


Fig. 55: Altitude Envelope (Landplane and Trimaran Seaplane [Retracted])

Table 15: Endurance and Range of each Flight Segment

| | Landplane | Seaplane [Rect] | Seaplane [Ext] |
|----------------|-----------|-----------------|----------------|
| Endurance [hr] | 3.28 | 3.11 | 2.88 |
| Range [km] | 1,136 | 1,017 | 933 |

With the weight parameters, endurance, and range, a payload range diagram was elaborated showing a comparison between the landplane and the trimaran seaplane, shown in Fig. 56. Last, Fig. 57 shows the manoeuvring and gust envelope of the trimaran seaplane. As in the landplane, the gust loads do not exceed the maneuvering loads. Finally, Table 16 shows the summary of both the landplane and seaplane performance parameters.

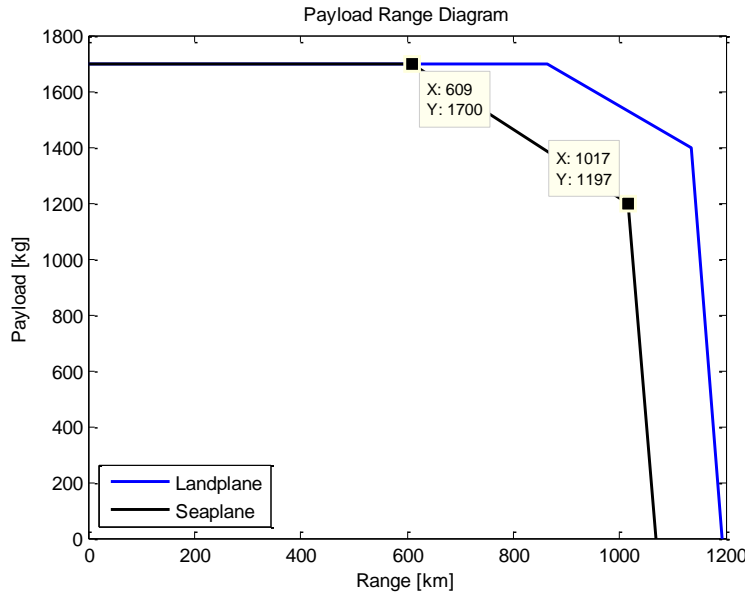


Fig. 56: Payload Range Diagram (Landplane and Trimaran Seaplane [Retracted])

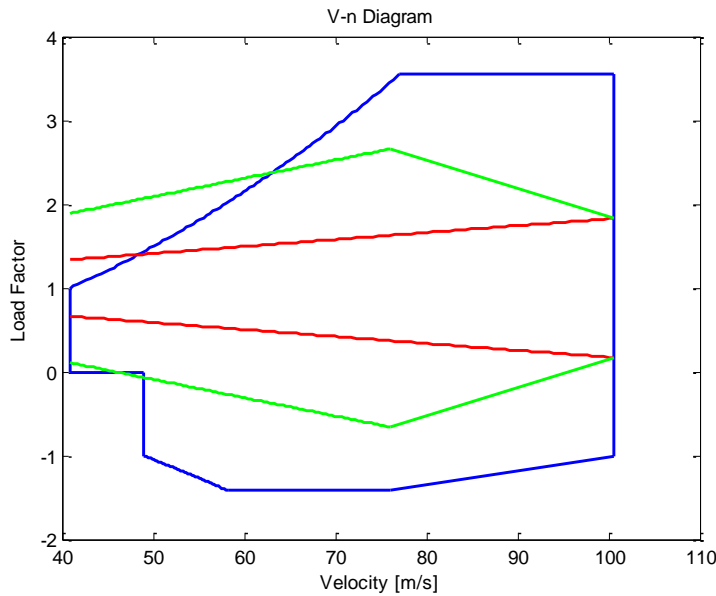


Fig. 57: Maneuvering and Gust Envelopes (Trimaran Seaplane)

Table 16: Summary of major design values (Landplane and Trimaran Seaplane)

| Parameters | Landplane | Seaplane |
|----------------------|-----------|----------|
| Gross Weight [kg] | 6,600 | 6,600 |
| Empty Weight [kg] | 3,900 | 4,300 |
| Max Speed [km/hr] | 392 | 370 |
| Rate of Climb [m/s] | 6.6 | 6.2 |
| Absolute Ceiling [m] | 7,273 | 7,089 |
| Endurance [hr] | 3.28 | 3.11 |
| Maximum Range [km] | 1,136 | 1,017 |

4.3. Design Analysis

4.3.1. SOLIDWORKS Computer Aided Design (CAD) Analysis

With the preliminary design of the amphibious aircraft finalized, a 3-D model was constructed using SOLIDWORKS. This model was used to analyze the center of gravity and center of buoyancy as well as to run Orca3D test cases. To obtain valid comparisons between the various analysis programs that were used to validate and improve the optimization code, it was very important to keep the 3-D model as true as possible to the final optimized design that was output by the sizing code.

While the output file specifies the exact geometry of boat hull, floats, and wing, it only provides general dimensions for the fuselage and engine, although the code does have relative positions for all the components. This means that these last two components must undergo detailed design not specified by the optimization code.

The sizing code output specifies the length, width and height of the boat hull fuselage of the aircraft, but does not specify any further details, such as the shape of the bottom of the forebody and afterbody. Both of these design factors affects the performance of the amphibious aircraft while it is on the water, especially in respect to its takeoff performance.

Some of the important aspects SOLIDWORKS performs are to identify the center of gravity of the model in the mass properties tool. This application calculates properties such as mass, density, and volume, based on the model geometry and material properties. This useful application was necessary to identify the center of gravity of the seaplane, and to compare the moments of inertia. With the center of gravity identified, it was useful to calculate the center of buoyancy of the model. The identified center of gravity and calculated center of buoyancy was compared to the identified centers elaborated by ORCA 3D.

An important concern that arises by placing a hull under a fuselage may be related to the structural force the fuselage must support. SOLIDWORKS performs basic structural analysis to analyze the stress and displacement of the model.

4.3.1.1. Results

SOLIDWORKS SimulationXpress offers an easy stress analysis tool for design analysis users. It performs a basic analysis of the effects of a force applied to a certain body of a model. For this case, a simple structural analysis of the boat hull was performed to analyze the impact the hull withstands at water landing.

SimulationXpress starts by identifying the body to analyze. In this case, the main hull is analyzed for water landing impact. Then, a fixture must be added. Applying a fixture keeps the

part from moving when loads are applied, though a face with fixtures are treated as perfectly rigid body, in which can cause unrealistic results. For this analysis, the fuselage is treated as the fixture, as shown in Fig. 58.

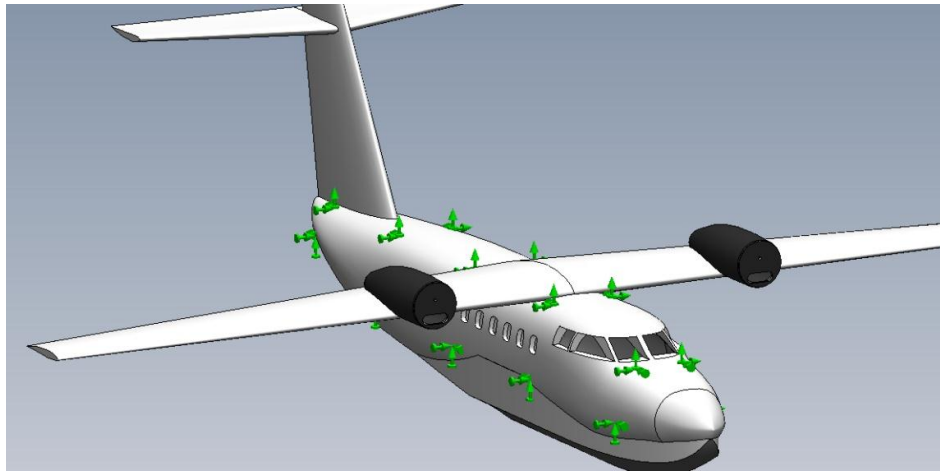


Fig. 58: Trimaran Seaplane Fuselage Fixture

Next, applying the force to the body (in this case the boat hull) must be selected. The total force applied was around 60,000 N, which is based on the Gross Weight at landing (6,200 kg). The force is applied at forebody of the hull since this is the main part of the hull that receives most of the landing impact, shown in Fig. 59.

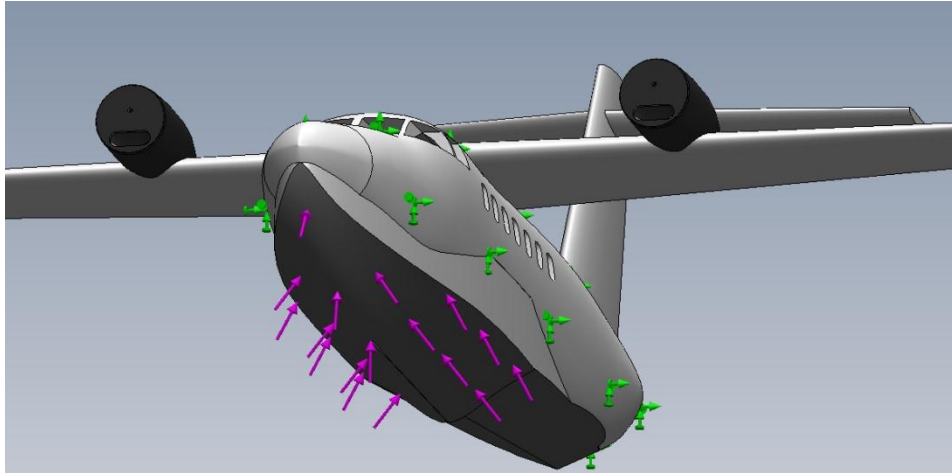


Fig. 59: Trimaran Seaplane Load Force at Afterbody Hull

The next step is to choose the material of the hull. It was decided to use composite materials, in this case Glass Laminate Aluminium Reinforced Epoxy (GLARE). This material is light, strong and has an advantage against corrosion. After selecting the fixture, the load and material, the simulation starts by meshing the model. SOLIDWORKS performs the meshing by the elaboration of Finite Element Analysis (FEA), which connects small pieces of the model called elements which then share common points called nodes. The example mesh figure of the trimaran seaplane is shown in Fig. 60.

Finally, the simulation performs a Von Mises Stress and a displacement analysis. The resultant action shows an image with the hull deformed. The image is a mere exaggeration just to visualize where the deformation is taken place. Most of the deformed body takes place around

the step of the hull. Since the seaplane must land in an angle, the deformation is found to be consistent to an actual realistic result. The maximum deformation encountered by the hull is of 4.5e-4 mm. Maximum Von Mises Stress is 0.052 N/mm² at the point shown in Fig. 61.

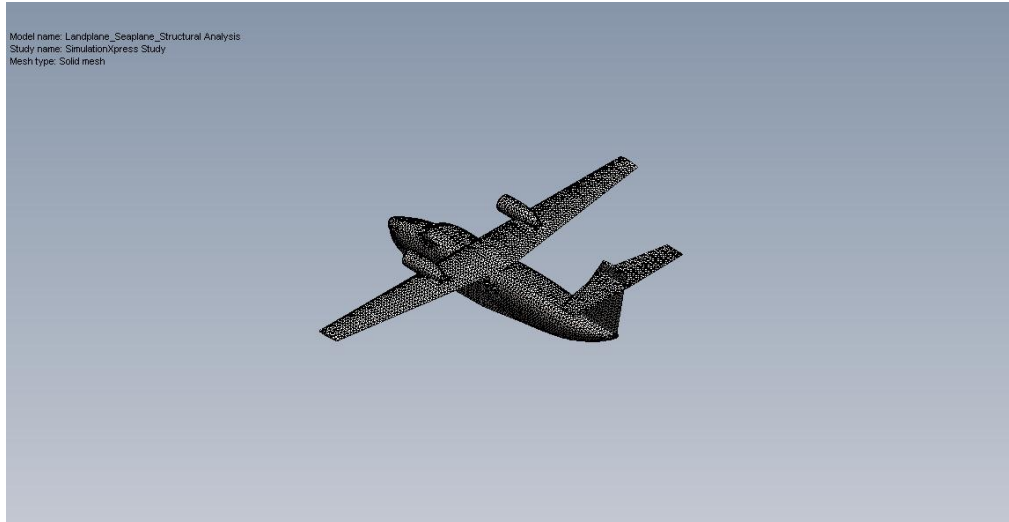


Fig. 60: Trimaran Seaplane Mesh

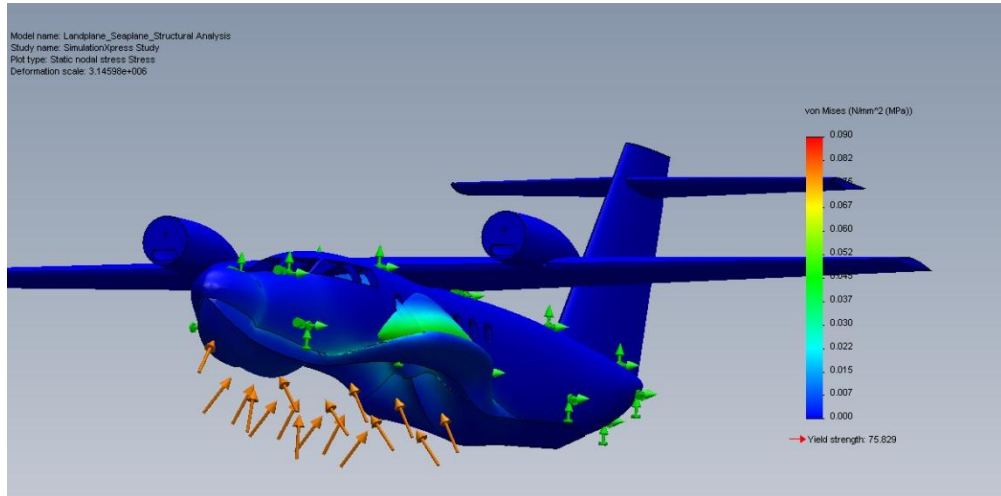


Fig. 61: Trimaran Seaplane Von Mises Stress Analysis

4.3.2. ORCA 3D

Orca3D is a suite of tools used for naval architectural design and analysis that were written as a plug-in for the Rhinoceros 3-D modeling software. For this research, Orca3D was used to determine if the amphibious aircraft that was output by the sizing code had satisfactory longitudinal and transverse stability in the water. The stability of the aircraft in water is determined by finding the location of the longitudinal and transverse metacenters.

Classically, Simpson's Rule was the primary tool used in designing boat hulls. Simpson's Rule is a method of numerical integration and is governed by

$$\int_b^a f(x)dx \approx \frac{b-a}{6} \left(f(a) + 4f\left(\frac{a+b}{2}\right) + f(b) \right) \quad (54)$$

Using this approximation, a designer could calculate the location of the longitudinal and transverse metacenters, as well as the center of buoyancy and center of floatation, of a boat hull being designed.

Computer aided hull design has been becoming more and more prominent in recent years, as it offers advantages over traditional design methods. A majority of CAD representations of a boat hull are curve-surfaces. Orca3D generates a mesh from this surface to calculate most of its hydrostatic and stability parameters. With a mesh created, Orca3D then uses Simpson's Rule to numerically integrate between the mesh nodes. This method of computer aided mesh generation and numerical analysis leads to more accurate results, as it doesn't rely on a manually calculated station model, which has a tendency to miss local hull features, such as discontinuities and curvature changes.

According to Sederberg [69], the de-facto CAD standard for representing curved surfaces since the 1970's has been the non-uniform rational B-splines (NURBS). NURBS are the only free-form surface type supported in the IGES file format, which is the most popular format for transferring data between CAD software. Unfortunately, NURBS have two weaknesses that impact hull design and analysis. First, to make hull optimization and analysis easier, it is helpful to have the entire hull represented with a single surface. Unfortunately, due to NURBS needing rectangular topography when making its mesh, a complicated hull cannot always be represented by a single surface. Secondly, control node points for a NURBS surface must lie in a rectangular grid, which leads to there being a large number of control points that carry no significant geometric information and only serve to increase calculation time. Fig. 62 illustrates the drawbacks of the NURBS model. The personal watercraft depicted is divided into 13 surfaces in order to maintain the required rectangular topography. Also, many of the nodal points are unnecessary and are merely included to satisfy rectangular shape constraints.

To address the limitations of using NURBS to model complex boat hulls, T-Splines were introduced. T-Splines are not limited to a rectangular geometry, which significantly reduces the number of superfluous points needed to complete the mesh as well as make the modeling of a complex body with a single surface possible. In the NURBS mesh, all the interior control points have a valence of four, which means that all the interior control points touch four edges. A T-Spline mesh (T-Mesh) allows control points to have valence other than four. These points are shown in Fig. 62 as yellow dots. The ability to have nodal points with different valence values gives T-Splines the ability to model any surface using a single T-Mesh. T-Splines were integrated into Orca3D to decrease calculation time as well as increase the accuracy of the calculations by removing discontinuities between surface meshes.

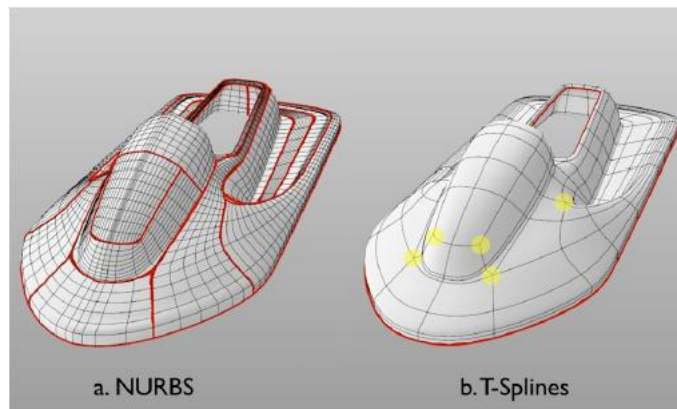


Fig. 62: Personal Watercraft Modeled as a NURBS and a T-Spline [69]

The 3-D model of the full scale optimized design was transferred from SolidWorks to Rhinoceros in the form of an IGES file. While Rhinoceros only accepts NURBS meshes, the Orca3D add-on allows for the creation of a single surface T-Spline mesh when performing stability and hydrostatic parameter calculations.

4.3.2.1. Results

Orca3D requires a number of parameters in order to output meaningful hydrostatic and stability data. The hull was designed so that the load water line (LWL) would have the aircraft sitting at a 1.5 degree trim angle in the water. During the design of the hull shape, the load water line was specified and the hull shaped to provide that attitude while in the water. Considerations were taken to keep the vertical tails out of the water during water operations. Next, Orca3D needs an input weight ($GW = 6,600 \text{ kg}$) and heel angle. The heel angle was set to 0 degrees. Finally, a vertical center of gravity position was needed, which directly affects the metacentric height of the craft, as that is the distance from the metacenter to the center of gravity. From this data and given aircraft geometry, Orca3D outputs the location of the center of buoyancy and center of flotation. It also gives the lateral and longitudinal metacentric heights, and draws in a waterline on the model to give a visual representation of its attitude on water (Fig. 63, Fig. 64).

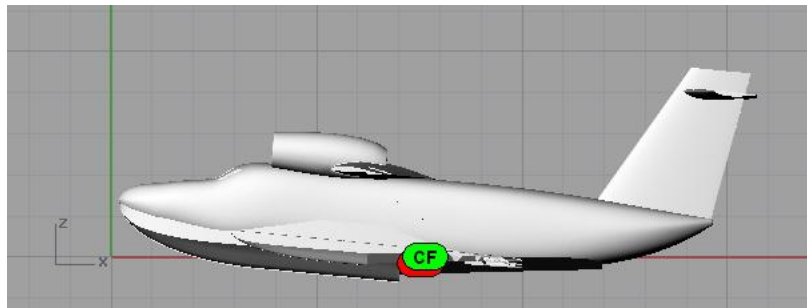


Fig. 63: Orca3D Results with Virtual Waterline of Trimaran Seaplane (Longitudinal)

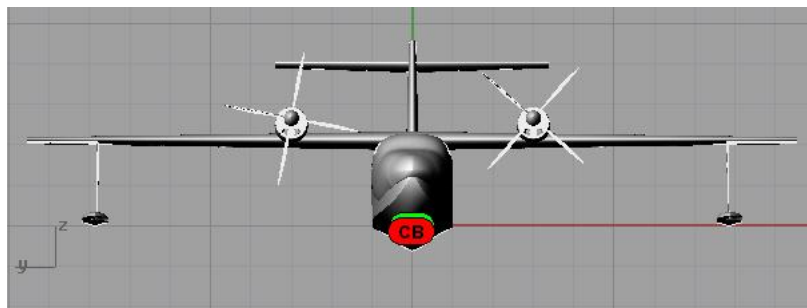


Fig. 64: Orca3D Results with Virtual Waterline of Wing Tip Floats Seaplane (Transverse)

The longitudinal and transverse metacentric heights of the trimaran seaplane were calculated to be 33.42 and 2.15 m. respectively. The values obtained by Orca3D are related to those shown from the theoretical calculations done by the FOTS code, shown in Table 12.

Another important aspect that was analyzed by Orca 3D is the overturn of the seaplane. This tool is useful in analyzing the conditions in which the seaplane can operate on rough, high wave water conditions. The overturn acts predominantly at the transverse stability. The seaplane is able to obtain a maximum heel angle before it overturns. Using the same criteria to calculate the metacentric height which needs input weight but now adding a heel angle, this analysis was performed. The maximum heel angle the trimaran seaplane could obtain is 12° before overturning as shown in Fig. 65.

Fig. 65 shows the trimaran seaplane when overturning. The outriggers turn in line with the seaplane, where the right outrigger is sunk inside the water and the left outrigger is out in the air. However, with the retractable float system, the outriggers are automated to stay in the water line, giving the seaplane more stability. Applying this system into the Orca 3D analysis, the maximum heel angle the seaplane trimaran can obtain increased to 18° .

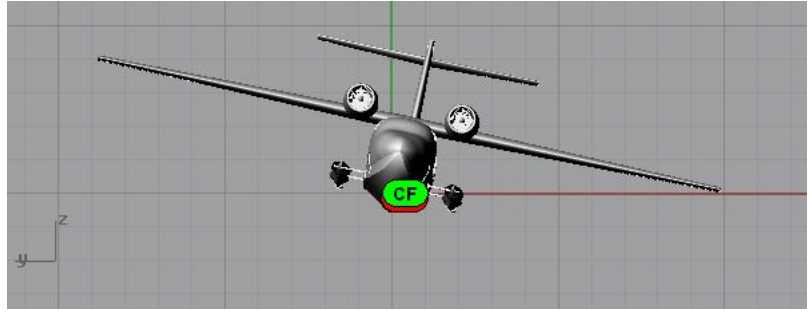


Fig. 65: Trimaran Seaplane at 12° Heel Angle before Overturning

Furthermore, the idea to obtain a seaplane that has outstanding water capability added the solution to fold the wings to increase the heel angle of the seaplane. Folding the wings gives the seaplane a better clearance when it is maneuvering in the water, especially in bodies of water with too congested boats or ships. Using the retractable float system and folded wings, the heel angle increased to 20° , shown in Fig. 66.

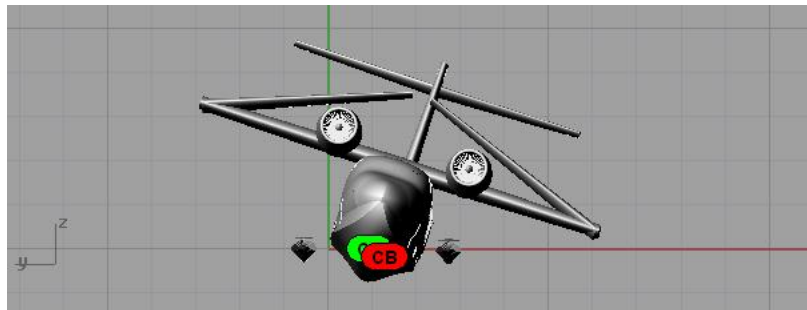


Fig. 66: Trimaran Seaplane at 20° Heel Angle before Overturning

4.3.3. Software Validation

Based on researched [70], CAD programs have a high validity and reliability, hence high accuracy for modeling. There are two common methods of 3-D models: Meshes and NURBS. NURBS method is more accurate than meshes since a mesh represents flat triangles, while NURBS are free form surfaces as explained before. SOLIDWORKS and Rhino uses NURBS when modeling, making the C.G. calculation very accurate. That means the x-,y-, or z-coordinate of any point can have a value ranging from as large as $\pm 10^{308}$ to as small as $\pm 10^{-308}$. Calculations can be accurate to 15 digits of precision in a range of $\pm 10^{20}$ to $\pm 10^{-20}$. In the end, there are a numerous industries that rely on CAD software such as SOLIDWORKS to perform design modeling. Such examples are the American Institute of Aeronautics and Astronautics at Arizona State University, BAE Systems, EAD Aerospace, Terrafugia, Inc., U.S. Army Research Laboratory among many others [71].

5. 2050 Visionary Concept: Future Seaplane Transport

5.1. Introduction

During the years of 1950 – 1980, the world was experiencing an exponential growth in technological advances due to the superpower rivalry between the United States and the Soviet Union. The aeronautical industry as well got caught in this expansion of technological exploration. The empirical guidelines during those days were: higher, further, and faster. In the late 1990's, this exponential growth reached its maximum peak. The world was experiencing economical problems, and certainly the aeronautical industry felt its effects. This "out of the box" thinking that emerged during the postwar era is restricted now to the same problems, money and social acceptance. Now, according to the European Vision 2020 guidelines, these have become: more affordable, safer, cleaner and quieter [19]. The old empirical guidelines are now forgotten, restricting the researcher's mind to explore radical aeronautical designs.

In order to expand the designer's mind, a modern vision with more radical, environmentally efficient, and innovative technologies was created. The new vision is called Future Air Transport Concept Technologies for 2050 in which the new guidelines will be: safer, quieter, cleaner and efficient. An efficient concept adapts the early guidelines (higher, further, and faster), with no restrictions in material, capital or infrastructure for planning, designing, testing, and constructing. The research addressed aspects such as new ideas in airborne vehicles, including design, new airport concepts as well as Air Traffic Management (ATM), alternative methods of air transport system operation and their integration with other transport modes. Let us recall this is just a radical way of thinking in order to expand the researcher's mind with no restrictions what so ever.

The purpose of this chapter was to create an example of this 2050 visionary aircraft concept, in this case an advanced amphibian aircraft. This amphibian aircraft was created on the basis of the proposed past research, however improving the design into creating a futuristic idea. The new proposed amphibian adapts advanced capabilities such as Unmanned Aerial Vehicle (UAV) mode, High Altitude and Long Endurance (HALE) capability, water and rescue missions, and water bomber operations. The advanced amphibian aircraft was created from a Blended Wing Body (BWB) aircraft and converted into an amphibian by adapting the trimaran design concept and the retracting float system creating an Advanced Amphibian Blended Wing Body Aircraft (AABWBA).

5.2. Review of Literature

The BWB is a type of tailless flying wing design in which the wing and fuselage are blended together into one seamless body in order to achieve significant improvements in performance over the conventional aircraft, example shown in Fig. 67. Unlike the flying wing design, in which the entire body of the aircraft is a wing, the BWB has a fuselage that is designed as a wing. Therefore, the BWB has a fuselage section that is thicker than the flying wing which allows it to accommodate more payloads. And, unlike a conventional aircraft, the BWB's fuselage acts as a lifting body allowing it to generate lift, rather than acting as an interference component [72].

In 1988, the McDonnell Douglas Company (now Boeing), along with NASA, conducted a large study on the feasibility of a BWB passenger transport aircraft as an alternative to the conventional cylindrical tube and wing transport. An initial study performed by Callaghan and Liebeck in 1990 [73] showed that an 800 passenger BWB, when compared to a conventional

transport, cruising at Mach 0.85 with a 7,000 nmi range offered an increase in lift to drag ratio (L/D) of 40%, and a 25% reduction in fuel burn. Another study performed [74] showed that the same 800 passenger BWB offered a decrease of 16% in takeoff gross weight (GW) and a reduction of 35% in fuel required. These improvements in performance are made possible because the BWB has an extremely low interference drag factor due to the absence of an interfering fuselage and tail. This allows for the improvement in L/D . In addition, due to the absence of these components, the BWB is able to achieve a significant decrease in wetted surface area, which also reduces friction drag.

Another recent and important study on the BWB concept is the European Union sponsored MOB (Multi-Disciplinary Design and Optimization for Blended Wing Body configurations) project. The MOB project is a joint project with participation from three aerospace companies, four research institutions and eight universities throughout the European Union. Publications put out by the project showed a 10%-19% savings in operating costs for a BWB when compared to the operating costs of the Boeing 747-400 aircraft [75].



Fig. 67: Example Blended Wing Body Aircraft [72]

5.3. Design Selection

5.3.1. Input Parameters

It was analyzed as the best choice in terms of productivity to use an aspect ratio of $AR = 14$ and W/S of 195 kg/m^2 on the BWB aircraft. The higher AR and relatively low W/S equates to a lower GW through requiring a lower engine thrust and lower fuel usage.

AR was varied between values of 8 to 14 and W/S was varied between 90 kg/m^2 and 400 kg/m^2 . The values of AR were chosen because research showed that these were typical values for flying wings [76]. The values of W/S were chosen because this range of W/S was typical for HALE type aircrafts.

An important point to notice is that as AR increases, GW decreases. This is in part due to the decrease in wing area that higher aspect ratios have. Another important point to notice from this is that the lowest GW occurs at W/S of 195 kg/m^2 . Since it is always important to optimize and lower the weight of a new aircraft, a W/S of 195 kg/m^2 was selected. Using this information, an AR of 14 would result in the lowest amount of thrust required. This combination of lowest GW and lowest thrust required with an AR of 14 and W/S of 195 kg/m^2 became the selected configuration for the BWB.

The unfortunate side effects of having such a large *AR* are structural effects due to bending, manoeuvrability, parasitic drag and low internal volume for fuel. Longer wings simply have more bending stress and lower roll rates, however these two drawbacks were deemed to be worth the risk due to advanced material selection which offers better structural strength and lower structural weight. The lower roll rates would also not affect the designed mission very much as the mission is not one that requires high maneuverability.

An increase in parasitic drag is partially offset by a reduction in induced drag from having a longer wing span, and especially offset by the huge reduction in equivalent aspect ratio due to the BWB configuration. Values calculated for the amount of fuel required for the designed mission indicate that the design has plenty of room for fuel within the wing of the plane.

5.3.2. Fuselage Thickness

In order to fit sizable payload into the fuselage, a wing thickness ratio of 17% was used. This value is much higher than typical transonic airfoils and it is the upper limit of thin airfoil theory [76].

5.3.3. Airfoil

The BWB design is a tailless aircraft, and therefore a reflexive airfoil is required to produce a positive pitching moment to counteract the negative pitching moment of the wing. The NACA 6400 series airfoils were selected due to the ready availability of data (drag polar, moment arm, etc) and because the cambered airfoil can achieve a higher lift coefficient at lower angles of attack [27]. While the NACA 6400 series is not a reflexive airfoil, the elevons can be trimmed in such a way to have a negative deflection, therefore creating a pseudo reflexive airfoil without sacrificing interior cabin space.

For the fuselage section of the aircraft, a NACA 6417 and 6416 were selected to utilize the maximum 17% *t/c* available. The NACA 6417 was placed in the middle of the aircraft, with the NACA 6416 on the outer edges of the fuselage. A NACA 6410 was then chosen to be the airfoil shape at the wing tips. The entire aircraft was then lofted together in such a way that the entire aircraft is one blended body.

The NACA 6410 airfoil has a $C_{L_{max}}$ of 1.3. From all of the calculations, this value was sufficient given the available thrust. Therefore, high lift devices such as slats were not used. In addition, high lift devices such as flaps could not be used because it increases the negative pitching moments of the aircraft [76] which cannot be counteract because it does not have a tail.

5.3.4. Wing Sweep (Λ)

Boeing's 800 passenger BWB used a Λ of 36° [76] from the quarter chord, which swept the tips of the wings back behind the engines, providing the inherently unstable BWB with increased stability and control. One of the drawbacks to having a highly swept wing is that air flow over the wing begins to divert and flow over the wing toward the tips in a diagonal manner, instead of in a straight line from front to rear. In order to address this problem, wing fences were constructed on the wing in an effort to redirect flow back into a better wing front to rear manner. Fig. 68 shows a top-down view of the BWB, showing the wing and wing fence design.

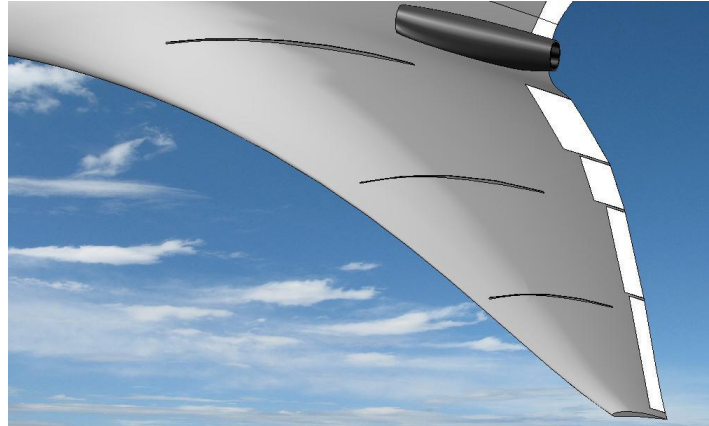


Fig. 68: Top-down view of BWB showing wing and wing fences

5.4. Preliminary Results

To compare the results obtained from the conventional advance amphibian aircraft, the same mission profile was used in order to size the AABWBA. As well, the same calculation process and design method was used to calculate the weights, dimensions, and performance of the AABWBA. A CAD Model and parameters of the BWB are shown in Table 17 and Fig. 69.

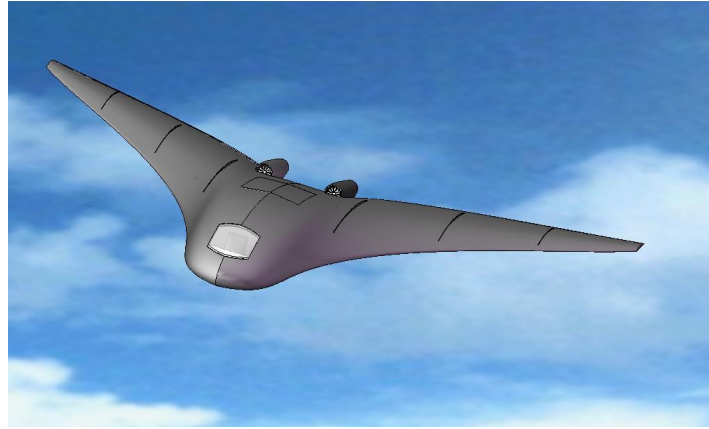


Fig. 69: Blended Wing Body Aircraft

Table 17: Blended Wing Body Parameters

| | |
|-------------------------------------|-------|
| Gross Weight [kg] | 7,600 |
| Fuselage Length [m] | 13.7 |
| Fuselage Max Height [m] | 2.4 |
| Fuselage Width [m] | 4.2 |
| C_{root} [m] | 10 |
| Wing Area [m^2] | 39.09 |
| Wing Span [m] | 23.47 |
| C_{Lmax} | 1.3 |
| Flat Plate Drag Area [m^2] | 0.445 |
| Aspect Ratio (AR) | 14 |
| Wing Loading (W/S) [kg/m^2] | 195 |

5.4.1. Geometric Properties (BWB)

5.4.1.1. Fuselage

The fuselage of the BWB uses a NACA 6417 airfoil and is divided into two sections: the crew cabin and the aft section. The crew cabin section of the fuselage houses the (optional) pilot and flight instrumentation and computer. The aft section of the fuselage is further divide into a cargo bay and engine bay. A cut view of the fuselage with the two (three) different sections is shown in Fig. 70.

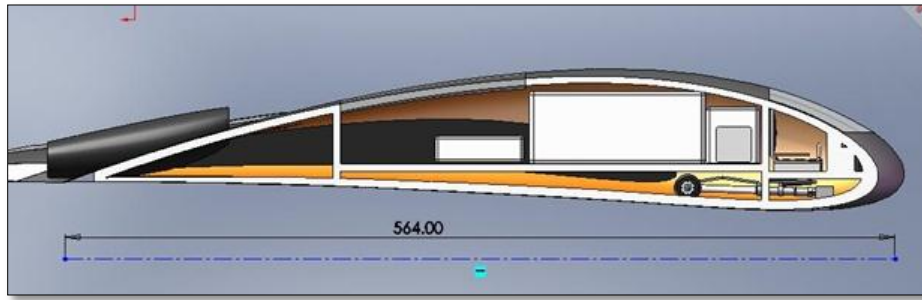


Fig. 70: Cut view of BWB fuselage

The fuselage was originally given a height of 1.82 m, which was theoretically enough space to accommodate for the tallest of the payload component. However, upon further investigation, this height proved to be insufficient, which left no room to account for spars, ribs, electrical and hydraulic lining and so on. Therefore, the height of the fuselage at the widest section was increased to 2.4 m. This value provided enough spacing within the fuselage to accommodate all payload, landing gear, system lines, bulkheads, and so forth.

In a similar fashion, a width of 4.2 m was assigned to the fuselage. From the assigned fuselage height of 2.4 m, and using a t/c ratio for the fuselage of 17%, the chord, or length from nose to aft, of the fuselage was calculated to be 14.3 m. As shown in Fig. 70, this length offers plenty of longitudinal length to fit engines, payload and (optional) pilot.

5.4.1.2. Wing

The wing of the BWB uses a NACA 6410 airfoil. A taper ratio (λ) of 10% was selected for the design. A value of 10% was selected based on appearance. The root chord of the wing has a chord equal to 80% of the chord of the entire fuselage. This was chosen not only for aesthetics, but also so that the wings would be swept back, enough for placing the control surfaces behind the engines for better handling.

5.4.1.3. Fuel Tanks

As calculated from LOTS, the weight of fuel needed to fly the mission profile, including reserves, was around 1,550 kg. Based on the density of Jet A-1 fuel (0.804kg/L) this correlates to a fuel volume of around 1,927 L or 1.9 m³. A CAD analysis of the design indicates that there is an available volume of around 11 m³ inside of each wing. Taking into account that not all 11 m³ within each wing can be used (due to structures, control surfaces, electrical and hydraulic lines, and so on), there is still more than enough volume inside of each wing to use for fuel storage. Fig. 71 shows the location of the BWB's fuel tanks. Due to the extremely large amount of free volume within the wings, the fuel tanks can be placed anywhere that is possible. CG analysis tells that the CG location is 8.65 m from the front. In order to minimize CG travel, the fuel tanks were placed right on the CG axis. Therefore, effectively eliminating CG travel.

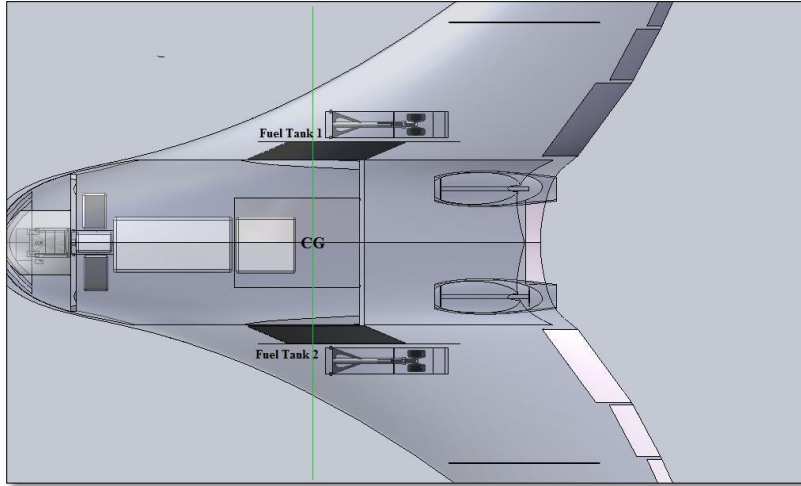


Fig. 71: BWB fuel tanks

5.4.2. Weight Breakdown

The values for the weight of the BWB and AABWBA are shown in Table 18. The calculated empty weight was elaborated using the equations from Appendix A.1. The only difference in calculating the empty weight of the BWB differs in which the “fuselage” of the BWB is not treated as a conventional fuselage. Equations for calculating the cabin and aft sections are given.

Table 18: BWB and AABWBA Weight Breakdown

| Weights [kg] | BWB | AABWBA |
|---------------------|------------|---------------|
| MTOW | 7,600 | 7,600 |
| Boat Hull | 0 | 225 |
| Floats | 0 | 150 |
| Strutting | 0 | 50 |
| Empty Weight | 4,600 | 5025 |
| Max Fuel | 1,550 | 1,550 |
| Payload | 1,450 | 1,025 |
| Max Payload | 1,800 | 1,800 |

5.4.3. Control Surfaces

The BWB aircraft has no vertical control surfaces to minimize the drag of the aircraft. This makes the aircraft unstable, so fly-by-wire (FBW) system in combination with a flight control computer (FCC) keeps the aircraft balanced and flying well. The control surfaces on the aircraft are modeled after the B-2 Spirit bomber. The control surfaces were sized to give the same area of control surface to area of wing as is found on the B-2 Spirit. Table 9.2 lists the dimensions of each of the control surfaces.

On the outermost portion of the wing is the deceleron, a vertically split airbrake that simultaneously opens up and down. The deceleron causes an increase in drag on the outer portion of the wing; and when only one deceleron is active, it causes a yawing moment on the aircraft. The deceleron is needed because there is no vertical tail to provide yaw control. There are three elevons inboard from the deceleron. The elevons take place of traditional elevators and ailerons. When the elevons are moved in the same direction on both wings, they act as elevators

and create a pitching force on the aircraft. When the elevons are moved in opposite directions unequally, they take place of the ailerons and produce a rolling force on the aircraft. At the center of the aircraft there is a single elevator that is used for pitch control. This center elevator is used to trim the aircraft so the outboard elevons can be freely used to control the aircraft. Although the aircraft has no vertical tail and hence no rudder, the pilot still has rudder pedals and a traditional stick for flight control. The inputs from these traditional controls are fed into the FCC which then operates the elevons and decelerons to complete the wanted manoeuvre. This way, training required for flying the BWB is kept to minimum as the layout of the controls is still the same as in a conventional aircraft. Fig. 72 shows the control surfaces of the BWB.

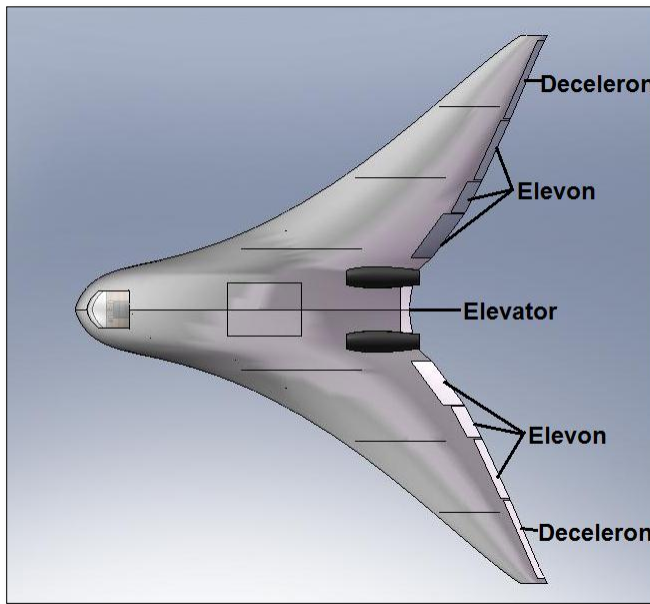


Fig. 72: Top view of BWB with control surfaces labeled

5.4.4. Trimaran Dimensions

The dimensions of the trimaran for the AABWBA obtained are shown in Table 19. With the parameters of the BWB and the trimaran, the AABWBA was constructed, shown in Fig. 73.

Table 19: Trimaran Dimensions (AABWBA)

| | <i>Main Hull</i> | <i>Outrigger</i> |
|--------------------------|------------------|------------------|
| <i>Slenderness Ratio</i> | 5.24 | 14 |
| <i>Spray Coefficient</i> | 0.0975 | 0.08 |
| <i>Beam [m]</i> | 2.61 | 0.48 |
| <i>Length [m]</i> | 13.69 | 6.74 |
| <i>Forebody [m]</i> | 6.61 | 3.19 |
| <i>Afterbody [m]</i> | 7.07 | 3.55 |
| <i>Bow Height [m]</i> | 1.70 | 0.04 |
| <i>Clearance [m]</i> | - | 2.35 |
| <i>Stagger [m]</i> | - | -0.86 |

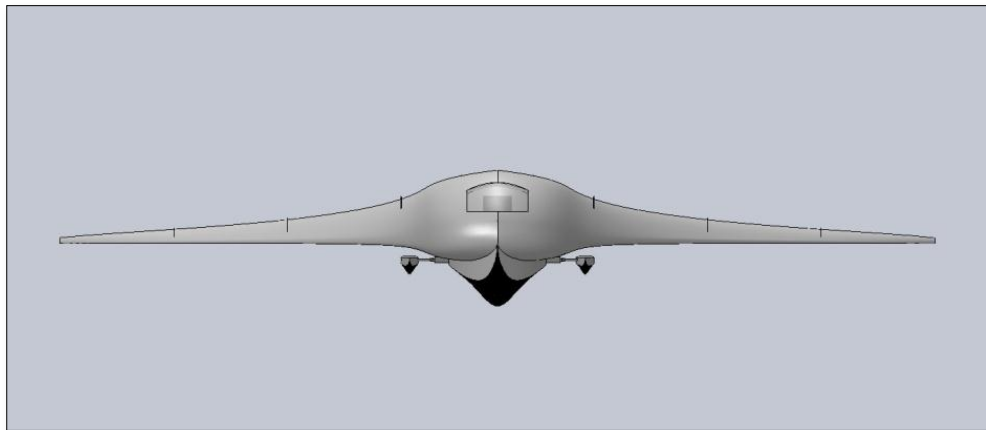


Fig. 73: CAD Model of AABWBA

5.4.5. Hydrostatic Stability

The following image (Fig. 74) was elaborated showing the locations of the waterline, CB , CG , and GM . Since the GM is positive, the AABWBA shows it has a positive transverse stability.

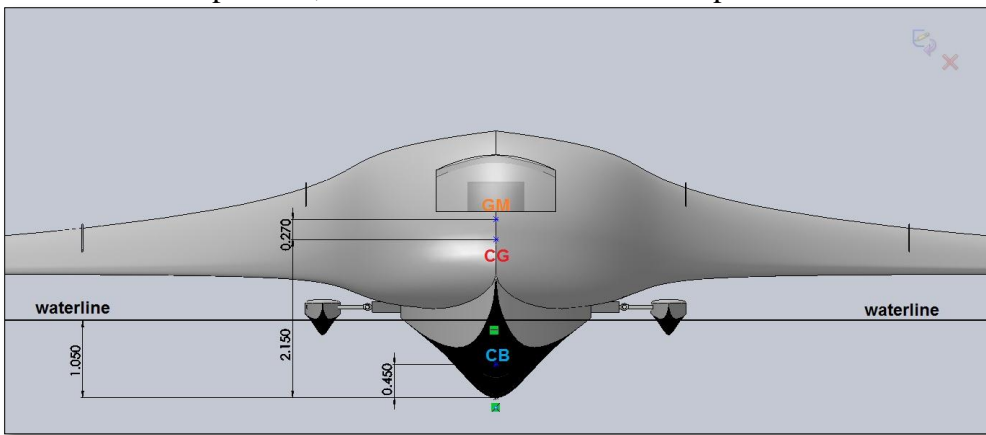


Fig. 74: Metacentric Height of AABWBA

5.4.6. Water Resistance

The graph shows trend lines of water resistance, thrust available of turboprop engine, turbojet, and turbofan engines as a function of velocity (Fig. 75). Using the static thrust available from the BWB of 40,500 N, the curves for turboprop, turbojet and turbofan engines were plotted using the empirical formulas from eqs (26) - (28). For this aircraft, the use of high lift devices was not necessary, since the high initial takeoff thrust generated by the jet engines made it possible for the aircraft to takeoff from water.

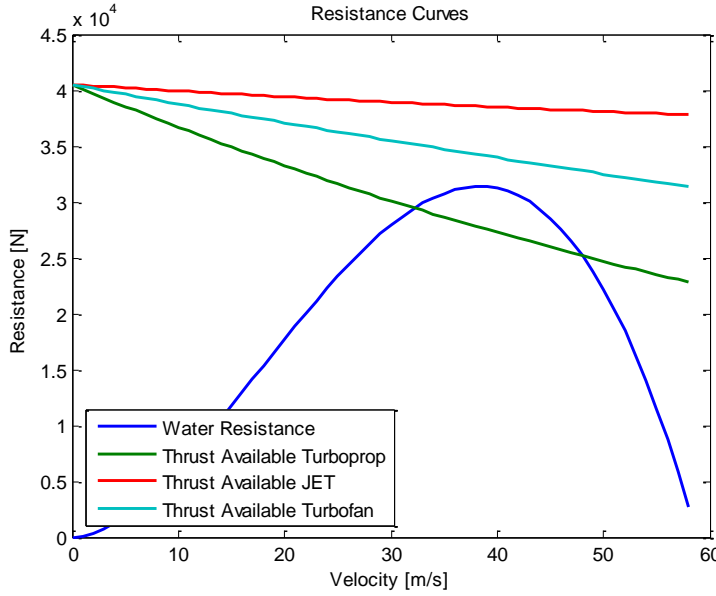


Fig. 75: Resistance Curves AABWBA

5.4.7. Air Performance

With the geometry of the trimaran calculated, the increase in parasite drag was then approached. The same approached for comparing the drag increment was elaborated in Table 20.

Table 20 shows the total drag that the landplane, the seaplane with extended floats, and retracted floats at cruising speed of 900 km/hr and an altitude of 12,200 m. Since the BWB does not feature a conventional fuselage, the “fuselage” section of the BWB is treated as a wing, then the flat plate drag area of the “fuselage” is calculated using the equations for wing component.

With the drag increase calculated for the AABWBA, a comparison of the flight performance for both the BWB and the AABWBA was elaborated. First, an altitude flight envelope was created, showing the stall speed, maximum speed, and service ceiling of both the landplane and seaplane, Fig. 76. The aircrafts can reach a supersonic speed at cruising altitude. Compressibility effects are taken into consideration and calculated as well.

Finally, Fig. 77 and Fig. 78 show the payload-range diagram and maneuvering envelope for the AABWBA. As can be seen from the figure, the gust loads do not exceed the maneuvering loads. This means that the aircraft will not need additional strengthening to withstand gust loads experienced in its flight envelope.

Table 20: Flat Plate Drag Area Breakdown Component

| Flat Plate Drag Area | Landplane | Seaplane | Seaplane |
|----------------------------------|------------------|-------------------|--------------------|
| <i>Breakdown [m²]</i> | | <i>[Extended]</i> | <i>[Retracted]</i> |
| <i>Aircraft</i> | 0.445 | 0.445 | 0.445 |
| <i>Boat Hull</i> | 0.000 | 0.128 | 0.128 |
| <i>Floats</i> | 0.000 | 0.067 | 0.000 |
| <i>Strutting</i> | 0.000 | 0.006 | 0.000 |
| <i>Total</i> | 0.445 | 0.646 | 0.573 |
| C_{DP} | 0.0114 | 0.0166 | 0.0147 |
| C_{DP} Increment | - | 0.0052 | 0.0033 |
| Drag Increase | - | 31.33% | 22.45% |

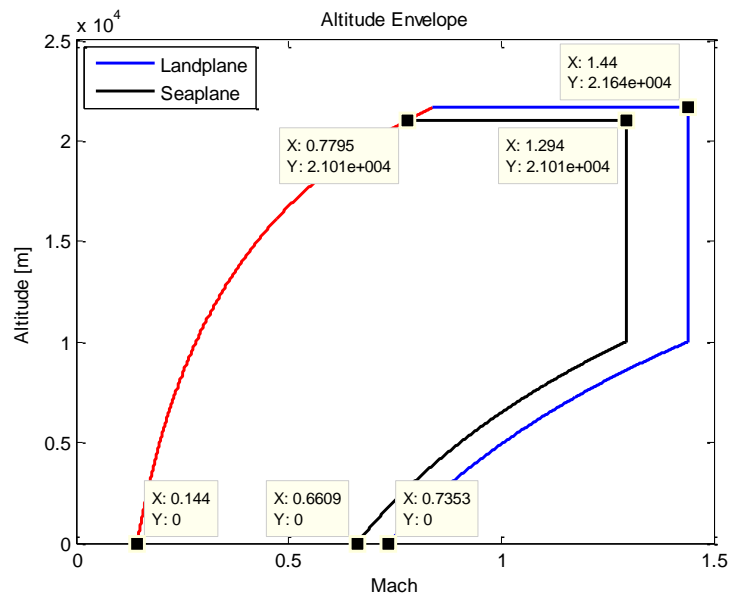


Fig. 76: Altitude Envelope of BWB and AABWBA

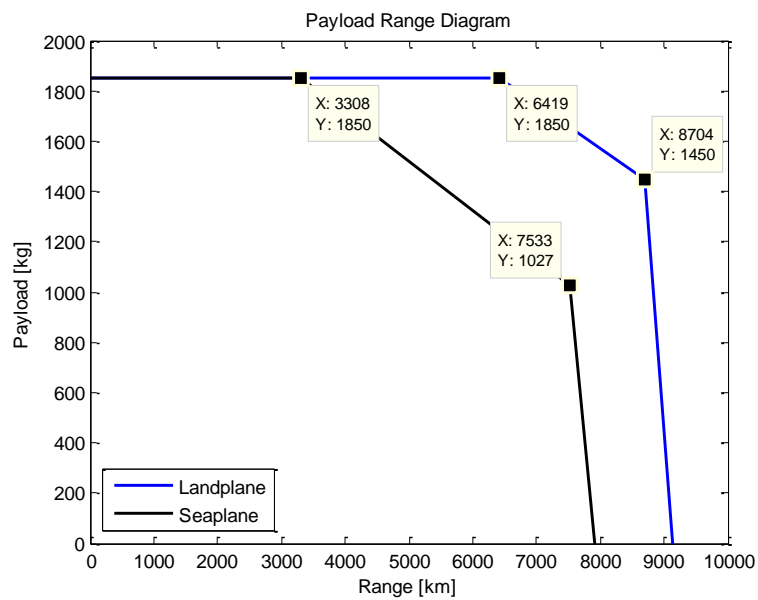


Fig. 77: Payload Range Diagram

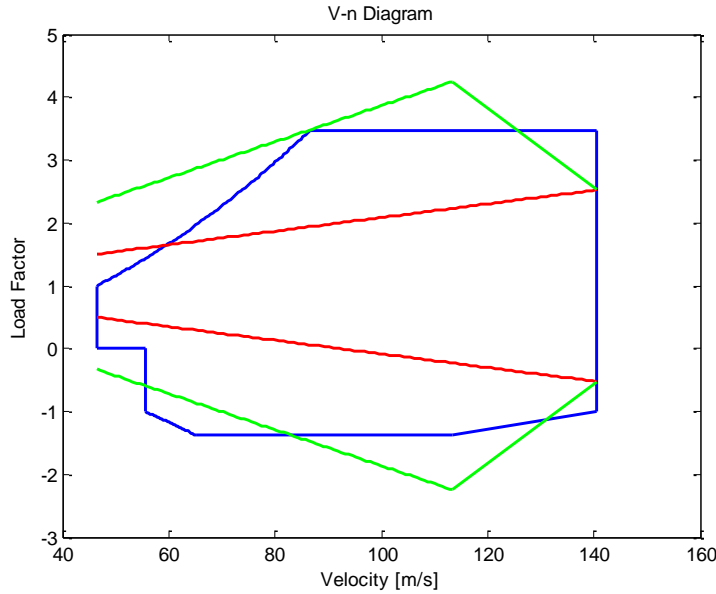


Fig. 78: Maneuvering and Gust Envelopes

5.5. Summary

The aim was to keep most of the AABWBA performance as close to the BWB performance. With the aid of the retracting system, and reducing weight using composite materials, this goal was possible, in which an overall reduction in flight performance of around 10% was observed from the BWB and AABWBA design. Table 21 summarizes the BWB and AABWBA comparison values.

In UAV mode, the aircraft uses an onboard computer with a flight controller and autopilot. The flight computer is linked to a base station through high bandwidth radios. The radios are capable of both uplink and downlink. This enables commands to the UAV to be both sent and received, letting the user have a choice between autonomous mode and remotely piloted mode. The flight controller uses a wide range of sensors to collect accurate data and flight conditions. Positioning data is provided by GPS, and transformation and rotation is collected through triple redundant accelerometers, in conjunction with IR sensors as an extra redundancy feature. Ambient and flight conditions are collected via Pitot tubes and laser readings.

In addition, an imaging system consisting of high resolution cameras capable of both still and moving images at the same time are mounted on board the AABWBA. These cameras are connected to a separate radio downlink to enable dedicated photo and live video streaming. The flight controller can be pre-programmed for missions and the uplink capable radio allows for mission changes during flight. In the remotely piloted role, the same sensors are used; however the flight controller switches off from autonomous mode so that a user can pilot the AABWBA from a remote location.

Another analysis made through this research is increment seaplane traffic. Suitable infrastructure (seaports) could be constructed in order to increase seaplane market and operations. The advance amphibian aircraft gets a futuristic design that will attract the attention of investors, and will get a high social acceptance. As a result, using SOLIDWORKS, models of this futuristic seaplane traffic model was elaborated shown in Fig. 79 and Fig. 80.

Table 21: Summary of major design values (BWB and AABWBA)

| Parameters | BWB | AABWBA |
|----------------------|--------|--------|
| Gross Weight [kg] | 7,600 | 7,600 |
| Empty Weight [kg] | 4,600 | 5,025 |
| Max Speed [km/hr] | 900 | 806 |
| Rate of Climb [m/s] | 18.12 | 17.59 |
| Absolute Ceiling [m] | 21,644 | 21,012 |
| Endurance [hr] | 10.75 | 10.35 |
| Maximum Range [km] | 8,704 | 7,533 |
| Thrust [N] | 40,500 | 40,500 |



Fig. 79: AABWBA at takeoff from seaport



Fig. 80: AABWBA taxiing at seaport

6. Conclusions and Recommendations

6.1. Conclusions

One of the main purposes of this research was to analyze the optimization and sizing methodology used in the creation of a preliminary design for an amphibious aircraft and to make suggestions about ways it can be improved. Of course, it is very difficult to create a perfect aircraft in every aspect (such as structures, aerodynamics, stability, etc.) analyzed that will then function perfectly after the first design iteration. The preliminary design aims to locate as many of the main issues as possible before beginning the detailed design. The optimization design method, especially on the design of the floating device, proves to be very simple and easy to handle by the designer, in which time and effort could be saved when deciding the type of amphibian aircraft to size. The results of the validation work done on the sizing code were very promising. The geometric parameters predicted by the LOTS were very accurate. The FOTS sizing code reasonably predicted the size of the floating device, with the largest error in the predicted performance.

Finally, the preliminary results show some of the advantages of using the trimaran concept into a seaplane design, and the increase in flight performance when the floats are retracted. For the flight performance, mounting the floats inside the hull decreases significantly the drag as compared to an extended position. This increases the flight performance of the seaplane in rate of climb, range, and endurance, shown in Fig. 55 and Table 15.

The design excels in hydrostatic stability. The trimaran proves to be a stable method as shown from the FOTS code and the design analysis performed by ORCA 3D. The metacentric height of this design has a positive value both in the transverse and longitudinal stability. The water speed that a trimaran shows is also significant, in which water resistance is less compared when using the wing tip floats or stabilizers as explained by the graph in Fig. 50.

With the help of the design analysis, an extended analysis of the structural strength of the hull was performed. The analysis shows to have some structural stress on the point where the step is located. Special attention on this matter has to be addressed. Of course, computer simulations may prove to be unrealistic and true practical tests are to be made. Finally, ORCA 3D help prove the theoretical hydrostatic analysis performed by the FOTS code. As well, it was a useful tool in analyzing wave simulations and finding the maximum heel angle the seaplane must be able to withstand before overturning. This tool seems useful in analyzing the retractable float system in water, in which it showed to improve the heel angle 6° when using the float system.

The second aim of this research was to design an “out of the box” idea that stands out not only because of its improved performance, as well as its unique design idea. On a long term basis, a brand new seaplane can be designed as well as suitable infrastructure (seaports) in order to increase seaplane market and operations. The creation of the Blended Wing Body Aircraft creates a more efficient landplane than a conventional configuration. Combining the advance trimaran concept to the blended wing body design, an advance amphibian aircraft emerges, exceeding both water performance and air performance on any kind of amphibian aircraft of its type. The theoretical design exceeds the “out of the box” thinking, as well as the aesthetic design. The advance amphibian blended wing body aircraft gets a futuristic design that attracts the attention of investors, and gets a high social acceptance.

The aim was to keep most of the AABWBA performance as closed to BWB performance. With the aid of the retracting system, and reducing weight using composite materials, this goal was possible, in which an overall reduction in flight performance of around 10% was observed

from the BWB and AABWBA design. The aerodynamic properties of the aircraft were deemed important and the drag reduction of the aircraft was carried out. For this reason, a BWB configuration was chosen. Another analysis made through this research is increment seaplane traffic. Suitable infrastructure (seaports) could be constructed in order to increase seaplane market and operations.

Finally, using SOLIDWORKS, models were elaborated to show a futuristic picture of this advance trimaran seaplane design shown in Fig. 81, Fig. 82, and Fig. 83.

6.2. Recommendations

6.2.1. Sizing Code Improvements

Drag estimation in the sizing code seemed to be quite consistent. However, wind tunnel testing must be elaborated to prove the validity of the sizing code results. The method of drag calculation used by the sizing code is purely theoretically. It doesn't take into account interference from one component to another. There is also the issue of the shape of the individual components. Also, unknown perturbances, e.g. drag due to flow separation at the step of the boat hull, are not taken into account so all of these factors may play an important role in calculating the real drag estimation of the model. It does not consider the blunt trailing edge of the floats or stabilizers. It also does not include the additional drag due to the scalloped cut outs in the fore and aft sections of the fuselage. One method of improving aerodynamic prediction could be the inclusion of a vortex panel code into the design code. This would completely replace the current aerodynamic calculations made in the sizing code and could hopefully help improve drag predictions.

A second issue that may be improved with the sizing code was during the analysis of its lateral and longitudinal stability on the water. While the aircraft was found to be stable in both the lateral and longitudinal directions, the values could also reflect other results as compared to real life tests. This is a difficult problem to solve, as it requires the designer to know the exact shape of the floating in order to calculate its center of buoyancy and metacentric heights. This requires a more detailed design than is currently being used and may not be feasible with the current approach. On the other hand, if a panel method could be implemented that could handle the complex geometries involved in detailed boat hull design, then it is possible that that geometry could have a sectioning method performed on it inside the sizing code to predict its on-water performance.

If a panel method was used that was allowed to change many of the geometrical parameters of the fuselage and other components, the smart use of penalty functions would be necessary to make sure that the geometry maintains a level of feasibility. This includes parameters such as length-to-beam ratio, which is currently user input. Care would need to be taken that it could not be made too large or too small, as either extreme is not feasible.

6.2.2. Technical Improvements

There are still more options that can be considered to further refine the seaplane aircraft. The landing gear can be refined to possibly reduce the length of the landing gear to reduce weight. Increasing the loads that the landing gear can take and absorb as the aircraft lands should also be looked into as it will allow the aircraft to land at higher speeds or in more turbulent weather. Also, more aspects of the design should be addressed, as structures, and stability in order to obtain a complete analysis of the aircraft. To obtain better manoeuvrability in water, the introduction of a water rudder could be used. The rudder could be deployed from under the tail

section of the hull, and retract inside the hull when the seaplane is at flight. Though, this complex device will increase the empty weight of the seaplane.

Of course, especial attention must be made to the elaboration of the floating devices, and practical testing must be elaborated to prove the results found from the LOTS and FOTS code

Some improvements done to the BWB design are more specified to the aerodynamics. Wing twist should be explored to create stall at the root wing before stall occurs at the wing tips. This will allow the decelerons to remain effective and be in control of the aircraft even if the root portion of the wings stalls.

To reduce the need to have the elevons always engaged to stabilize the aircraft and balance the pitching moment of the wings, a reflexive airfoil should be researched and applied to the aircraft. Although with today's active and computerized flight control systems, a nonreflexed airfoil is allowed.

Right now, the BWB has enough space to allow more fuel to be stored onboard without the need for external fuel tanks. This can greatly increase the endurance of the aircraft and provide for longer surveillance and scientific monitoring. A system for air refueling should also be looked into to extend the range and endurance of the aircraft. Since the aircraft can be operated pilotless; with air refueling, the aircraft can then be operated well over more than ten hours.

The model used to calculate the weight of the wing, fuselage cabin and aft developed by [76] was sufficient, but more time could be used to refine it for different scaling factors. A better model for weights would also provide for better CG estimates and a more accurate drag build up.

The BWB was based on the Boeing BWB studies, which were for an 800 passenger aircraft. A CFD analysis could be performed in the future to verify and validate the designs and models. In addition, should be given more time, more design variables could have been examined in LOTS and FOTS to be used as varying parameters in order to find the most suitable HALE BWB design.



Fig. 81: Futuristic CAD Model of Amphibians at a Modern Sea Port



Fig. 82: Futuristic CAD Model of a Turboprop Seaplane and AABWBA

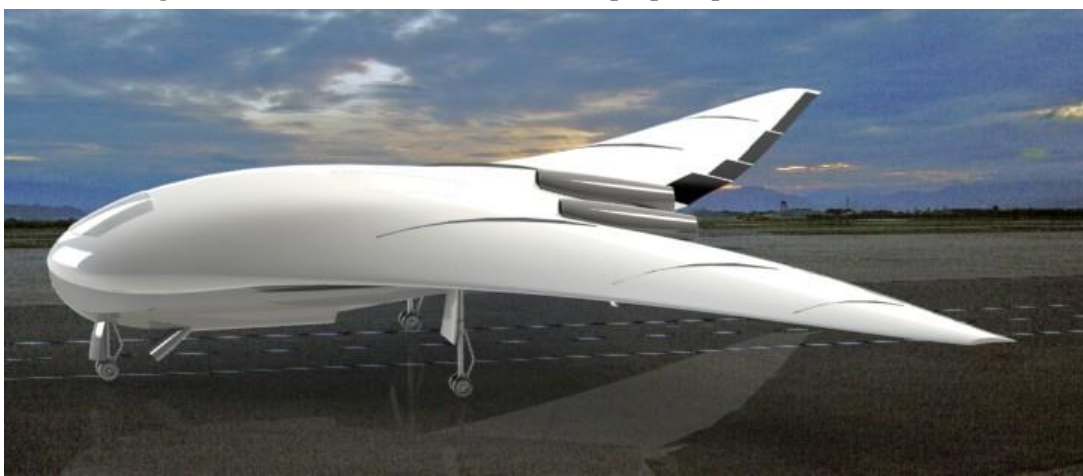


Fig. 83: Futuristic CAD Model of AABWBA at taxi

References

- [1] "Design", (2012) Google search engine [online]; <http://dictionary.cambridge.org/search/british/?q=design>
- [2] Nicolaou, S., " Flying boats and seaplanes: A history from 1905 ", Bay View Books Ltd, 1996
- [3] Syed, H., "Amphibian Aircraft Concept Design Study," Individual Project, University of Glasgow, 2009.
- [4] Gunston, B., "World Encyclopedia of Aircraft Manufacturers: From the Pioneers to the Present Day", 2nd Edition, The History Press Ltd, 29 Sept 2005
- [5] Curtiss, G. H., and Post, A., "The Curtiss Aviation Book", The Frederick A. Stokes Company, New York, US, 1912
- [6] Knott, R., " Flying Boats of the Empire. The Rise and Fall of the Ships of the Sky ", Robert Hale Limited, London, UK, 2011
- [7] "Spruce Goose", google.com 2012; <http://www.theaviationzone.com/factsheets/hk1.asp> [Cited Feb 15, 2012]
- [8] "Advance Amphibious Vehicles", google.com 2012; <http://www.army-technology.com/projects/efv/> [Cited Mar 13, 2012]
- [9] University of New South Wales., "Ekranoplans & Very Fast Craft", Sydney, Australia, Dec. 1996
- [10] Dornier, I., "Mission Dream: Adventures of an aviator", Airborne Grafix, Dec. 27, 2011
- [11] Frawley, G., "The International Directory of Civil Aircraft", Aerospace Publications, US, 2003
- [12] "Beriev" beriev.com 2011; http://www.beriev.com/eng/core_e.html [Cited Jan 26, 2011]
- [13] Halirova, J., "Business and Cost Analysis of Seaplanes," Erasmus Individual Project, Czech Technical University, Prague, Czech Republic, 2011
- [14] Lightening B., "Road Map for Fullfilling Market and Operator Needs in Seaplane Operation within Europe", Individual Pilot Feedback Report, Fusetra, 2011.
- [15] "Seaplane Facilities," Seaplane Pilots Association, US Department of Commerce
- [16] Canamar, A., Galbraith, R., Gobbi, G., Halirova, J., Smrcek, L., "Long term future opportunities for seaplanes operations," FUSETRA Report, Workshop Proceedings & Presentations, University of Glasgow, 2011.
- [17] Mohr, B., Schomann, J., "Today's Seaplane Operations; Results from the 2010 online survey," FUSETRA Report, Malta Workshop Proceedings & Presentations, University of Munich, 2010.
- [18] Gobbi, G., Canamar, A., "Visionary Concepts for Future European Seaplane Operations," 3rd CEAS Air & Space Conference Paper, University of Glasgow, 2011.
- [19] Report of the group of personalities, "European aeronautics: a vision for 2020. Meeting society' needs and winning global leadership", Luxembourg: Office for Official Publications of the European Communities, 2001.
- [20] "Seaplane Environmental Impact," google.com 2011; <http://www.seaplanes.org/advocacy/environment.pdf> [Cited Feb 3, 2011]
- [21] "Seaplane Environmental Impact" google.com 2011; <http://www.usace.army.mil/environment/Pages/home.aspx> [Cited Feb 3, 2011]
- [22] Cronin Millar Consulting Engineers, "Seaplane Environmental Impact Information Report," The Mews Cobh Co. Cork, 21 Dec 2009
- [23] Office for National Statistics, "An investigation into the location and commuting patterns of part-time and full-time workers in the United Kingdom, using information from the 2001 Census| Alistair Dent & Stephen Bond", Executive Summary, UK, 2008.
- [24] Department of Transport, "Public experience of and attitudes towards air travel", UK, 29th July 2010.
- [25] "Aircraft Accidents," google.com 2011; [http://www\(aaib.gov.uk/home/index.cfm](http://www(aaib.gov.uk/home/index.cfm) [Cited Feb 3, 2011]
- [26] Transportation Safety Board of Canada, "A Safety Study of Survivability in Seaplane Accidents," Report Number SA9401, Canada, 1994.
- [27] Raymer, D. P., "Aircraft Design, A Conceptual Approach", American Institute of Aeronautics and Astronautics, Inc., Washington D.C., USA, 1992
- [28] Smrcek, L., "Aircraft Design for Performance 3" Lecture notes, University of Glasgow, 20011.
- [29] "Dornier Do.228" google.com 2011; <http://www.raf.mod.uk/equipment/islander.cfm> [Cited Jan 26, 2011]
- [30] "Britten Norman BN 2" google.com 2011; <http://www.raf.mod.uk/equipment/islander.cfm> [Cited Jan 26, 2011]
- [31] "BAe 146" baesystems.com 2011; http://www.baesystems.com/Newsroom/NewsReleases/2009/autoGen_10903093820.html [Cited Jan 26, 2011]
- [32] "Antonov AN-72" aerospaceweb.org 2011; <http://www.aerospaceweb.org/aircraft/transport-m/an72/> [Cited Feb 2, 2011]
- [33] Taylor, J., Allen, J.E., Smith, A.G., "Flight Investigations of Some Airworthiness problems of Civil Boat Seaplanes", Ministry of Supply, Aeronautical research Council Reports and Memoranda, 1958.

- [34] "Seaplane Design Features," Quest for Performance: The Evolution of Modern Aircraft, <http://www.hq.nasa.gov/pao/History/SP-468/ch8-2.htm> [retrieved 15 May 2011].
- [35] Tomaszewski, K. M., "Hydrodynamic Design of Seaplanes." A.R.C. Technical Report. Ministry of Supply. Aeronautical Research Council. London, United Kingdom, 1950.
- [36] Vargas, F., "Concept Design of Seaplane Floats", Individual Dissertation Project, University of Glasgow, 2011
- [37] Benson, J., Bidwell J., "Bibliography and Review of Information relating to the Hydrodynamics of Seaplanes", NACA Advance Confidential Wartime Report, 1945
- [38] Dathe, I., "Hydrodynamic Characteristics of Seaplanes as Affected by Hull Shape Parameters," A.I.A.A. Advance Marine Vehicles Journal, United States of America, 1989.
- [39] Fletcher, G. L., Llewelyn-Davies, D. I., "Note on Some Tank Tests on the Sunderland III for Takeoff at Extreme Overload", British R.A.E. Report, Aero 1887, UK, 1943.
- [40] Davis B., W., "Analysis of Results - Hydrodynamic Research Project", Boeing Aircraft Company, Rep. No. D-5558, USA, 1944.
- [41] Brimm, D. J., "Seaplanes: Maneuvering, Maintaining, Operating", Pitman Publishing Corporation, New York, NY, 1937.
- [42] Langley, M., "Seaplane Float and Hull Design", Sir Isaac Pitman & Sons, LTD, London, UK, 1935.
- [43] Garner, H. M., Coombes, L. P., "Seaplane Hulls and Floats: An Epitome of Present Knowledge with Suggestions for Future Research," Aircraft Engineering and Aerospace Technology, Vol. 2, No. 9, 1930, pp. 221-225.
- [44] Munro, W., "Marine Aircraft Design", Sir Isaac Pitman & Sons, LTD., London, 1933
- [45] Nelson, W., "Seaplane Design", 1st ed. McGraw-Hill Book Company, Inc., New York, NY, 1934.
- [46] Carter, A. W., "Recent N.A.C.A. Research on High Length-Beam Ratio Hulls," Journal of the Aeronautical Sciences, Vol. 17, No. 3, 1949, pp. 167-183.
- [47] Benson, J. K., Lina, L. J., "The Use of a Retractable Planning Flap Instead of a Fixed Step on a Seaplane," NACA L-257, 1943.
- [48] Mottard, E. J., "A Brief Investigation of the Effect of Waves on the Take-Off Resistance of a Seaplane," NASA TN-D-165, 1959.
- [49] Jenkinson, L. R., Marchman, J. F., 1993, "Aircraft design projects: for engineering students", American Institute of Aeronautics and Astronautics, Inc.; Oxford: Butterworth-Heinemann, Reston, VA, 1993.
- [50] Klemin, A., Pierson, J.D., Storer, E. M., "An Introduction to Seaplane Porpoising," Journal of the Aeronautical Sciences, Vol. 6, No. 8, 1939, pp. 311-318.
- [51] Smith, A.G., White H. G., "A review of Porpoising Instability of Seaplanes," A.R.C. Technical Report. Ministry of Supply. Aeronautical Research Council. London, United Kingdom, 1954
- [52] Vagianos, N. J., Thurston, D. B., "Hydrofoil Seaplane Design," Thurston Aircraft Corp., Rept. to Department of the Navy Air Systems Command, Sanford, ME, 1970.
- [53] "The Hydrofoil and Float Combination," Seaplane Pilots Association, Aug. 2008, http://www.seaplanes.org/mambo/index.php?option=com_content&task=view&id=221&Itemid=245 [retrieved 20 June 2011].
- [54] Wood, R., "Performance Multihulls Part 1 and 2", Multihull Review Magazine, UK, 2007.
- [55] Brown, J., "The Case for the Cruising Trimaran", BookSpecs Publishing, Pennsville, NJ 08070, USA, 2010.
- [56] Mohanty, P., "Concept Design of Seaplane Hulls", Individual Dissertation Project, Aerospace Engineering, University of Glasgow, 2011
- [57] Bertorello, C., Bruzzone, D., Cassella, P., Zotti, I. "Trimaran Model Test Results and Comparison with Different High Speed Craft." Elsevier Science Ltd. Italy, 2001.
- [58] Begovic, E., Bertorello, C., Cassella, P., "Calm Water Experimental Research On Geosims Of High Speed Trimaran Hydrodynamic Characteristics And Model-Ship Correlation", Practical Design of ships and other floating structures, Elsevier Science limited, 2001.
- [59] "Retractable Floats", google.com 2011; <http://www.tigerfishaviation.net/> [Cited April 21, 2011]
- [60] Raymer, D. P., "Aircraft Design, A Conceptual Approach", Chapter XII "Aerodynamics", page 285, American Institute of Aeronautics and Astronautics, Inc., Washington D.C., USA, 1992
- [61] Raymer, D. P., "Aircraft Design, A Conceptual Approach", Chapter XV "Weights", page 395, American Institute of Aeronautics and Astronautics, Inc., Washington D.C., USA, 1992.
- [62] Bradley, K. R., "A sizing methodology for the conceptual design of blended-wing-body transports". CR 2004-213016, NASA, September 2004.
- [63] Schaufele, R. D., "The Elements of Aircraft Preliminary Design". Aries Publications, 2000.

- [64] Langley, M., “*Seaplane Float and Hull Design*”, Chapter IV “*Float Design*”, page 65, Sir Isaac Pitman & Sons, LTD, London, UK, 1935.
- [65] Parkinson, J. B., “*Design Criterions for the Dimensions of the Forebody of a Long-Range Flying Boat,*” Wartime Report 3K08. National Advisory Committee for Aeronautics, Washington, USA, 1943
- [66] “*Main Float Buoyancy,*” FAR 23.751, Federal Aviation Administration, 2011.
- [67] Comstock, J., “*Principles of Naval Architecture.*” New York: Society of Naval Architects and Marine Engineers. 1967.
- [68] Wells, V., “*Review of Aircraft Aerodynamics,*” Course Notes, Dept of Aerospace Engineering, Arizona State University, 2008.
- [69] Sederberg, M. T., Sederberg, T. W., “*T-Splines: A Technology for Marine Design with Minimal Control Points*”, Chesapeake Powerboat Symposium, Annapolis, MD, March 2010.
- [70] Dahlmo KI Andersson M., Gellerstedt M., and Karlsson S., “*Methods to assess the accuracy of a CAD program,*” Nobel Biocare, S-402 26 Goteborg, Sweden.
- [71] “*Industries using SOLIDWORKS,*” google.com 2013 <http://www.solidworks.com/sw/successes/overview-results.htm> [Cited Feb. 19, 2013]
- [72] Amihan, C., Chen E., Nadzakovic, Z., Pickering, R., “*The High-Altitude, Long Endurance, Blended Wing Body*” Final Year Project, Dept of Aerospace Engineering, Arizona State University, 2010
- [73] Callaghan, J. T., and Liebeck, R. H., “*Some thoughts on the design of subsonic aircraft for the 21st century*”. SAE Paper No. 901987, October 1990.
- [74] Liebeck, R. H., Page, M. A., Rawdon, B. K., Scott, P. W., and W. R. A. “*Concepts for advanced subsonic transports*”. CR 4624, NASA, September 1994.
- [75] Ko, Y. A. “*The Multidisciplinary Design Optimization of a Distributed Propulsion Blended-Wing-Body Aircraft*”. PhD thesis, Virginia Tech, Blacksburg, VA., April 2003.
- [76] Bradley, K. R., “*A sizing methodology for the conceptual design of blended-wing-body transports*”. CR 2004-213016, NASA, September 2004.
- [77] Jedlicka,L., “*Seaplane Conversion Artistic Images,*” UG student of VSVU Bratislava (Slovakia)

Appendix

Appendix A. Empirical Equations

A.1 Empty Weight Breakdown Equations

A.1.1. Structures

Wing For composites $ff = 0.6528$, else $ff = 0.768$. Value of 0.768 is a multiplicative factor for flying wings.

$$W_{wing} = 0.036 S_w^{0.758} W_{fw}^{0.0035} \left(\frac{AR}{\cos^2 \Lambda} \right)^{0.6} q^{0.006} \lambda^{0.04} \frac{100 t}{\cos^2 \Lambda} (N_z GW)^{0.49} ff \quad (\text{A.1.1})$$

where ff =Fudge Factors, N_z =Ultimate Load Factor; $=1.5x$ limit load factor, t =Wing Thickness, S_w =Trapezoidal Wing Area, W_{fw} =Weight of Fuel in Wing.

Fuselage For a conventional aircraft the equation for the weight of the fuselage is as follows. For advanced composites $ff = 0.9$, else $ff = 1$.

$$W_{fuselage} = [0.052 S_f^{1.086} (N_z GW)^{0.177} L_t^{-0.051} (L_f/d)^{-0.072} q^{0.241}] ff + W_{press} \quad (\text{A.1.2})$$

$$W_{press} = 11.9 + (V_{pr} \Delta P)^{0.271} \quad (\text{A.1.3})$$

where S_f =Fuselage Wetted Area, L_t =Tail Length, L_f =Total Fuselage Length, d =Fuselage Structural Depth, W_{press} =Weight Penalty due to Pressurization, V_{pr} =Volume of Pressurized Section, ΔP =Pressure Difference

Centerbody For a Blended Wing Body (BWB) aircraft, the fuselage or centerbody is split into two sections, the crew cabin and the aft section, in order to predict the weight accurately.

Cabin The weight of the BWB cabin is taken from [62], who derived the equation from the weight equation of a cigar shaped fuselage.

$$W_{cabin} = 1.8032 GW^{0.166552} S_{cabin}^{1.061158} ff \quad (\text{A.1.4})$$

where S_{cabin} =Cabin Wetted Area.

Aft Eq. (A.1.5), also taken from [62], estimates the weight of the aft section as if it were a horizontal tail, but with modifications in the equation to include engine placement.

$$W_{aft} = (1 + 0.05 N_{en}) 0.53 S_{aft} GW^{0.2} (\lambda_{aft} + 0.5) ff \quad (\text{A.1.5})$$

where N_{en} =Number of engines, S_{aft} =Fuselage Aft Area

Horizontal Tail For advanced composites $ff = 0.83$, else $ff = 1$.

$$W_{horizontal\ tail} = 0.016 (N_z GW)^{0.414} q^{0.168} S_{ht}^{0.896} \left(\frac{100 t/c}{\cos \Lambda_{ht}} \right)^{-0.12} \left(\frac{A}{\cos^2 \Lambda_{ht}} \right)^{0.043} \lambda_h^{-0.02} ff \quad (\text{A.1.6})$$

where t =Wing thickness.

Vertical Tail For advanced composites $ff = 0.83$, else $ff = 1$.

$$W_{vertical\ tail} = 0.073 \left(1 + 0.2 \frac{H_t}{H_v} \right) (N_z GW)^{0.376} q^{0.122} S_{vt}^{0.873} \left(\frac{100 t/c}{\cos \Lambda_{vt}} \right)^{-0.49} \left(\frac{AR}{\cos^2 \Lambda_{ht}} \right)^{0.357} \lambda_{vt}^{0.039} ff \quad (\text{A.1.7})$$

where H_t =Horizontal Tail Height above Fuselage, H_v =Vertical Tail Height above Fuselage

Landing Gear $ff = 0.95$ for advanced composites for both landing gear types.

Main Landing Gear (MLG)

$$W_{MLG} = 0.095(N_l GWL)^{0.768} \left(\frac{L_m}{12}\right)^{0.409} ff \quad (A.1.8)$$

Nose Landing Gear (NLG)

$$W_{NLG} = 0.125(N_l GWL)^{0.566} \left(\frac{L_n}{12}\right)^{0.845} ff \quad (A.1.9)$$

where N_l =Ultimate Landing Load Factor, GWL =Landing Design Gross Weight, L_m =Length of Main Landing Gear, L_n =Length of Nose Landing Gear.

A.1.2. Propulsion Engine

$$W_{installed\ engine} = 2.575 W_{en}^{0.922} N_{en} \quad (A.1.10)$$

Fuel System

$$W_{fuel\ system} = 2.49 V_t^{0.726} \left(\frac{1}{1 + V_i/V_t}\right)^{0.363} N_t^{0.242} N_{en}^{0.157} \quad (A.1.11)$$

where W_{en} =Engine Weight, V_t =Total Fuel Volume, V_i =Integral Tanks Volume, N_t =Number of Fuel Tanks

A.1.3. Equipment Flight Control

$$W_{flight\ control} = 0.053 L_f^{1.536} b^{0.371} (N_z GW x 10^{-4})^{0.8} \quad (A.1.12)$$

Hydraulics

$$W_{Hydraulics} = 0.001 GW \quad (A.1.13)$$

Avionics

$$W_{avionics} = 2.117 W_{uav}^{0.933} \quad (A.1.14)$$

Electrical

$$W_{electrical} = 12.57 (W_{fuelsystem} + W_{avionics})^{0.51} \quad (A.1.15)$$

Anti-Ice System

$$W_{Hydraulics} = 0.002 GW \quad (A.1.16)$$

where W_{UAV} =Uninstalled Avionics Weight

A.2 Flat Plate Drag Area Breakdown Equations

In addition to lift, the wing and body traveling through the air generates drag. The drag consists of viscous or parasite drag as well as lift-induced drag. Most aircraft today travel fast enough that they also have an additional drag arising from compressibility effects.

A useful measure of the parasite drag is the equivalent flat plate-drag area, f . Therefore, the total parasite drag is:

$$D_p = f \frac{1}{2} \rho V^2 \quad (A.2.1)$$

To calculate f is done by doing a drag component buildup. Each exterior component of the airplane is considered separately, and the f of each component is found. The total f of each component is finally sum together of all the drag areas. The equivalent flat plate drag area can be computed from the following expression:

$$f_i = C_f F_i Q_i S_{wet_i} \quad (A.2.2)$$

Where C_f is the friction coefficient, F is the form factor, Q is the interference factor, and S_{wet} is the wetter Area.

Friction coefficient depends on the Reynolds number and the surface roughness, and is affected whether the flow is laminar or turbulent. Friction coefficient can be computed by the following expression:

$$C_f = \frac{0.455}{(\log Re)^{2.58}} \quad (\text{A.2.3})$$

From equation (A.2.3) Re is the Reynolds number. Reynolds number is computed as follows:

$$Re = \frac{\rho V l}{\mu} \quad (\text{A.2.4})$$

l is the characteristic length of the specific component. For wings, and tails it will be the mean aerodynamic chord, while for nacelles, fuselage and other components it would be the length. V will represent velocity, and μ is the dynamic viscosity. Equation (A.2.4) is only valid up to transonic Mach range.

"The form factor (F) is a measure on how "streamlined" the component is. It thus has a major influence on the pressure drag since thin bodies exhibit lower adverse pressure gradients and, therefore, less boundary-layer thickening near the trailing edge" [68]. This factor is a function of the component thickness to length ratio. The following are expressions of the form factor of some the major aircraft components:

$$F_{wing} = 1 + Z \frac{t}{c} + 100 \left(\frac{t}{c} \right)^4 \quad (\text{A.2.5})$$

$$Z = \frac{(2 - M_\infty^2) \cos \Lambda}{\sqrt{1 - M_\infty^2 \cos^2 \Lambda}} \quad (\text{A.2.6})$$

From expression (A.2.5), $\frac{t}{c}$ is the thickness ratio of the wing, therefore, the lower the thickness ratio, the lower the form factor. From (A.2.6) M_∞^2 is Mach number and Λ is the sweep angle. Equations (A.2.5) and (A.2.6) can also be used to find the form factors for tail surfaces, pylons and struts.

The following equation is used to find the form factor of the fuselage, smooth canopies, pods, flying boat hulls, nacelles, and external stores such as auxiliary fuel tanks.

$$F_{Fuselage} = 1 + \frac{60}{(l/d)^3} + \frac{l/d}{400} \quad (\text{A.2.7})$$

$$\frac{l}{d} = \frac{l}{\sqrt{(4/\pi) A_{max}}} \quad (\text{A.2.8})$$

The form factor for squared sided fuselages should increase by about 40%, by about 50% for flying boat hull, and 7% for transport-type canopies.

The interference factor Q is the aerodynamic interference between the component and its surrounding components. For example, the dynamic pressure can be increased or reduced at a junction between a fuselage and tail surface, which alters the drag of the tail relative to its isolated drag. This interference factors tend to have values from about 1 for the fuselage and well-filletted wing to about 1.5 for fuselage-mounted nacelles.

The wetted area S_{wet} is the actual area exposed to the air. The air can only create stress on surfaces that it touches, so the relevant area over which the friction or the pressure will act is the wetted area. Calculations of this value are determined by the geometry of the aircraft and even Computer Aided Design (CAD) software can help calculate this value.

The components of the aircraft that do not fit to equation (A.2.2) should be computed using different equations. If the fuselage has an upsweep, the flat plate drag area should be computed by the following:

$$f_{ups} = 3.83 u^{2.5} A_{max} \quad (\text{A.2.9})$$

Where u is the upsweep angle and A_{max} is the fuselage cross sectional area. For wind milling propeller engines the following expression is used to calculate the flat plate drag area:

$$f_{prop} = \begin{cases} 0.1\sigma A_{disk} & feathered \\ 0.8\sigma A_{disk} & stopped \end{cases} \quad (\text{A.2.10})$$

Where A_{disk} is the disk area, and σ is expressed as follows:

$$\sigma = \frac{B c_{avg}}{\pi R} \quad (\text{A.2.11})$$

And B is the number of blades, c_{avg} is the average blade chord, and R is the propeller radius. Finally, to calculate the coefficient of parasite drag, first calculate drag from the following:

$$D = \frac{1}{2} C_D \rho_0 V^2 S_{wing} \quad (\text{A.2.12})$$

Then replacing equation (A.2.12) to (A.2.1) and deriving the coefficient of drag the following is obtained:

$$C_{DP} = \frac{f}{S_{wing}} \quad (\text{A.2.13})$$

So the total flat plate drag area depends on the wing area. So as the wing area increases, parasite drag decreases. But as the flat plate drag area increases, parasite drag increases.

A.3 Aircraft Flight Performance Equations

The performance of an aircraft is important parameters that are calculated in order to compare the aircraft with other competitors and to evaluate the whole aircraft performance in the conceptual design. So the computations that were done in this project for the performance of this aircraft is required thrust and power, level flight airspeed, total time of flight on take-off, climb, cruise, descent and landing, endurance and range and finally steady level turns.

Equation (A.3.1) is the expression for lift coefficient.

$$C_L = \frac{2mg}{\rho_0 S_{wing} V^2} \quad (\text{A.3.1})$$

To calculate the minimum or stall speed the following expression is utilized:

$$V_{min} = V_{so} = \sqrt{\frac{2mg}{C_{Lmax} \rho_0 S_{wing}}} \quad (\text{A.3.2})$$

To calculate the equivalent airspeed is as follows:

$$V_{EAS} = V_{TAS} \sqrt{\sigma} \quad (\text{A.3.3})$$

$$\sigma = \frac{\rho}{\rho_0} = \frac{20000 - H}{20000 + H} \quad (\text{A.3.4})$$

To calculate the service and absolute ceiling of an aircraft is necessary to calculate the climb speed, climb angle and the climb gradient. The following shows the equations for climb speed, climb angle and climb gradient, respectively:

$$V_c = \frac{(T_A - T_R)V_{TAS}}{mg} = \frac{(P_A - P_R)}{mg} \quad (\text{A.3.5})$$

$$\theta = \arcsin\left(\frac{V_c}{V_{TAS}}\right) = \arcsin\left(\frac{T_A - T_R}{mg}\right) \quad (\text{A.3.6})$$

$$grad_c = \tan(\theta) \times 100 \quad (\text{A.3.7})$$

Where T_A and P_A are the thrust available and power available generated by the engines of the aircraft. Another important parameter of the climb section useful in the performance of an aircraft is the time and distance climb. The following equations are useful to calculate the time and distance of climb:

$$t_{c_{1,2}} = \int_{H_1}^{H_2} \frac{dH}{V_{C(h)}} \cong \frac{\Delta H}{V_{Ca}} \quad (\text{A.3.8})$$

$$l_{c_{1,2}} = \int_{t_1}^{t_2} V_{TAS} \cos(\theta) dt \quad (\text{A.3.9})$$

For aircraft with low power to weight ratio it can be assumed that $\cos(\theta) \approx 1$. Therefore, (A.3.9) is derived as follows:

$$l_{c_{1,2}} = \int_{t_1}^{t_2} V_{TAS} dt \cong \Delta V_{TASa} \quad (\text{A.3.10})$$

Finally, with the climb speeds of the aircraft the absolute and service ceiling can be calculated. Same rules apply for the descent characteristics of the aircraft, however using different equations. Since the aircraft is not descending at a perfect vertical line, an angle of descent must be added to calculate the lift coefficient at descent. The following equation is used:

$$C_L = \frac{2mg}{\rho_0 V_{EAS}^2 S_{wing}} \cos(\theta) \quad (\text{A.3.11})$$

The angle of descent can be established by the aircraft to calculate the required thrust or it can be calculated by the following derivation:

$$\theta = \arctan\left(\frac{D}{L}\right) = \arctan\left(\frac{C_D}{C_L}\right) = \arctan\left(\frac{V_D}{V_x}\right) \quad (\text{A.3.12})$$

Where V_D is the speed of descent and V_x is the horizontal speed and are derived from the following expressions:

$$V_D = V_{TAS} \sin \theta \quad (\text{A.3.13})$$

$$V_x = V_{TAS} \cos \theta \quad (\text{A.3.14})$$

where $V_{TAS} = \frac{1}{(C_L^2 + C_D^2)^{\frac{1}{4}}} \sqrt{\frac{2mg}{S_{wing} \rho}}$ (A.3.15)

To calculate the required thrust Newton's second law is applied, where:

$$D - T_R = mg \sin \theta \quad (\text{A.3.16})$$

Deriving T_R and simplifying Drag (D), the following is obtained:

$$T_R = \frac{1}{2} C_D \rho_0 V_{EAS}^2 S_{wing} - mg \sin \theta \quad (\text{A.3.17})$$

The same equations to calculate the time of descent and distance of descent (A.3.8) and A.3.10) apply as in the climb section, however changing the climb speed to speed of descent.

Two other aspects that are calculated on the flying segment of an aircraft are the take-off and landing. Most aircraft required large amounts of thrust in order to perform the required take-off specified by the aviation authorities. So to calculate the required thrust for the aircraft to perform the take-off segment, it must be calculated the acceleration. The acceleration will be divided on the ground run, and acceleration on air. To calculate acceleration on ground, Applying Newton's Second Law, the following is obtained:

$$acc = \frac{(T_A - D - F)}{m} \quad (\text{A.3.18})$$

Where T_A is the thrust available, D is Drag Force and F is the Gear drag or Friction Force. To calculate F the following is used:

$$F = \mu(mg - L) \quad (\text{A.3.19})$$

μ is the friction coefficient. When the aircraft is at the air, F is removed from equation (A.3.18):

$$acc = \frac{(T_A - D)}{m} \quad (\text{A.3.21})$$

With the acceleration of the aircraft on both on the ground run and air, the time and distance to take-off can be calculated. This time will be calculated until the aircraft reaches lift-off speed before it starts the transition arc. To calculate the lift-off speed (V_{LOF}) and take-off safety speed (V_r) the following is used:

$$V_r = 1.1V_{S0} \quad (\text{A.3.22})$$

$$V_{LOF} = 1.2V_{S0} \quad (\text{A.3.23})$$

Then to calculate the distance of take-off until the aircraft reaches take-off safety speed is as follows:

$$l_t = l_{t-\Delta t} + \Delta l \quad (\text{A.3.24})$$

$$\Delta l = \frac{(V_t + V_{t-\Delta t})}{2} \Delta t \quad (\text{A.3.25})$$

and finally to calculate the real time speed necessary to calculate the distance, since $acc = \frac{dV}{dt}$, deriving from this expression:

$$V_t = V_{t-\Delta t} + \Delta V \quad (\text{A.3.26})$$

$$\Delta V = acc \Delta t \quad (\text{A.3.27})$$

So this method of calculation requires loop iterations where acceleration depends on Lift, and Drag Force; Lift and Drag Force requires speed; and speed depends on acceleration.

So after the aircraft had reached take-off safety speed (V_t), the aircraft must perform a transition arc, in which a lift load factor is required. With the lift load factor calculated, the radius of transition arc, the angle of climb, the length of transition arc, the increment of altitude and the time of transition arc are derived by the following, respectively:

$$n_L = \frac{L}{mg} = \left(\frac{V_{LOF}}{V_{S0}} \right)^2 \quad (\text{A.3.28})$$

$$r = \frac{V_{LOF}^2}{g(n_L - \cos\theta)} \quad (\text{A.3.29})$$

$$\theta = \arcsin\left(\frac{T_A - T_R}{mg}\right) \quad (\text{A.3.30})$$

$$l_3 = r\sin\theta \quad (\text{A.3.31})$$

$$h_3 = r(1 - \cos\theta) \quad (\text{A.3.32})$$

$$t_3 = \frac{l_3}{V_{LOF}} \quad (\text{A.3.33})$$

Finally for the final climb up to 10.5 m (35ft), the following equations to calculate the length of climb and time of climb are used:

$$l_4 = \frac{H - h_3}{\theta} \quad (\text{A.3.34})$$

$$t_4 = \frac{l_4}{V_{LOF}\cos\theta} \quad (\text{A.3.35})$$

For the landing segment, the same iteration loop that is used to calculate the take-off segment is also applied. First the available speed and the touchdown speed should be calculated:

$$V_A = 1.3V_{S0} \quad (\text{A.3.36})$$

$$V_{TD} = 1.05V_{S0} \quad (\text{A.3.37})$$

Therefore, first the descent from altitude of 15m (50ft) must be calculated. So using equations (A.3.34) and (A.3.35) the initial length of climb and time are calculated, where h_3 will be from (A.3.32) and r will come from (A.3.29). The only difference to the equations above will be replacing V_{LOF} with V_A . The same will be apply to the transition arc segment at landing, however a new airspeed at the end of the arc must be calculated and an end time using the following derivations:

$$V_F = \sqrt{V_A^2 - 2gh_3} \quad (\text{A.3.38})$$

$$t_2 = \frac{2l_3}{(V_A + V_F)} \quad (\text{A.3.39})$$

So for the deceleration on the air and ground same rule applies as in the take-off segment. However, the acceleration will be calculated differently. Since no thrust is required at landing and the drag force will act in the opposite side, a new derivation for the acceleration (deceleration) on the air is being calculated:

$$acc = \frac{(-D)}{m} \quad (\text{A.3.40})$$

As the aircraft touches the ground, the acceleration force will add the gear drag and the following is applied:

$$acc = \frac{(-D - F)}{m} \quad (\text{A.3.41})$$

where

$$F = \mu_f F_f + \mu_m F_m \quad (\text{A.3.42})$$

and

$$F_f = \frac{(mg - L)X_G - (acc \cdot m + D)Y_G}{X_F} \quad (\text{A.3.43})$$

$$F_m = mg - L - F_f \quad (\text{A.3.44})$$

F_f stands for force on front gear, F_m is the force on the main gears, X_G is the horizontal arm of centre of gravity, Y_G is the vertical arm of centre of gravity, X_F is the horizontal arm of front gear, μ_f is the friction coefficient when no brakes are applied and μ_m is the friction coefficient when brakes are applied. After the acceleration is calculated, the speed is calculated using equation (A.3.27), and finally the distance is calculated until the aircraft reaches 0 speed using equation (A.3.25).

Calculating the performance time and distance of take-off, climb, descent, and landing, it can be calculated the cruise time and distance using the maximum fuel capacity the aircraft can carry. From equation (11) the fuel for level flight is calculated using the following:

$$m_{fL} = m_f - m_{fTAXI} - m_{fTO} - m_{fC} - m_{fD} - m_{fLN} - m_{fH} \quad (\text{A.3.45})$$

Where m_f is the total mass of the fuel, L is level flight, $Taxi$ is fuel at taxi segment, TO stands for take-off, C is climb, D is for descent, LN is for landing, and H is for holding fuel or fuel reserve. To calculate the mass of the fuel for each segment the following equation is used:

$$m_{fi} = t_i FC_{hr} \quad (\text{A.3.46})$$

t_i is the total time of each flight segment and FC_{hr} is the Fuel consumption per hour derived from the following:

$$FC_{hr} = SFC \times P \quad (\text{A.3.47})$$

SFC is the specific fuel consumption and P is the shaft power of the engine. Engines have different ratings in which the engine can be operating depending on the flight segment; maximum contingency, maximum take-off, maximum continuous, and idle. At take-off the engines operate at maximum take-off, at climb and level flight engines are operating at maximum continuous rating, and for descent and landing engines operate at idle rating. Once the mass of the fuel at level flight is calculated using equation (A.3.45), the time of flight can be calculated using equation (A.3.46). The distance at level flight is computed from the following:

$$l_L = V_{cruising} t_L \quad (\text{A.3.48})$$

The sum of the all the distance segments will give the range of the aircraft. Finally, another aspect of the performance of the aircraft that can be calculated is the steady level turns. This is obtained if the available thrust equals the required thrust, expressed as followed:

$$T_A = T_R = \frac{1}{2} C_D \rho S_{wing} V^2 \quad (\text{A.3.49})$$

A.4 Hull geometrical empirical formulas

Bow Height:

$$h_b = 0.65b \quad (\text{A.4.1})$$

Step Height:

$$S_b = 0.09b \quad (\text{A.4.2})$$

Flat forebody length:

$$l_c = 1.7b \quad (\text{A.4.3})$$

Chine Flare Length:

$$c_b = 0.08b \quad (\text{A.4.4})$$

Appendix B. Artistic impressions of the conversion of current certified aircraft to a seaplane

The following images are an impression of the artist of some certified aircraft that could be converted into a seaplane [77]. The characteristics of this aircrafts are shown in Table 2.



Fig. 84: Artistic Impression of LET L-410 [77]

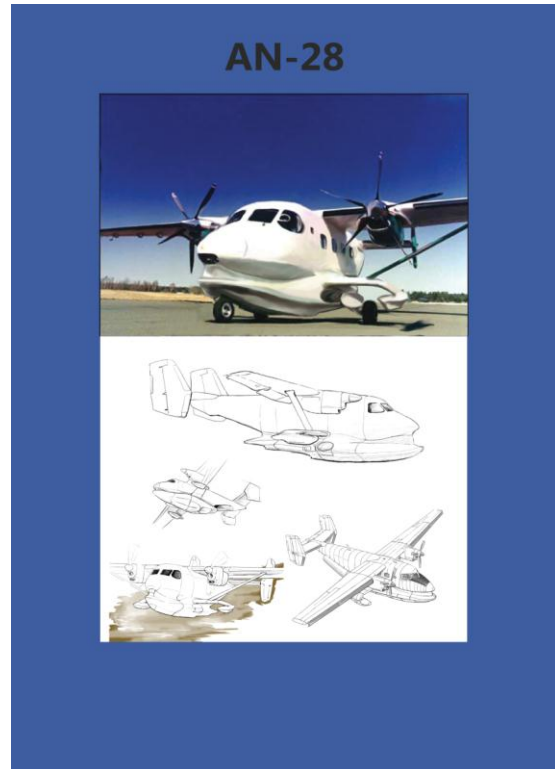


Fig. 85: Artistic Impression of Antonov AN28 [77]



Fig. 86: Artistic Impression of BAE 146 [77]



Fig. 87: Artistic Impression of Dornier DO-228 [77]

Appendix C. MATLAB Optimization Source Code

```

%% Floating Device Optimized Testing Source Code %%
%%% by Alan Canamar %%%
clc; clear all

%% Input Parameters

global GW g0 rho0 rhos ...
Sexp2 CLmax0 d L

prompt = {'Enter Maximum Takeoff Weight [kg]:',...
    'Enter Main Landing Gear Weight [kg]:',...
    'Enter Nose Landing Gear Weight [kg]:','Enter Empty Weight [kg]:',...
    'Enter Maximum Fuel Weight [kg]:','Enter Maximum Payload Weight
[kg]:',...
    'Enter Wing Area [m^2]:','Enter Fuselage Diameter [m]:'};
prompt2 = {'Enter Fuselage Length [m]:','Enter Wing Span [m]:',...
    'Enter Maximum Lift Coefficient:','Enter Plate Drag Breakdown [m^2]:',...
    'Enter Cruising Speed [km/hr]:','Enter Cruising Altitude [m]:',...
    'Enter Center of Gravity of Landplane from Bottom [m]:',...
    'Enter Thrust Available of Aircraft [N]:'};
dlg_title = 'Input Initial Aircraft Parameters';
num_lines = 1;
def = {'7600','80','70','4600','1550','1850','39.02','2.4'};
def2 = {'13.69','23.47','1.3','0.445','900','12200','0.7','40500'};
C = inputdlg(prompt,dlg_title,num_lines,def);
C2 = inputdlg(prompt2,dlg_title,num_lines,def2);
GW = str2double(C(1,1));           %Maximum Takeoff Weight [kg]
MLG = str2double(C(2,1));         %Main Landing Gear Weight [kg]
NLG = str2double(C(3,1));         %Nose Landing Gear Weight [kg]
EW = str2double(C(4,1));          %Empty Weight [kg]
MF = str2double(C(5,1));          %Maximum Weight of Fuel [kg]
Wpay = str2double(C(6,1));        %Maximum Payload Weight [kg]
Sexp2 = str2double(C(7,1));       %Wing Area [m^2]
d = str2double(C(8,1));          %Diameter of Fuselage [m]
L = str2double(C2(1,1));         %Length of Fuselage [m]
b2 = str2double(C2(2,1));        %Wing Span [m]
CLmax0 = str2double(C2(3,1));    %Maximum Lift Coefficient of the Wing
ftotal_air = str2double(C2(4,1)); %Aircraft Flat Plate Breakdown [m^2]
Vel = str2double(C2(5,1));        %Cruising speed [km/hr]
ALT = str2double(C2(6,1));        %Cruising altitude [m]
CGL = str2double(C2(7,1));        %Center of Gravity [m]
TA = str2double(C2(8,1));        %Thrust Available [N]

%% Global Inputs
rhoW = 1000;                      %Density of Water [kg/m^3]
rhoS = 1025;                       %Average Density of Salt Water [kg/m^3]
g0 = 9.80665;                      %Gravitational Constant [m/s^2]
rho0 = 1.225;                      %Density of air at Sea Level [kg/m^3]

%% WEIGHTS
%Weight of Landing Gear
WLG = MLG+NLG;

%Total Gross Weight with no Landing Gear [kg]

```

```

GW0 = GW - WLG;

%Weight of Boat Hull [kg]
Wb = round(GW0*0.12); %Aluminum Material
Wbc = round(GW0*0.03); %Composite Materials

%Weight of Floats [kg]
nf = 2; %Total number of floats
if nf == 0;
    Wft = 0;
else
    Wf = round(GW0*0.02);
    Wft = Wf*nf; %Total Weight of floats [kg]
end
Wftc = round(Wft*0.5); %Composite Materials

%Weight of Mid Wing Stabilizers [kg]
nMW = 2; %Total number of stabilizers
if nMW == 0;
    WMW = 0;
else
    WMW = round(GW*0.02);
    WMW = WMW*nMW; %Total Weight of stabilizers [kg]
end
WMWc = round(WMW*0.5); %Composite Materials

%Weight of Wing Tip Stabilizers [kg]
nWT = 2; %Total number of stabilizers
if nWT == 0;
    WWT = 0;
else
    WWT = round(GW*0.012);
    WWT = WWT*nWT; %Total Weight of stabilizers [kg]
end
WWTc = round(WWT*0.5); %Composite Materials

%Total Empty Weight Seaplane with Floats, Boat Hull [kg]
Ewt = EW+Wb+Wft; %Aluminum Material
Ewc = EW+Wbc+Wftc+50; %Composite Materials

%Total Empty Weight Seaplane with Mid Wing, Boat Hull [kg]
EWMt = EW+Wb+WMW; %Aluminum Material
EWMc = EW+Wbc+WMWc; %Composite Materials

%Total Empty Weight Seaplane with Wing Tip, Boat Hull [kg]
EWWTt = EW+Wb+WWT; %Aluminum Material
EWWTc = EW+Wbc+WWTc; %Composite Materials

%Reduced Payload Weight, Using Max Fuel [kg]
WPa = GW - EW - MF; %Landplane
WPs = GW - Ewt - MF; %Aluminum Seaplane
WPSc = GW - Ewc - MF; %Composite Seaplane

%Reduced Fuel Weight, Using Max Payload [kg]
WFa = GW - EW - Wpay; %Landplane

```

```

WFs = GW - Ewt - Wpay;      %Aluminum Seaplane
WFsc = GW - Ewc - Wpay;     %Composite Seaplane

%% Trimaran Dimensions
[b,Lh,bo,Lo,y,h,ho] = Trimaran_Dimensions();

%% Stabilizer Dimensions
[bstab,Lstab,dstab,l,VF1] = Stabilizer_Dimensions(CGL);

%% WingTip Floats Dimensions
[bstabWT,LstabWT,dstabWT,VFWT1] = Wingtip_Dimensions(CGL,b2);

%% Hydrostatics of Seaplane
[GMS,GMSy,Dras] = Hydrostatics(b,Lh,h,bo,Lo,ho,y,CGL,b2,bstab,Lstab,dstab, ...
    l,bstabWT,LstabWT,dstabWT,VF1,VFWT1);

%% Water Loads
[a] = WaterLoads(b,Dras);

%% Drag Curves
[DPi,DPis] = Drag_Curves(L,b2,d,b,Lh,bo,Lo,TA,ALT);

%% Aerodynamic Drag Comparison
[Cd,Cdsi,Cdsie,ftotal_air] = Aero_Drag(Lh,b,Lo,bo,Vel,ALT);

%% Aircraft Drag
[Cd,D] = Aircraft_Drag(ftotal_air,b2,Vel,ALT);

%% Seaplane Drag Increase
[Cdsi,Cdsie,Cdsist,Cdsiest,CdsiWT,CdsieWT] = Seaplane_Drag(Lh,b,Lo,bo, ...
    bstab,Lstab,bstabWT,LstabWT,Vel,ALT);

%% Water Performance
[FTm,Rw] = Water_Resistance(Lh,Lo,b,h,bo,ho,Lstab,bstab, ...
    dstab,bstabWT,LstabWT,dstabWT,VF1,VFWT1,TA,CLmax0,ALT);

%% Flight Performance TurboProp Engine
[Ttotal,Ltotal,Ttotalse,Ltotalsej,Vmax,Vmaxs] = Flight_Performance...
    (EW,EWC,MF,Wpay,Cd,Cdsi,Cdsie,Lh,Lo,b,bo,TA,ALT,Vel);

%% Flight Performance JET Engine
[Ttotalj,Ltotalj,Ttotalsej,Ltotalsej,Vmax,Vmaxs] = Flight_Performance_JET...
    (EW,EWC,MF,Wpay,Cd,Cdsi,Cdsie,Lh,Lo,b,bo,TA,ALT,Vel);

%% Gust Envelope
[Vstall] = Gust(ALT,Vel);

%% Results
fprintf('-----')
fprintf('\n Weight Parameters\n')
fprintf('\n Total Gross Weight no Landing Gear [kg] = %g\n', GW0)
fprintf('\n Total Weight of Floats [kg] = %g\n', Wftc)
fprintf('\n Total Weight of Boat Hull [kg] = %g\n', Wbc)
fprintf('\n Total Weight of Stabilizers [kg] = %g\n', WMWc)

```

```

fprintf('\n Total Weight of Wing Tip Floats [kg] = %g\n', WWTc)
fprintf('\n Empty Weight of Seaplane Trimaran [kg] = %g\n', EWC)
fprintf('\n Empty Weight of Seaplane Mid Wing [kg] = %g\n', EWMc)
fprintf('\n Empty Weight of Seaplane Wing Tip [kg] = %g\n', EWWTC)
fprintf('\n Payload Weight of Seaplane w/Max Fuel [kg] = %g\n', WPsc)
fprintf('\n Fuel Weight of Seaplane w/Max Payload [kg] = %g\n', WFsc)
fprintf('\n-----\n')

%% Sizing Trimaran Geometry Code Created by Alan Canamar %%

function [b,Lh,bo,Lo,y,h,ho] = Trimaran_Dimensions()
%% Declare global variables
global GW rhos L

%% Trimaran Dimensions
% clc; clear all
% GW = 6600; %Total Gross Weight of Aircraft [kg]
% rhos = 1025; %Density of Salt Water [kg/m^3]
% L = 14.47; %Length of Fuselage [m]
% CGL = 1.594; %Landplane Centre of Gravity [m]
% b2 = 19.08; %Wingspan [m]
BouyR = 1.9; %Bouyancy Reserve [Percent]
HullR = 1.5; %Hull Displacement [Percent]
OutR = BouyR - HullR; %Outrigger Displacement [Percent]
delT = BouyR*GW; %Aircraft Total Displacement on Water [kg]
delb = HullR*GW; %Boat Hull Total Displacement [kg]
del0 = OutR*GW; %Outriggers Total Displacement [kg]
del1 = del0/2; %Displacement on one Outrigger [kg]

%% Boat Hull Design
lf_lah = 2.07; %Afterbody Forebody Ratio [Percent]
Bhh = 0.65; %Bow height increment [Percent]
Shh = 0.09; %Step Height increment [Percent]
chh = 0.08; %Chine Flare increment [Percent]
Lch = 1.7; %Flat Forebody increment [Percent]
V = delb./rhos; %Displacement Volume [m^3]
Lh = Inf; %Length [m]
SLR = 20; %Slenderness Ratio
precision = 0.01;
precisionK = 0.0001;
minK = 0.0525;
maxK = 0.0975;
matK = [(minK:precisionK:maxK)', Inf(length(minK:precisionK:maxK),1), ...
          Inf(length(minK:precisionK:maxK),1), ...
          Inf(length(minK:precisionK:maxK),1)];
i = 1;
for K = minK:precisionK:maxK
    while Lh > L
        Lf_b = SLR/lf_lah; %Forebody Ratio
        Cv0 = K*Lf_b^2; %Static Load Coefficient
        b = (delb/(rhos*Cv0))^(1/3); %Beam Width [m]
        Lh = SLR*b; %Length [m]
        Lhf = (1/lf_lah)*L; %Forebody Length [m]
        Lha = L-Lhf; %Afterbody Length [m]
        h = b*Bhh; %Bow Height [m]
        S = b*Shh; %Step Height [m]
    end
end

```

```

ch = b*chh;           %Chine Flare [m]
Lc = b*Lch;           %Flat Forebody Length [m]
if Lh > L
    SLR = SLR - precision;
end
matK(i,2) = SLR;
matK(i,3) = Lh;
matK(i,4) = b;
i=i+1;
Lh = Inf;
SLR = 20;
end

%Calculations for Boat Hull
[SLR, idx] = max(matK(:,2));
K = matK(idx,1);
Lf_b = SLR/lf_lah;      %Forebody_beam Ratio
Cv0 = K*Lf_b^2;          %Static Load Coefficient
b = (delb/(rhos*Cv0))^(1/3); %Beam Width [m]
Lh = SLR*b;              %Length [m]
Lhf = (1/lf_lah)*Lh;     %Forebody Length [m]
Lha = Lh-Lhf;             %Afterbody Length [m]
h = b*Bhh;                %Bow Height [m]
S = b*Shh;                %Step Height [m]
ch = b*chh;                %Chine Flare [m]
Lc = b*Lch;                %Flat Forebody Length [m]
Vha = (0.45)*Lh*b*h;      %Actual Volume [m^3]
disp(' ')
if V <= Vha
    fprintf('Hull = Pass');
else
    fprintf('Hull = Fail');
end

%% Outrigger Design part 2
Lb = 14;                  %Length to Beam Ratio
k = 0.08;                  %Spray Coefficient
L_Lo = 0.4925;             %Outrigger to Hull Length ratio
lf_lao = 2.11;              %Afterbody_Forebody Ratio [Percent]
Bho = 0.9;                  %Bow height increment [Percent]
Sho = 0.09;                  %Step Height increment [Percent]
chho = 0.08;                 %Chine Flare increment [Percent]
lco = 1.7;                  %Flat Forebody increment [Percent]
Vo = dell./rhos;            %Displacement Volume [m^3]
Lo = L_Lo*Lh;                %Length [m]
bo = Lo/Lb;                  %Beam width [m]
lf = Lo/lf_lao;              %Forebody Length [m]
la = Lo-lf;                  %Afterbody Length [m]
ho = bo*Bho;                  %Bow Height [m]
Sh = bo*Sho;                  %Step Height [m]
cho = bo*chho;                %Chine Flare [m]
lc = bo*lco;                  %Flat Forebody Length [m]
y = Lh*0.12;                  %Y displacement of Outrigger from main Hull [m]
x = Lh*(-0.0625);            %X displacement of Outrigger from main Hull [m]
Voa = (1/2)*Lo*bo*ho;        %Actual Volume [m^3]

```

```

disp(' ')
if Voa <= Voa
    fprintf('Outrigger = Pass');
else
    fprintf('Outrigger = Fail');
end
disp(' ')

%% Results
fprintf('-----')
fprintf('\n Dimensional Parameters\n')
fprintf('\n Boat Hull Dimensions\n')
fprintf('\n Bouyancy Volume [m^3] = %g\n', V)
fprintf('\n Slenderness Ratio = %g\n', SLR)
fprintf('\n Spray Coefficient = %g\n', K)
fprintf('\n Beam [m] = %g\n', b)
fprintf('\n Length [m] = %g\n', Lh)
fprintf('\n Forebody Length [m] = %g\n', Lhf)
fprintf('\n Afterbody Length [m] = %g\n', Lha)
fprintf('\n Bow Height [m] = %g\n', h)
fprintf('\n Step Height [m] = %g\n', S)
fprintf('\n Chine Flare [m] = %g\n', ch)
fprintf('\n Flat Forebody Length [m] = %g\n', Lc)
fprintf('\n Forebody deadrise angle [deg] = 30\n')
fprintf('\n Afterbody deadrise angle [deg] = 22\n')
fprintf('\n Afterbody Keel angle [deg] = 7\n')
fprintf('\n Actual Volume [m^3] = %g\n', Vha)
disp(' ')
fprintf('\n Outriggers Dimensions\n')
fprintf('\n Bouyancy Volume [m^3] = %g\n', Voa)
fprintf('\n Length to Beam Ratio = %g\n', Lb)
fprintf('\n Spray Coefficient = %g\n', k)
fprintf('\n Beam [m] = %g\n', bo)
fprintf('\n Length [m] = %g\n', Lo)
fprintf('\n Forebody Length [m] = %g\n', lf)
fprintf('\n Afterbody Length [m] = %g\n', la)
fprintf('\n Step Height [m] = %g\n', Sh)
fprintf('\n Flat Forebody Length [m] = %g\n', lc)
fprintf('\n Bow height [m] = %g\n', ho)
fprintf('\n Chine Flare [m] = %g\n', cho)
fprintf('\n Forebody deadrise angle [deg] = 30\n')
fprintf('\n Afterbody deadrise angle [deg] = 25\n')
fprintf('\n Afterbody Keel angle [deg] = 7\n')
fprintf('\n Y displacement [m] = %g\n', y)
fprintf('\n X displacement [m] = %g\n', x)
fprintf('\n Actual Volume [m^3] = %g\n', Voa)
fprintf('\n-----\n')

```

%% HydroStatics code of Trimaran Technology created by Alan Canamar

```

function [GMS,GMSy,Dras] = Hydrostatics(b,Lh,h,bo,Lo,ho,y,CGL,b2,bstab, ...
Lstab,dstab,l,bstabWT,LstabWT,dstabWT,VF1,VFWT1)
%% Declare global variables
global GW rhos

```

%% Input Parameters

```

% clc; clear all
% b = 2.60; %Hull beam [m]
% Lh = 13.69; %Main Hull Length [m]
% h = 1.69; %Hull Bow Height [m]
% bo = 0.48; %Outrigger Beam [m]
% Lo = Lh*0.5; %Outrigger Length [m]
% ho = 0.43; %Outrigger Bow Height [m]
% y = 2.35; %Lateral Distance between Hull and Outrigger [m]
% bstab = 0.95; %Beam of stabilizer [m]
% Lstab = 3.82; %Length of stabilizer [m]
% dstab = 0.48; %Depth of stabilizer [m]
% l = 3; %Distance of Center of Stabilizing Float [m]
% VF1 = 3.48; %Float Volume [m^3]
% bstabWT = 0.65; %Beam of Wing Tip Float [m]
% LstabWT = 2.60; %Length of Wing Tip Float [m]
% dstabWT = 0.32; %Depth of Wing Tip Float [m]
% b2 = 23.47; %Wing Span [m]
% VFWT1 = 1.10; %Float Volume [m^3]
% CGL = 0.70; %Centre of Gravity of Landplane [m]
% GW = 7600; %Total Gross Weight of Aircraft [kg]
% rhos = 1025; %Density of Salt Water [kg/m^3]
BouyR = 1.9; %Bouyancy Reserve [Percent]
HullR = 1.5; %Hull Displacement [Percent]
OutR = BouyR - HullR; %Outrigger Displacement [Percent]
delt = BouyR*GW; %Trimaran Displacement Weight [kg]
delH = HullR*GW; %Hull Displacement Weight [kg]
delO = OutR*GW; %Outrigger Displacement Weight [kg]
delO1 = delO/2; %One Outrigger Displacement Weight [kg]
delF = VF1*rhos; %Displacement Weight of Stabilizer Float [kg]
delFWT = VFWT1*rhos; %Displacement Weight of WingTip Float [kg]
V = delH/rhos; %Hull Displacement Volume [m^3]
Vo = delO/rhos; %Twin Outrigger Displacement Volume [m^3]
Vo1 = delO1/rhos; %One Outrigger Displacement Volume [m^3]
VT = V+Vo; %Trimaran Displacement Volume [m^3]
VS = delt/rhos; %Seaplane Displacement Volume [m^3]

%% Airfoil Area Calculation
KA = 0.7; %Proportionality Coefficient
AHull = KA*Lh*b; %Area of Load Water Plane of Hull [m^2]
Afloat = KA*Lo*bo; %Area of Load Water Plane Float [m^2]
ASTAB = KA*Lstab*bstab; %Area of Load Water Plane Float Stabilizer[m^2]
AWT = KA*LstabWT*bstabWT;%Area of Load Water Plane WingTip Float [m^2]

%% Stability Calculation
%%% Draft Level and Center of Bouyancy in the Lateral Direction [x]
%%% Draft Level and Center of Bouyancy for Hull
Draft = 0.95; %Draft line [Percent]
Drah = V/AHull; %Draught [m]
KBh = Draft*Drah; %Center of Bouyancy [m]
%%% Draft Level and Center of Bouyancy for Outrigger
Drao = Vo/AFloat; %Draught [m]
KBo = Draft*Drao; %Center of Bouyancy [m]
%%% Draft Level and Center of Bouyancy for Stabilizer Float
Drastab = VF1/ASTAB; %Draught [m]
KBstab = Draft*Drastab; %Center of Bouyancy [m]
%%% Draft Level and Center of Bouyancy for Wing Tip Float

```

```

DraWT = VFWT1/AWT;           %Draught [m]
KBWT = Draft*DraWT;         %Center of Bouyancy [m]
%%% Draft Level and Center of Bouyancy for Twin Outrigger
Draot = Vo/(2*AFloat);      %Draught [m]
KBot = Draft*Draot;         %Center of Bouyancy [m]
%%% Draft Level and Center of Bouyancy for Trimaran Outrigger
AT = AHull+(2*AFloat);      %Area of Load Water Plane [m^2]
DraT = VT/AT;                %Draught [m]
KBT = Draft*DraT;           %Center of Bouyancy [m]
%%% Draft Level and Center of Bouyancy for Trimaran Stabilizer
ATs = AHull+(2*ASTAB);      %Area of Load Water Plane [m^2]
DraTs = VT/ATs;              %Draught [m]
KBTs = Draft*DraTs;         %Center of Bouyancy [m]
%%% Draft Level and Center of Bouyancy for Trimaran Wing Tip Float
ATW = AHull+(2*AWT);         %Area of Load Water Plane [m^2]
DraTW = VT/ATW;              %Draught [m]
KBTW = Draft*DraTW;          %Center of Bouyancy [m]
%%% Draft Level and Center of Bouyancy for Seaplane
As = AT;                     %Area of Load Water Plane [m^2]
Dras = VS/As;                %Draught [m]
KBS = Draft*Dras;            %Center of Bouyancy [m]

%%%% METACENTRIC HEIGHT Transverse [x]
%%% Metacentric Height of Hull
% KGh = 0.85;                 %Center of Gravity from keel [m]
Ka = 1.3;
KGh = Ka*(h/2);              %Center of Gravity from keel [m]
K1 = 0.036;                   %Proportionality Coefficient
Ih = K1*Lh*b^3;              %Moment of Inertia [m^4]
BMh = (Ih/V);                %Distance from CB to Metacentre [m]
BGh = KGh - KBh;              %Distance from CG to CB [m]
GMh = BMh - BGh;              %Metacentric Height [m]
%%% Metacentric Height of Outrigger
% KGo = 0.37;                  %Center of Gravity from keel [m]
KGo = Ka*(ho/2);              %Center of Gravity from keel [m]
Io = K1*Lo*bo^3;              %Moment of Inertia [m^4]
BMo = (Io/Vo1);              %Distance from CB to Metacentre [m]
BGo = KGo - KBo;              %Distance from CG to CB [m]
GMO = BMo - BGo;              %Metacentric Height [m]
%%% Metacentric Height of Stabilizer Float
% KGo = 0.37;                  %Center of Gravity from keel [m]
KGstab = Ka*(dstab/2);        %Center of Gravity from keel [m]
Istab = K1*Lstab*bstab^3;%Moment of Inertia [m^4]
BMstab = (Istab/VF1);         %Distance from CB to Metacentre [m]
BGstab = KGstab - KBstab;%Distance from CG to CB [m]
GMstab = BMstab - BGstab;%Metacentric Height [m]
%%% Metacentric Height of Wing Tip Float
% KGo = 0.37;                  %Center of Gravity from keel [m]
KGWT = Ka*(dstabWT/2);        %Center of Gravity from keel [m]
IWT = K1*LstabWT*bstabWT^3;%Moment of Inertia [m^4]
BMWWT= (IWT/VFWT1);          %Distance from CB to Metacentre [m]
BGWT = KGWT - KBWT;           %Distance from CG to CB [m]
GMWT = BMWWT - BGWT;          %Metacentric Height [m]
%%% Metacentric Height of Twin Outrigger
% KGT = 0.42;                  %Center of Gravity from keel [m]
KGT = KGo + 0.08;              %Center of Gravity from keel [m]
It = 2*(Io+(AFloat*y^2));    %Moment of Inertia [m^4]

```

```

BMt = (It/Vo); %Distance from CB to Metacentre [m]
BGT = KGt - KBot; %Distance from CG to CB [m]
GMT = BMt - BGt; %Metacentric Height [m]
%%% Metacentric Height of Twin Stabilizer
% KGt = 0.42; %Center of Gravity from keel [m]
KGts = KGstab + 0.08; %Center of Gravity from keel [m]
Its = 2*(Istab+(ASTAB*1^2));%Moment of Inertia [m^4]
BMTs = (Its/(VF1*2)); %Distance from CB to Metacentre [m]
BGTs = KGts - KBstab; %Distance from CG to CB [m]
GMTs = BMTs - BGts; %Metacentric Height [m]
%%% Metacentric Height of Twin Wing Tip Float
% KGt = 0.42; %Center of Gravity from keel [m]
KGtW = KGWT + 0.08; %Center of Gravity from keel [m]
ITW = 2*(IWT+(AWT*(b2/2)^2));%Moment of Inertia [m^4]
BMTW = (ITW/(VFWT1*2)); %Distance from CB to Metacentre [m]
BGTW = KGtW - KBWT; %Distance from CG to CB [m]
GMTW = BMTW - BGtW; %Metacentric Height [m]
%%% Metacentric Height of Trimaran Outrigger
% KGT = 0.826; %Center of Gravity from keel [m]
KGT = (KGh/2.15) + KGt; %Center of Gravity from keel [m]
IT = Ih + It; %Moment of Inertia [m^4]
BMT = (IT/VT); %Distance from CB to Metacentre [m]
BGT = KGT - KBT; %Distance from CG to CB [m]
GMT = BMT - BGT; %Metacentric Height [m]
%%% Metacentric Height of Trimaran Stabilizer
% KGT = 0.826; %Center of Gravity from keel [m]
KGts = (KGh/2.15) + KGts;%Center of Gravity from keel [m]
ITS = Ih + Its; %Moment of Inertia [m^4]
BMTs = (ITS/VT); %Distance from CB to Metacentre [m]
BGTs = KGts - KBTs; %Distance from CG to CB [m]
GMTs = BMTs - BGts; %Metacentric Height [m]
%%% Metacentric Height of Trimaran Wing Tip Float
% KGT = 0.826; %Center of Gravity from keel [m]
KGtW = (KGh/2.15) + KGtW;%Center of Gravity from keel [m]
ITW = Ih + ItW; %Moment of Inertia [m^4]
BMTW = (ITW/VT); %Distance from CB to Metacentre [m]
BGTW = KGtW - KBTW; %Distance from CG to CB [m]
GMTW = BMTW - BGtW; %Metacentric Height [m]
%%% Metacentric Height of Seaplane Trimaran
KGS = 1.75; %Center of Gravity from keel [m]
% KGS = CGL + (KGT*1.75); %Center of Gravity from keel [m]
IS = IT; %Moment of Inertia of Trimaran[m^4]
BMS = (IS/VS); %Distance from CB to Metacentre [m]
BGS = KGS - KBS; %Distance from CG to CB [m]
GMS = BMS - BGS; %Metacentric Height [m]
%%% Metacentric Height of Seaplane Stabilizer
KGSS = 1.84; %Center of Gravity from keel [m]
% KGSS = CGL + (KGts/3.5);%Center of Gravity from keel [m]
ISS = ITS; %Moment of Inertia of Trimaran[m^4]
BMSs = (ISS/VS); %Distance from CB to Metacentre [m]
BGSS = KGSS - KBTs; %Distance from CG to CB [m]
GMSS = BMSs - BGSS; %Metacentric Height [m]
%%% Metacentric Height of Seaplane Wing Tip Float
KGSW = 1.84; %Center of Gravity from keel [m]
% KGSW = CGL + (KGtW/3.5);%Center of Gravity from keel [m]
ISW = ITW; %Moment of Inertia of Trimaran[m^4]
BMSW = (ISW/VS); %Distance from CB to Metacentre [m]

```

```

BGSW = KGSW - KBTW;           %Distance from CG to CB [m]
GMSW = BMSW - BGSW;          %Metacentric Height [m]

%%%% METACENTRIC HEIGHT LONGITUDINAL [y]
%%% Metacentric Height of Hull
Ihy = K1*Lh^3*b;             %Moment of Inertia [m^4]
BMhy = (Ihy/V);              %Distance from CB to Metacentre [m]
GMhy = BMhy - BGh;           %Metacentric Height [m]
%%% Metacentric Height of Outrigger
Ioy = K1*Lo^3*bo;            %Moment of Inertia [m^4]
BMoy = (Ioy/Vo1);            %Distance from CB to Metacentre [m]
GMoy = BMoy - BGo;           %Metacentric Height [m]
%%% Metacentric Height of Twin Outrigger
Ity = 2*(Ioy+(Afloat*y^2)); %Moment of Inertia [m^4]
BMy = (It*y/Vo);             %Distance from CB to Metacentre [m]
GMy = BMy - BGT;             %Metacentric Height [m]
%%% Metacentric Height of Trimaran
ITy = Ih + Ity;              %Moment of Inertia [m^4]
BMTy = (ITy/VT);             %Distance from CB to Metacentre [m]
GMTy = BMTy - BGT;           %Metacentric Height [m]
%%% Metacentric Height of Seaplane
ISy = ITy;                   %Moment of Inertia of Trimaran[m^4]
BMSy = (ISy/VS);              %Distance from CB to Metacentre [m]
GMSy = BMSy - BGS;           %Metacentric Height [m]

%% Air Ministry Minimum Requirements for Stability
fprintf(' Air Ministry Minimum Requirements for Stability')
disp(' ')
%Stability of Hull
TGMh = 4*(V)^(1/3);          %Transverse Metacentric Height
LGMh = 6*(V)^(1/3);          %Longitudinal Metacentric Height
if GMh >= TGMh
    fprintf('GMh = Pass');
else
    fprintf('GMh = Fail');
end
disp(' ')
if GMhy >= LGMh
    fprintf('GMhy = Pass');
else
    fprintf('GMhy = Fail');
end
disp(' ')
% Stability of Outrigger
TGMo = 4*(Vo1)^(1/3); %Transverse Metacentric Height
LGMo = 6*(Vo1)^(1/3); %Longitudinal Metacentric Height
if GMo >= TGMo
    fprintf('GMo = Pass');
else
    fprintf('GMo = Fail');
end
disp(' ')
if GMoy >= LGMo
    fprintf('GMoy = Pass');
else
    fprintf('GMoy = Fail');

```

```

end
disp(' ')
%Stability of Twin Floats
TGMt = 4*(Vo)^(1/3); %Transverse Metacentric Height
LGMt = 6*(Vo)^(1/3); %Longitudinal Metacentric Height
if G Mt >= TGMt
    fprintf('GMt = Pass');
else
    fprintf('GMt = Fail');
end
disp(' ')
if GMty >= LGMt
    fprintf('GMty = Pass');
else
    fprintf('GMty = Fail');
end
disp(' ')
% Stability of Trimaran
TGMT = 4*(VT)^(1/3); %Transverse Metacentric Height
LGMT = 6*(VT)^(1/3); %Longitudinal Metacentric Height
if GMT >= TGMT
    fprintf('GMT = Pass');
else
    fprintf('GMT = Fail');
end
disp(' ')
if GMTy >= LGMT
    fprintf('GMTy = Pass');
else
    fprintf('GMTy = Fail');
end
disp(' ')
% Stability of Seaplane
TGMS = 4*(VS)^(1/3); %Transverse Metacentric Height
LGMS = 6*(VS)^(1/3); %Longitudinal Metacentric Height
if GMS >= TGMS
    fprintf('GMS = Pass');
else
    fprintf('GMS = Fail');
end
disp(' ')
if GMSy >= LGMS
    fprintf('GMSy = Pass');
else
    fprintf('GMSy = Fail');
end

%% Righting Moment
theta = 0:90;
%%% Float Track location
RM = delT*y*cos(theta*(pi/180));
%%% Float Track location
RMF = delT*l*cos(theta*(pi/180));
%%% Float Track location
RMFWT = delT*(b2/2)*cos(theta*(pi/180));
%%% Righting Moment for Hull
RMh = delH*sin(theta*(pi/180))*GMh;

```

```

%%% Righting Moment for Outrigger
RMO = delO1*sin(theta*(pi/180))*GMo;
%%% Righting Moment for Stabilizer Float
RMstab = delF*sin(theta*(pi/180))*GMstab;
%%% Righting Moment for Wing Tip Float
RMWT = delFWT*sin(theta*(pi/180))*GMWT;
%%% Righting Moment for Seaplane Trimaran
RMS = delT*sin(theta*(pi/180))*GMS;
%%% Righting Moment for Seaplane Stabilizer
RMSS = delT*sin(theta*(pi/180))*GMSS;
%%% Righting Moment for Seaplane Wing Tip Float
RMSW = delT*sin(theta*(pi/180))*GMSW;

%Maximum Righting Moment and Max angle of tilting
thetamax = 90; %Max angle of Tilting [deg]
RMSmax = delT*sin(thetamax*(pi/180))*GMS; %Max Rigthing Moment [kg m]
phi = RMSmax./(delT*y);
phimax = acos(phi)*(180/pi); %Max allowed angle of Tilting

%% Stability in Wind
B = y; %Beam between the centerlines of the outer hulls [m]
CE = GMSy; %Height of the center of effort above the CG [m]
SA = 0:50; %Sail Area [m^2]
SF = 9.48*sqrt((0.5*B*GW)./(SA*CE)); %Wind Speed [m/s]

%% Plots
figure
plot(theta,RMS,'k',theta,RMSS,theta,RMSW,'Linewidth',2)
xlabel('Angle of Inclination [deg]')
ylabel('Righting Moment [Kg m]')
title('Righting Moment Transverse Stability')
legend('Seaplane Trimaran','Seaplane Stabilizer','Seaplane Wing Tip Float')

%% Results
disp(' ')
fprintf('-----')
fprintf('\n Stability Parameters\n')
disp(' ')
fprintf('\n Centre of Bouyancy, Centre of Gravity and Draft Line\n')
fprintf('\n Hull \n')
fprintf('\n Draft [m] = %g\n', Drah)
fprintf('\n Centre of Bouyancy [m] = %g\n', KBh)
fprintf('\n Centre of Gravity [m] = %g\n', KGh)
fprintf('\n Metacentre Transverse [m] = %g\n', BMh)
fprintf('\n Metacentric Height Transverse [m] = %g\n', GMh)
fprintf('\n Metacentre Longitudinal [m] = %g\n', BMhy)
fprintf('\n Metacentric Height Longitudinal [m] = %g\n', GMhy)
disp(' ')
fprintf('\n Outrigger \n')
fprintf('\n Draft [m] = %g\n', Drao)
fprintf('\n Centre of Bouyancy [m] = %g\n', KBo)
fprintf('\n Centre of Gravity [m] = %g\n', KGo)
fprintf('\n Metacentre Transverse [m] = %g\n', BMo)
fprintf('\n Metacentric Height Transverse [m] = %g\n', GMo)
fprintf('\n Metacentre Longitudinal [m] = %g\n', BMoy)
fprintf('\n Metacentric Height Longitudinal [m] = %g\n', GMoy)

```

```

disp(' ')
fprintf('\n Stabilizer Float \n')
fprintf('\n Draft [m] = %g\n', Drstab)
fprintf('\n Centre of Bouyancy [m] = %g\n', KBstab)
fprintf('\n Centre of Gravity [m] = %g\n', KGstab)
fprintf('\n Metacentre Transverse [m] = %g\n', BMstab)
fprintf('\n Metacentric Height Transverse [m] = %g\n', GMstab)
disp(' ')
fprintf('\n Wing Tip Float \n')
fprintf('\n Draft [m] = %g\n', DraWT)
fprintf('\n Centre of Bouyancy [m] = %g\n', KBWT)
fprintf('\n Centre of Gravity [m] = %g\n', KGWT)
fprintf('\n Metacentre Transverse [m] = %g\n', BMWT)
fprintf('\n Metacentric Height Transverse [m] = %g\n', GMWT)
disp(' ')
fprintf('\n Twin Floats \n')
fprintf('\n Draft [m] = %g\n', Drao)
fprintf('\n Centre of Bouyancy [m] = %g\n', KBo)
fprintf('\n Centre of Gravity [m] = %g\n', KGt)
fprintf('\n Metacentre Transverse [m] = %g\n', BMt)
fprintf('\n Metacentric Height Transverse [m] = %g\n', GMT)
fprintf('\n Metacentre Longitudinal [m] = %g\n', BMty)
fprintf('\n Metacentric Height Longitudinal [m] = %g\n', GMty)
disp(' ')
fprintf('\n Trimaran \n')
fprintf('\n Draft [m] = %g\n', DraT)
fprintf('\n Centre of Bouyancy [m] = %g\n', KBT)
fprintf('\n Centre of Gravity [m] = %g\n', KGT)
fprintf('\n Metacentre Transverse [m] = %g\n', BMT)
fprintf('\n Metacentric Height Transverse [m] = %g\n', GMT)
fprintf('\n Metacentre Longitudinal [m] = %g\n', BMTy)
fprintf('\n Metacentric Height Longitudinal [m] = %g\n', GMTy)
disp(' ')
fprintf('\n Seaplane Trimaran\n')
fprintf('\n Draft [m] = %g\n', Dras)
fprintf('\n Centre of Bouyancy [m] = %g\n', KBS)
fprintf('\n Centre of Gravity [m] = %g\n', KGS)
fprintf('\n Metacentre Transverse [m] = %g\n', BMS)
fprintf('\n Metacentric Height Transverse [m] = %g\n', GMS)
fprintf('\n Metacentre Longitudinal [m] = %g\n', BMSy)
fprintf('\n Metacentric Height Longitudinal [m] = %g\n', GMsy)
disp(' ')
fprintf('\n Seaplane Stabilizer\n')
fprintf('\n Draft [m] = %g\n', DraTs)
fprintf('\n Centre of Bouyancy [m] = %g\n', KBTs)
fprintf('\n Centre of Gravity [m] = %g\n', KGSS)
fprintf('\n Metacentre Transverse [m] = %g\n', BMSS)
fprintf('\n Metacentric Height Transverse [m] = %g\n', GMSS)
disp(' ')
fprintf('\n Seaplane Wing Tip Float\n')
fprintf('\n Draft [m] = %g\n', DraTW)
fprintf('\n Centre of Bouyancy [m] = %g\n', KBTW)
fprintf('\n Centre of Gravity [m] = %g\n', KGSW)
fprintf('\n Metacentre Transverse [m] = %g\n', BMSW)
fprintf('\n Metacentric Height Transverse [m] = %g\n', GMSW)
fprintf('\n-----\n')

```

```

%% Water Loads Code Created by Alan Canamar %%


function [a] = WaterLoads(b,Dras)
%% Declare global variables
global GW g0 rho0 rhos Sexp2 CLmax0 d L

%% Water Landing Impact
% clc; clear all
% GW = 6600; %Total Gross Weight of Aircraft [kg]
% rhos = 1025; %Density of Salt Water [kg/m^3]
% g0 = 9.80665; %Gravitational Constant [m/s^2]
% rho0 = 1.225; %Density of air at Sea Level [kg/m^3]
% Sexp2 = 34.86; %Wing Area [m^2]
% b = 2.03; %Boat Hull Beam [m]
% Dras = 0.46; %Seaplane Draft Line from keel [m]
% d = 1.92; %Diameter of Fuselage [m]
% L = 14.47; %Length of Fuselage [m]
% CLmax0 = 1.63; %Maximum Lift Coefficient
Vso = sqrt((2*GW*g0)/(rho0*Sexp2*CLmax0));%Stall Speed [m/s]
B = 0:50; %Forebody deadrise angle
C = 0.012; %Seaplane Operation Factor
nwsB = (C.*Vso.^2)./((tan(B*(pi/180)).^(2/3)).*GW.^(1/3));%Water Load Formula

%% Chine intensity Loading
n = 8; %Load Factor
LWL = Dras/2; %Half length of the L.W.L forward of the step [m]
a = (6*n*GW)./(5*2*b*LWL);%Intensity of Loading at Chine [kg/m^2]
bm = 0:0.1:5; %Beam Matrix [m]
am = (6*n*GW)./(5*2*bm*LWL);%Intensity of Loading at Chine matix [kg/m^2]

%% Plots
figure
plot(B,nwsB,'Linewidth',2)
xlabel('Forebody Deadrise Angle [deg]')
ylabel('Load Factor')
title('Load Factor Curve')
figure
plot(bm,am)
xlabel('Beam [m]')
ylabel('Intensity Loading at Chine [kg/m^2]')
title('Intensity Loading vs Beam')

%% Aircraft Drag Breakdown
% Created by Alan Canamar %

function [DPi,DPis] = Drag_Curves(L,b2,d,b,Lh,bo,Lo,TA,ALT)
%% Declare global variables
global GW g0 Sexp2 rho0

%% Inputs
% clc; clear all
% GW = 6600; %Gross Weight [kg]
% Sexp2 = 34.86; %Wing Area [m^2]
% g0 = 9.80665; %Gravitational Constant [m/s^2]
% rho0 = 1.225; %Density of air at Sea Level [kg/m^3]
% L = 14.47; %Fuselage Length [m]

```

```

% b2 = 19.08;                               %Wing Span [m]
% d = 1.92;                                %Fuselage Height [m]
% b = 2.03;                                 %Hull beam [m]
% Lh = L;                                   %Main Hull Length [m]
% bo = 0.59;                                %Outrigger Beam [m]
% Lo = 0.5*Lh;                             %Outrigger Length [m]
% TA = 25500;                               %Thrust Available [N]
% ALT = 4200;                               %Cruising altitude [m]
Vel = 150;                                  %Speed [m/s]

%% Initial Calculations
dV = 1;                                     %Speed Change
V = 15:dV:Vel;                            %Speed Matrix
h0 = 0;                                     %Altitude at sea level [m]
G = 1.4;                                    %Ratio of specific heat of air (gamma)
R = 286.9;                                 %Gas constant [J/kg*K]
T0 = 287.827;                            %Temperature at sea level [K]
a_L = -0.0065;                            %Lapse Rate [K/m]
T = T0;                                     %Temperature altitude gradient [K]
rho = rho0;                                %Density altitude gradient [kg/m^3]
a = sqrt(G*R.*T);                         %Local speed of sound [m/s]
M = V./a;                                  %Mach number
q = 0.5*rho*V.^2;                          %Dynamic Pressure [Pa]

%% Calculation of Dynamic Viscosity of air
T00 = 291.15;                            %Reference Temperature [K]
v0 = 18.27*10^-6;                        %Reference Viscosity [Pa-s]
C = 120;                                   %Sutherlands Constant [K]
v = v0;                                    %v = v0.*((T00+C)./(T+C)).*((T./T00).^(3/2));%Dynamic viscosity [Pa-s]

%% Flat plate drag area of the fuselage
%Fuselage Geometry
%1 stands for fuselage
if L == 0;
    f1 = 0;
else
    Ln = 3.52;                             %Length of the Nose of Fuselage [m]
    Lt = 4.87;                             %Length of the Tail of Fuselage [m]
    Lfu = L-Ln-Lt;                         %Length of Fuselage [m]
    Swetn = 0.75*pi*d*Ln;                 %Wetted area of the nose [m^2]
    Swetf = (0.5*pi*d^2)+(pi*d*Lfu);    %Wetted area of fuselage [m^2]
    Swet1 = Swetn+Swetf;                  %Wetted Area [m^2]
    Q = 1;                                  %Interference Factor
    Rel = (V*L*rho)/v;                   %Reynolds Number
    Cf1 = 0.455./(log10(Rel)).^2.58;%Friction coefficient
    Amax = (pi*d^2)/4;                    %Fuselage Cross Area [m^2]
    ld = L/sqrt((4/pi)*Amax);           %Fineness ratio
    F1 = 1+(60/(ld^3))+(ld/400);        %Fuselage Form Factor
    f1 = Cf1*F1*Q*Swet1;                %Flat plate drag area [m^2]
end

%% Flat Plate Drag Area of the wing

```

```

%Wing Geometry
%2 stands for wing
if b2 == 0;
    f2 = 0;
else
    cT2 = 1.12;                                %Wing Tip Chord [m]
    cr2 = 2.534;                               %Wing Root Chord [m]
    zeta2 = 0;                                  %Wing Sweep Angle [degree]
    tc2 = 0.18;                                 %Wing thickness ratio
    zeta_rad2 = zeta2*(pi/180);                %Sweep Angle [rad]
    if tc2 < 0.05;
        Swet2 = 2.003*Sexp2;
    else
        Swet2 = Sexp2*(1.977+(0.52*tc2));      %Wetted Wing Area [m^2]
    end
lamda2 = cT2/cr2;                            %Taper ratio
mac2 = (2/3)*cr2*(1+lamda2-(lamda2/(1+lamda2))); %Aerodynamic moment [m]
Re2 = (V*rho*mac2)/v;                         %Reynolds Number
Cf2 = 0.455./log10(Re2).^2.58;                 %Friction Coefficient
z2 = ((2-M.^2).*cos(zeta_rad2))./sqrt((1-M.^2).*cos(zeta_rad2).^2);
F2 = 1+(z2*tc2)+(100*tc2^4);                  %Wing Form Factor
f2 = Cf2.*F2.*Q.*Swet2;                        %Wing drag area [m^2]
end

%% Flat Plate Drag area of the horizontal tail
%Tail Geometry
%3 stands for tail
b3 = 1.799;                                    %Horizontal Tail Span [m]
if b3 == 0;
    f3 = 0;
else
    cT3 = 1.054;                               %Horizontal Tail Taper Chord [m]
    cr3 = 1.799;                               %Horizontal Tail Root Chord [m]
    zeta3 = 5;                                  %Horizontal Tail Sweep Angle
    [degree]
    tc3 = 0.12;                                %Horizontal Tail Thickness ratio
    Sexp3 = 9.56;                               %Horizontal Tail Area [m^2]
    zeta_rad3 = zeta3*(pi/180);                %Sweep Angle [rad]
    if tc3 < 0.05;
        Swet3 = 2.003*Sexp3;
    else
        Swet3 = Sexp3*(1.977+(0.52*tc3));      %Wetted Tail Area [m^2]
    end
lamda3 = cT3/cr3;                            %Taper ratio
mac3 = (2/3)*cr3*(1+lamda3-(lamda3/(1+lamda3))); %Aerodynamic moment [m]
Re3 = (V*rho*mac3)/v;                         %Reynolds Number
Cf3 = 0.455./log10(Re3).^2.58;                 %Friction Coefficient
z3 = ((2-M.^2).*cos(zeta_rad3))./sqrt((1-M.^2).*cos(zeta_rad3).^2);
F3 = 1+(z3*tc3)+(100*tc3^4);                  %Tail Form Factor
f3 = Cf3.*F3.*Q.*Swet3;                        %Tail Drag Area [m^2]
end

%% Flat Plate Drag area of the vertical tail
%Vertical Tail Geometry
%4 stands for Vertical tail
b4 = 3.31;                                     %Vertical Tail Span [m]

```

```

if b4 == 0;
    f4 = 0;
else
    cT4 = 1.47;                                %Vertical Tail Taper Chord [m]
    cr4 = 2.94;                                %Vertical Tail Root Chord [m]
    zeta4 = 35;                                 %Vertical Tail Sweep Angle [degree]
    tc4 = 0.12;                                 %Vertical Tail Thickness ratio
    Sexp4 = 7.298;                             %Vertical Tail Area [m^2]
    zeta_rad4 = zeta4*(pi/180);                 %Sweep Angle [rad]
    if tc4 < 0.05;
        Swet4 = 2.003*Sexp4;
    else
        Swet4 = Sexp4*(1.977+(0.52*tc4));      %Wetted Tail Area [m^2]
    end
    lamda4 = cT4/cr4;                           %Taper ratio
    mac4 = (2/3)*cr4*(1+lamda4-(lamda4/(1+lamda4))); %Aerodynamic moment [m]
    Re4 = (V*rho*mac4)/v;                      %Reynolds Number
    Cf4 = 0.455./log10(Re4).^2.58;              %Friction Coefficient
    z4 = ((2-M.^2).*cos(zeta_rad4))./sqrt((1-M.^2).*cos(zeta_rad4).^2);
    F4 = 1+(z4*tc4)+(100*tc4^4);                %Tail Form Factor
    f4 = Cf4.*F4.*Q.*Swet4;                     %Tail Drag Area [m^2]
end

%% Flat Plate Drag Area of Engines
%Engine Geometry
%5 stands for Engine
n5 = 2;                                         %Number of Engines
if n5 == 0;
    f5 = 0;
else
    L5 = 2.8;                                  %Engine Length [m]
    d5 = 1;                                    %Engine Diameter [m]
    Sexp5 = (0.5*pi*d5^2)+(pi*d5*L5);        %Engine Area [m^2]
    Q5 = 1.5;                                 %Interference factor
    g5 = L5/d5;                               %Effective Fineness ratio
    Re5 = (V*rho*L5)/v;                      %Reynolds Number
    Cf5 = 0.455./log10(Re5).^2.58;            %Friction Coefficient
    F5 = 1+(0.35/g5);                        %Form Factor
    f5 = Cf5.*F5.*Q5.*Sexp5.*n5;             %Engine Drag Area [m^2]
end

%% Flat Plate Drag Area of Pylons
%Pylon Geometry
%6 stands for Pylon
n6 = 0;                                         %Number of Pylons
if n6 == 0;
    f6 = 0;
else
    cT6 = 0;                                  %Pylon Taper Chord [m]
    cr6 = 0;                                  %Pylon Root Chord [m]
    zeta6 = 0;                                %Pylon Sweep Angle [degree]
    tc6 = 0;                                 %Pylon Thickness ratio
    Sexp6 = 0;                                %Pylon Area [m^2]
    zeta_rad6 = zeta6*(pi/180);               %Sweep Angle [rad]
    if tc6 < 0.05;
        Swet6 = 2.003*Sexp6;
    end
end

```

```

else
    Swet6 = Sexp6*(1.977+(0.52*tc6)); %Wetted Pylon Area [m^2]
end
lamda6 = cT6/cr6; %Taper Ratio
mac6=(2/3)*cr6*(1+lamda6-(lamda6/(1+lamda6))); %Aerodynamic moment [m]
Re6 = (V*rho*mac6)/v; %Reynolds Number
Cf6 = 0.455./log10(Re6).^2.58; %Friction Coefficient
z6=((2-M^2)*cos(zeta_rad6))/sqrt((1-M^2)*cos(zeta_rad6)^2);
F6=1+(z6*tc6)+(100*tc6^4); %Form Factor
f6 = Cf6.*F6.*Q.*Swet6.*n6; %Pylon Drag Area [m^2]
end

%% Flat Plate Drag Area of the Propeller
%Propeller Geometry
Nb = 0; %Number of Blades
if Nb == 0;
    fprop = 0;
else
    cb = 0.85; %Average Blade Chord [m]
    R = 1.04; %Propeller Radius [m]
    r = 0.5; %Radius of disk [m]
    s = 0.6; %Height of disk [m]
    Adisk = (pi*r*s)+(pi*r^2); %Disk Area [m^2]
    nu = (Nb*cb)/(pi*R);
    Pf = 1;
    if Pf == 1;
        fprop = 0.1*nu*Adisk; %Flat Area Propeller [m^2]
    else
        fprop = 0.8*nu*Adisk; %Flat Area Propeller [m^2]
    end
end

%% Flat plate drag area of the Boat Hull
%Boat Hull Geometry
%b stands for Boat Hull
rb = (b/2); %Radius of Boat Hull [m]
KA = 0.7; %Proportionality Coefficient
AHull = KA*Lh*b; %Area of Load Water Plane of Hull [m^2]
Swetb = 0.5*((pi*rb^2)+AHull+(pi*rb*Lh)); %Wetted area of Boat Hull [m^2]
Qb = 1.25; %Interference Factor
Reb = (V*Lh*rho)/v; %Reynolds Number
Cfb = 0.455./log10(Reb).^2.58; %Friction coefficient
Amaxb = (pi*(rb/2)^2)/4; %Boat Hull Cross Area [m^2]
ldb = Lh/sqrt((4/pi)*Amaxb); %Fineness ratio
Fb = 1+(60/(ldb^3))+(ldb/400); %Boat Hull Form Factor
fb = Cfb.*Fb.*Qb.*Swetb; %Flat plate drag area [m^2]

%% Flat Plate Drag Area of Floats
%Float Geometry
%f stands for Float
nf = 2; %Number of Outriggers
if nf == 0;
    ff = 0;
else
    ro = (bo/2); %Radius [m]
    Afloat = KA*Lo*bo; %Area of Load Water Plane Float [m^2]
end

```

```

Sexpf = (0.5*pi*ro^2)+AFloat+(pi*ro*Lo); %Float Exposed Area [m^2]
Qf = 1.5;                                     %Interference factor
gf = Lo/bo;                                    %Effective Fineness ratio
Ref = (V*rho*Lo)/v;                           %Reynolds Number
Cff = 0.455./log10(Ref).^2.58;                 %Friction Coefficient
Ff = 1+(0.35/gf);                            %Form Factor
ff = Cff.*Ff.*Qf.*Sexpf.*nf;                  %Floats Drag Area [m^2]
end

%% Flat Plate Drag Area of the Upsweep
%Upsweep Geometry
mu = 15;                                       %Upsweep angle [Deg]
if mu == 0;                                     %Upsweep angle [Deg]
    fups = 0;
else
    mu_rad = mu*(pi/180);                      %Upsweep angle [Rad]
    fups = 3.83*(mu_rad^2.5)*Amax;              %Flat Drag Area Upsweep [m^2]
end

%% Miscellaneous Flat Plate Drag Area of Landplane [m^2]
fsub=f1+f2+f3+f4+f5+f6+fups+fprop;           %Subtotal flat plate drag area
fmisc=0.05*fsub;                                %Miscellaneous flat plate drag area
ftotal_air=fsub+fmisc;                          %Total Flat plate drag area of Landplane

%% Miscellaneous Flat Plate Drag Area of Seaplane [m^2]
fsub=f1+f2+f3+f4+f5+f6+fups+fprop+fb+ff;     %Subtotal flat plate drag area
fmisc=0.05*fsub;                                %Miscellaneous flat plate drag area
ftotal_sea=fsub+fmisc;                          %Total Flat plate drag area of seaplane

%% Parasite Drag Coefficient of Landplane and Seaplane
CDP = ftotal_air/Sexp2;
CDPs = ftotal_sea/Sexp2;

%% Induced Drag
AR = b2^2./Sexp2;                             %Aspect Ratio
if zeta2 == 0;
    e = (1.78*(1-(0.045*(AR.^0.68))))-0.64;
else
    e = (4.61*(1-(0.045*(AR.^0.68)))*(cos(zeta2).^0.15))-3.1;
end
K = 1./(pi*AR*e);
CL = (GW*g0)./(q*Sexp2);                      %Coefficient of Lift
Cdi = CL.^2.*K;                                %Induced Drag Coefficient

%% Compressibility Drag
Mdiv = (-0.25.*CL)+0.91;
mdiff = M-Mdiv;
CDC = 0.002.*exp(21.652.*mdiff);

%% Total Drag of Aircraft no Floats or Boat Hull [N]
DP = q.*Sexp2.*CDP;                            %Parasite Drag Lanplane[N]
Di = q.*Sexp2.*Cdi;                            %Induced Drag [N]
Dc = q.*Sexp2.*CDC;                            %Compressibility Drag [N]
DPI = DP + Di;                                %Incompressible Total Drag [N]
Cd = CDP+Cdi;                                 %Total Drag Coefficient

```

```

%% Total Drag of Seaplane [N]
Dps = q.*Sexp2.*CDPs; %Parasite Drag Seaplane[N]
DPis = DPS + Di; %Incompressible Total Drag [N]
Cds = CDPs+Cdi; %Total Drag Coefficient

%% Thrust Available
Ta0 = TA*exp(-0.0099*V); %Available Thrust [N]
teta = T./T0; %Temperature Ratio
BPR = 10; %Bypass Ratio
TAFAN = TA.* (1+((G-1)/2)*M.^2).^(G./(G-1)).*(1-(sqrt(teta*0.25).*M)).*(1-(0.1*BPR.*M));
TAJET = TA.* (1+((G-1)/2)*M.^2).^(G./(G-1)).*(1-(sqrt(teta*0.25).*M));
%% Plots
figure
plot(V,Di,V,DPi,'LineWidth',2)
xlabel('Velocity [m/s]')
ylabel('Force [N]')
title('Drag Curves')
legend('Induce Drag','Parasite Drag','Total Drag')
figure
plot(V,DPi,V,DPis,'k',V,Ta0,'LineWidth',2)
xlabel('Velocity [m/s]')
ylabel('Force [N]')
title('Thrust Curves')
legend('Thrust Required Landplane','Thrust Required Seaplane',...
'TurboProp Engine')

%% WATER RESISTANCE CODE Created By Alan Canamar

function [FTm,Rw] = Water_Resistance(Lh,Lo,b,h,bo,ho,Lstab,bstab,... % Declare global variables
dstab,bstabWT,LstabWT,dstabWT,VF1,VFWT1,TA,CLmax0,ALT)
global GW g0 rho0 rhos Sexp2

%% Water Resistance of Seaplane at Takeoff
% Airplane Inputs
% clc; clear all
% GW = 6600; %Total Gross Weight of Aircraft [kg]
% rhos = 1025; %Density of Salt Water [kg/m^3]
% g0 = 9.80665; %Gravitational Constant [m/s^2]
% rho0 = 1.225; %Density of air at Sea Level [kg/m^3]
% Sexp2 = 34.86; %Wing Area [m^2]
% Cds = 0.0082; %Drag increment due to Seaplane configuration extended
% Lh = 14.47; %Length [m]
% b = 2.03; %Beam [m]
% h = 1.319; %Bow Height [m]
% Lo = 7.13; %Length [m]
% bo = 0.509; %Beam [m]
% ho = 0.46; %Bow Height [m]
% Lstab = 3.82; %Length [m]
% bstab = 0.95; %Beam [m]
% dstab = 0.48; %Bow Height [m]
% LstabWT = 2.60; %Length [m]
% bstabWT = 0.65; %Beam [m]
% dstabWT = 0.32; %Bow Height [m]

```

```

% CLmax0 = 1.63;           %Max Coefficient of Lift
% TA = 25000;              %Thrust Available [N]
% ALT = 4200;               %Cruising Altitude [m]
% VF1 = 1.7423;
% VFWT1 = 0.5479;
incCLflap = 0.45;          %Increment of CL due to flap configuration
CLmax18 = CLmax0;%Max Coefficient of Lift due to Flap
v = 1.83*10^-6;            %Dynamic Viscosity of Salt Water [m^2/s]
VS1 = sqrt((2*GW*g0)./(CLmax18*rho0*Sexp2));%Stall Speed [m/s]
Vlof = 1.2*VS1;             %Lift off Speed [m/s]
V = 0:Vlof;                 %Takeoff Speed [m/s]

%% Volume Calculations
BouyR = 1.9;                %Bouyancy Reserve [Percent]
HullR = 1.5;                 %Hull Displacement [Percent]
OutR = BouyR - HullR;        %Outrigger Displacement [Percent]
delt = BouyR*GW;             %Trimaran Displacement Weight [kg]
delH = HullR*GW;             %Hull Displacement Weight [kg]
delO = OutR*GW;              %Outrigger Displacement Weight [kg]
delO1 = delO/2;              %One Outrigger Displacement Weight [kg]
Vol = delH/rhos;             %Hull Displacement Volume [m^3]
Vo = delO/rhos;              %Twin Outrigger Displacement Volume [m^3]
Vol1 = delO1/rhos;            %One Outrigger Displacement Volume [m^3]
VT = Vol+Vo;                 %Trimaran Displacement Volume [m^3]
VS = delt/rhos;              %Seaplane Displacement Volume [m^3]

%% Avialable Thrust Curves
h0 = 0;                      %Altitude at sea level [m]
G = 1.4;                      %Ratio of specific heat of air (gamma)
R = 286.9;                     %Gas constant [J/kg*K]
T0 = 287.827;                  %Temperature at sea level [K]
Pasl = 101325;                  %Atmospheric Pressure at Sea Level [Pa]
a_L = -0.0065;                  %Lapse Rate [K/m]
T = T0+(a_L*(ALT-h0));         %Temperature altitude gradient [K]
a = sqrt(G*R.*T0);              %Local speed of sound [m/s]
Mach = V./a;                   %Mach Number
BPR = 10;                      %Bypass Ratio
C = 0.25;                      %Thrust Constant
T_cruise = T0+(a_L*(h0));       %Temperature altitude gradient [K]
T_T0 = T_cruise./T0;             %Temperature Ratio
TATOF = TA*exp(-0.0099*V);      %Max Take-off Thrust Curve at 0 Altitude [N]
TAFAN = TA.*((1+((G-1)/2)*Mach.^2)).^(G./(G-1)).*(1-
(sqrt(T_T0*C).*Mach)).*(1-(0.1*BPR.*Mach));
TAJET = TA.*((1+((G-1)/2)*Mach.^2)).^(G./(G-1)).*(1-(sqrt(T_T0*C).*Mach));

%% Water Resistance of Boat Hull
% Inputs
KA = 0.7;                      %Proportionality Coefficient
AHull = KA*Lh*b;                %Area of Load Water Plane of Hull [m^2]
Afloat = KA*Lo*bo;                %Area of Load Water Plane Float [m^2]
ASTab = KA*Lstab*bstab;          %Area of Load Water Plane Float [m^2]
AWT = KA*LstabWT*bstabWT;        %Area of Load Water Plane Float [m^2]
Velh = 5.07*sqrt(Lh);             %Hull Speed [m/s]
Reh = (Velh*Lh)./v;               %Reynolds Number for Boat Hull
Cfh = 0.075./((log10(Reh)-2).^2); %Friction Coefficient
Kh = 19*((Vol./((Lh*b*h)).*(b/Lh)).^2); %Form Factor

```

```

CVh = (1+Kh)*Cfh; %Coefficient of Viscous Resistance
Fnh = Velh./ (sqrt(g0*Lh)); %Froude Number
CWh = CVh/0.6; %Wave Coefficient
CTh = CVh + CWh; %Coefficient of Friction Resistance
Fh = CTh*0.5*rhos*A Hull.*Velh.^2; %Frictional Resistance [N]

%% Water Resistance of Floats
% Inputs
Velo = 5.07*sqrt(Lo); %Hull Speed [m/s]
Reo = (Velo*Lo)./v; %Reynolds Number for Boat Hull
Cfo = 0.075./((log10(Reo)-2).^2); %Friction Coefficient
Ko = 19*((Vo1./ (Lo*bo*ho)) * (bo/Lo))^2;%Form Factor
CVo = (1+Ko)*Cfo; %Coefficient of Viscous Resistance
Fno = Velo./ (sqrt(g0*Lo)); %Froude Number
CWo = CVo/0.6; %Wave Coefficient
CTo = CVo + CWo; %Coefficient of Friction Resistance
Fo = CTo*0.5*rhos*AFloat.*Velo.^2;%Frictional Resistance [N]
Kst = 19*((VF1./ (Lstab*bstab*dstab)) * (bstab/Lstab))^2;%Form Factor
KWT = 19*((VFWT1./ (LstabWT*bstabWT*dstabWT)) * (bstabWT/LstabWT))^2;%Form Factor

%% Total Water Resistance of Trimaran [N]
Velt = 5.07*sqrt(Lh+(2*Lo)); %Hull Speed [m/s]
FnT = Velt./ (sqrt(g0*(Lh+(2*Lo))));%Froude Number
CTT = CTh + (2*CTo); %Coefficient of Friction Resistance
FT = CTT*0.5*rhos*(A Hull+(2*AFloat)).*Velt.^2;%Frictional Resistance [N]
FT1 = Fh+(2*Fo); %Total Frictional Resistance [N]

%% Water Resistance Curves

%Resistance Calculation for Boat Hull
deltaAreaMax = 0.8; %Max Hull Area
deltaAreaMin = 0; %Min Hull Area
deltaArea = str2double(sprintf('%.4f', deltaAreaMax/length(V)));
AHullm = AHull*(deltaAreaMax:-deltaArea:deltaAreaMin);%Matrix
Rehm = ((V.*Lh)./v); %Reynolds Number for Boat Hull
Cfhm = 0.075./((log10(Rehm))-2).^2;%Friction Coefficient
CVhm = (1+Kh)*Cfhm; %Coefficient of Viscous Resistance
CWhm = CVhm/0.6; %Wave Coefficient
CThm = CVhm + CWhm; %Coefficient of Friction Resista
Fnhm = V./ (sqrt(g0*Lh)); %Froude Number
Fhm = (CThm*0.5*rhos.*AHullm.*V.^2);%Frictional Resistance [N]
%Resistance Calculation for Outriggers
AFloatm = AFLOAT*(deltaAreaMax:-deltaArea:deltaAreaMin);%Matrix
Reom = ((V.*Lo)./v); %Reynolds Number for Boat Hull
Cfom = 0.075./((log10(Reom))-2).^2;%Friction Coefficient
CVom = (1+Ko)*Cfom; %Coefficient of Viscous Resistance
CWom = CVom/0.6; %Wave Coefficient
CTom = CVom + CWom; %Coefficient of Friction Resistance
Fnom = V./ (sqrt(g0*Lo)); %Froude Number
Fom = (CTom*0.5*rhos.*AFloatm.*V.^2);%Frictional Resistance [N]
%Resistance Calculation for Stabilizers
Astabm = AStab*(deltaAreaMax:-deltaArea:deltaAreaMin);%Matrix
Restm = ((V.*Lstab)./v); %Reynolds Number for Boat Hull
Cfstm = 0.075./((log10(Restm))-2).^2;%Friction Coefficient
CVstm = (1+Kst)*Cfstm; %Coefficient of Viscous Resistance

```

```

CWstm = CVstm/0.6; %Wave Coefficient
CTstm = CVstm + CWstm; %Coefficient of Friction Resistance
Fstm = (CTstm*0.5*rhos.*Astabm.*V.^2);%Frictional Resistance [N]
%Resistance Calculation Wing Tip Floats
AWTm = AWT*(deltaAreaMax:-deltaArea:deltaAreaMin);%Matrix
ReWTm = ((V.*LstabWT)./v); %Reynolds Number for Boat Hull
CfWTm = 0.075./(((log10(ReWTm))-2).^2);%Friction Coefficient
CVWTm = (1+KWT)*CfWTm; %Coefficient of Viscous Resistance
CWWTm = CVWTm/0.6; %Wave Coefficient
CTWTm = CVWTm + CWWTm; %Coefficient of Friction Resistance
FWTm = (CTWTm*0.5*rhos.*AWTm.*V.^2);%Frictional Resistance [N]
%Total Water Resistance
FTm = (Fhm+(2.*Fom)); %Total Frictional Resistance [N]
FTstm = (Fhm+(2.*Fstm)); %Total Frictional Resistance [N]
FTWTm = (Fhm+(2.*FWTm)); %Total Frictional Resistance [N]
FnTm = Fnhm + (2*Fnom); %Froude Number
% %Boat Hull
Q = 0.80; %Hull Shape Constant
Rw = Q*GW*((V./Vlof) - (V.^2./Vlof.^2));%Water Resistance [N]

%% Plots
figure
plot(V,FTm,V,TATO,V,TAJET,V,TAFAN,'Linewidth',2)
xlabel('Velocity [m/s]')
ylabel('Resistance [N]')
title('Resistance Curves')
legend('Water Resistance','Thrust Available Turboprop',...
    'Thrust Available JET','Thrust Available Turbofan')

%% Results
fprintf('-----')
fprintf('\n Water Resistance\n')
disp(' ')
fprintf('\n Boat Hull\n')
fprintf('\n Speed Hull [m/s]= %g\n', Velh)
fprintf('\n Reynolds Number = %g\n', Reh)
fprintf('\n Friction Coefficient = %g\n', Cfh)
fprintf('\n Form Factor = %g\n', Kh)
fprintf('\n Coefficient of Viscous Resistance = %g\n', CVh)
fprintf('\n Froude Number = %g\n', Fnh)
fprintf('\n Wave Resistance Coefficient = %g\n', CWh)
fprintf('\n Total Water Resistance Coefficient = %g\n', CTh)
fprintf('\n Water Frictional Resistance [N] = %g\n', Fh)
disp(' ')
fprintf('\n Outrigger\n')
fprintf('\n Speed Hull [m/s]= %g\n', Velo)
fprintf('\n Reynolds Number = %g\n', Reo)
fprintf('\n Friction Coefficient = %g\n', Cfo)
fprintf('\n Form Factor = %g\n', Ko)
fprintf('\n Coefficient of Viscous Resistance = %g\n', CVo)
fprintf('\n Froude Number = %g\n', Fno)
fprintf('\n Wave Resistance Coefficient = %g\n', CWo)
fprintf('\n Total Water Resistance Coefficient = %g\n', CTo)
fprintf('\n Water Frictional Resistance [N] = %g\n', Fo)
disp(' ')
fprintf('\n Trimaran\n')

```

```

fprintf('\n Speed Hull [m/s]= %g\n', VelT)
fprintf('\n Froude Number = %g\n', FnT)
fprintf('\n Total Water Resistance Coefficient = %g\n', CTT)
fprintf('\n Water Frictional Resistance [N] = %g\n', FT1)
fprintf('\n-----\n')

%% Flight Performance Code
% Created by Alan Canamar %

function [Ttotal,Ltotal,Ttotalse,Ltotalse,Vmax,Vmaxs] = Flight_Performance...
    (EW,EWc,MF,Wpay,Cd,Cdsi,Cdsie,Lh,Lo,b,bo,TA,ALT,Vel)
%% Declare global variables
global GW g0 rho0 Sexp2 CLmax0

%% General Inputs
% clc; clear all
% GW = 6600;           %Total Gross Weight of Aircraft [kg]
% EW = 3900;           %Empty Weight of Aircraft [kg]
% EWc = 4220;          %Empty Weight of Seaplane [kg]
% MF = 1300;           %Maximum Fuel Weight [kg]
% Wpay = 1710;          %Maximum Payload Weight [kg]
% g0 = 9.80665;        %Gravitational Constant [m/s^2]
% rho0 = 1.225;         %Density of air at Sea Level [kg/m^3]
% Sexp2 = 34.86;        %Wing Area [m^2]
% CLmax0 = 1.63;        %Maximum Lift Coefficient
% Cd = 0.038;           %Coefficient of Drag of Landplane
% Cdsi = 0.0074;         %Drag increment due to Seaplane configuration extended
% Cdsie = 0.0058;        %Drag increment due to Seaplane configuration retracted
% Lh = 14.47;            %Length of Hull [m]
% Lo = Lh*0.5;           %Length [m]
% b = 2.03;              %Hull beam [m]
% bo = 0.509;             %Outrigger Beam [m]
% TA = 30500;            %Thrust Available [N]
% ALT = 4200;             %Cruising Altitude [m]
% Vel = 470;              %Maximum Landplane Speed at cruising altitude [km/hr]
GWL = GW*0.97;           %Total Gross Weight of Aircraft at Landing [kg]

%% Maximum Speed
% Inputs
h0 = 0;                  %Altitude at sea level [m]
G = 1.4;                 %Ratio of specific heat of air (gamma)
R = 286.9;                %Gas constant [J/kg*K]
T0 = 287.827;             %Temperature at sea level [K]
a_L = -0.0065;            %Lapse Rate [K/m]

%Aircraft Turbo Prop Speeds
% Maximum Airspeeds of Landplane
Vmaxj = Vel*(1000/3600);      %Maximum Speed [m/s]
if Vmaxj <= 120
    Vmax = Vmaxj;
else
    Vmax = Vmaxj.*0.71;       %Max Jet Speed [m/s]
end

% Maximum Airspeeds of Seaplane Retracted
Vmaxs = sqrt((Cd*Vmax^2)./(Cd+Cdsie));

```

```

%% Takeoff Segment
[ttoff,ltoff] = Take_off(GW,g0,rho0,Sexp2,CLmax0,Cd,TA);
[ttoffse,ltoffse] = Take_offs(GW,g0,rho0,Sexp2,CLmax0,Cd,TA,Cdsi);

%% Climb Segment for TURBOPROP
[tclimb,tclimbse,lclimb,lclimbse,VEAS,VEASS] = Climb(GW,g0,rho0,Sexp2, ...
    CLmax0,Cdsie,Vmax,Vmaxs,ALT,TA);

%% Descent Segment
[tdes,ldes,tdese,lde] = Descent(GWL,g0,rho0,Sexp2,Cd,ALT,Cdsie, ...
    Vmax,Vmaxs);

%% Landing Segment
[tland,lland] = Landing(GWL,g0,rho0,Sexp2,CLmax0,Cd);
[tlandse,llandse] = Landingse(GWL,g0,rho0,Sexp2,CLmax0,Cd,Cdsie, ...
    Lh,Lo,b,bo);

%% Cruise Segment
% Inputs
% Landplane
VS0 = sqrt((2*GW*g0)/(rho0*Sexp2*CLmax0)); %Stall Speed [m/s]
T_cruise = T0+(a_L*(ALT-h0)); %Temperature altitude gradient [K]
T_T0 = T_cruise./T0; %Temperature Ratio
Vper = 0.90; %Speed Percentage
Vcruise = Vper*Vmax; %Cruise Speed [m/s]
a_toff = sqrt(G*R.*T0); %Local speed of sound at takeoff [m/s]
a_conti = sqrt(G*R.*T_cruise); %Local speed of sound at takeoff [m/s]
Mach_toff = VEAS./a_toff; %Mach Number at Takeoff
Mach_max = Vmax./a_conti; %Mach Number at Cruise
Mach_idle = VS0./a_toff; %Mach Number at Cruise

%Thrust Specific Fuel [kg/hr/N]
ftoff = 0.91; %Throttle Setting at Takeoff
fconti = 0.79; %Throttle Setting at Cruise
fidle = 0.13; %Throttle Setting at Idle
TSFC_toff = ftoff*(0.34+0.19*Mach_toff).*sqrt(T_T0);
TSFC_conti = fconti*(0.34+0.19*Mach_max).*sqrt(T_T0);
TSFC_idle = fidle*(0.34+0.19*Mach_idle).*sqrt(T_T0);
%Thrust Available [N]
TA_toff = TA*exp(-0.0099*VEAS);
TA_conti = TA*exp(-0.0099*Vmax);

%%% Fuel Calculations
%Fuel Consumtion [kg/hr]
FCtoff = TA_toff.*TSFC_toff;
FCconti = TA_conti.*TSFC_conti;
FCidle = TA_conti.*TSFC_idle;

%%% Fuel Mass calculation [kg]
% Landplane
mtoff = FCtoff*(ttoff/60); %Takeoff Weight Fuel [kg]
mcclimb = FCidle*(tclimb/60); %Climb Weight Fuel [kg]
mdes = FCidle*(tdes/60); %Descent Weight Fuel [kg]
mland = FCidle*(tland/60); %Landing Weight Fuel [kg]

```

```

%%% Seaplane
% Inputs
Vcruises = Vper*Vmaxs; %Cruise Speed [m/s]
Mach_toffs = VEASS./a_toff;%Mach Number at Takeoff
Mach_maxs = Vmaxs./a_conti;%Mach Number at Cruise

%Thrust Specific Fuel [kg/hr/N]
TSFC_toffs = ftoff*(0.34+0.19*Mach_toffs).*sqrt(T_T0);
TSFC_contis = fconti*(0.34+0.19*Mach_maxs).*sqrt(T_T0);
TSFC_idles = fidle*(0.34+0.19*Mach_idle).*sqrt(T_T0);
%Thrust Available [N]
TA_toffs = TA*exp(-0.0099*VEASS);
TA_contis = TA*exp(-0.0099*Vmaxs);

%%% Fuel Calculations
%Fuel Consumtion [kg/hr]
FCtoffs = TA_toffs.*TSFC_toffs;
FCcontis = TA_contis*TSFC_contis;
FCidles = TA_contis*TSFC_idles;
%Calculations for Seaplane [Rec]
mtoffse = FCtoffs*(ttoffse/60);%Takeoff Weight Fuel [kg]
mclimbse = FCidles*(tclimbse/60);%Climb Weight Fuel [kg]
mdesse = FCidles*(tdese/60); %Descent Weight Fuel [kg]
mlandse = FCidles*(tlandse/60);%Landing Weight Fuel [kg]

%% Fuel Mass Calculation of Cruise, Descent and Landing [kg]
% Landplane
V = (Vcruise*3600)./1000; %Speed [km/hr]
msubtotal = mtoff+mclimb+mland+mdes;%Subtotal Weight [kg]
mcruise = MF - msubtotal; %Reserve Fuel Weight Fuel [kg]
E = mcruise./FCidle; %Endurance [hr]
R = E*V; %Range Distance [km]

% Seaplane [Rect]
Vs = (Vcruises*3600)./1000; %Speed [km/hr]
msubtotalse = mclimbse+mdesse+mtoffse+mlandse;%Subtotal Weight [kg]
mcruisese = MF - msubtotalse; %Reserve Fuel Weight Fuel [kg]
Ese = mcruisese./FCidles; %Endurance [hr]
Rse = Ese*Vs; %Range Distance [km]

%Total time [hr] and distance [km]
% Landplane
tsubmin = (ttoff+tclimb+tland+tdes)/60; %Subtotal [hr]
ttotal = E+tsubmin; %Total Time [hr]
ltotal = ltoff+lclimb+ldes+lland+R; %Total Distance [km]

% Seaplane [Rect]
tsubminse = (ttoffse+tclimbse+tlandse+tdese)/60;%Subtotal [hr]
ttotalse = Ese+tsubminse; %Total Time [hr]
ltotalse = ltoff+lclimbse+ldes+lland+Rse;%Total Distance [km]

%% Payload Range Diagram
%Calculations for Aircraft
mf = GW - EW - Wpay; %Fuel Weight w/Max Payload [kg]

```

```

Wpaymax = GW - EW - MF; %Payload Weight w/Max Fuel [kg]
Wcruise = mf - (msubtotal); %Cruise Fuel Weight w/Max Pay
T = Wcruise/FCidle; %Total Cruise Time [hr]
L = V*T; %Cruise Distance [km]
Ttotal = T+tsubmin; %Total Time [hr]
Ltotal = ltoff+lclimb+ldes+lland+L; %Total Distance [km]

%Calculations for Seaplane [Rect]
mfs = GW - EWC - Wpay; %Fuel Weight w/Max Payload [kg]
Wpaymaxs = GW - EWC - MF; %Payload Weight w/Max Fuel [kg]
Wcruisese = mfs - (msubtotsel); %Cruise Fuel Weight [kg]
Tse = Wcruisese/FCidles; %Total Cruise Time [hr]
Lse = Vs*Tse; %Cruise Distance [km]
Ttotalsel = Tse+tsubminse; %Total Time [hr]
Ltotalsel = ltoffse+lclimbse+ldesse+llandse+Lse;%Total Distance [km]

%% Plots
figure
pay = [Wpay Wpay Wpaymax 0];
rangep = [0 Ltotal ltotal (ltotal+(ltotal*0.05))];
payse = [Wpay Wpay Wpaymaxs 0];
rangemse = [0 Ltotsel ltotsel (ltotsel+(ltotsel*0.05))];
plot(rangep,pay,'b',rangemse,payse,'k','LineWidth',2)
legend('Landplane','Seaplane')
xlabel('Range [km]')
ylabel('Payload [kg]')
title('Payload Range Diagram')

%% Results
fprintf('-----\n')
fprintf('\n Range, Time and Fuel Mass Fly Breakdown\n')
disp(' ')
fprintf('\n Endurance | Landplane | Seaplane|\n')
fprintf('\n Takeoff [min] | %g | %g |\n', ttoff,ttoffse)
fprintf('\n Climb [min] | %g | %g |\n', tclimb,tclimbse)
fprintf('\n Cruising [hr] | %g | %g |\n', E,Ese)
fprintf('\n Descent [min] | %g | %g |\n', tdes,tdes)
fprintf('\n Landing [min] | %g | %g |\n', tland,tlandse)
fprintf('\n Total [hr] | %g | %g |\n', ttotall,ttotalse)
disp(' ')
fprintf('\n Range [km] | Landplane | Seaplane|\n')
fprintf('\n Takeoff | %g | %g |\n', ltoff,ltoffse)
fprintf('\n Climb | %g | %g |\n', lclimb,lclimbse)
fprintf('\n Cruising | %g | %g |\n', R,Rse)
fprintf('\n Descent | %g | %g |\n', ldes,ldes)
fprintf('\n Landing | %g | %g |\n', lland,llandse)
fprintf('\n Total | %g | %g |\n', ltotal,ltotalse)
disp(' ')
fprintf('\n Fuel Weight [kg] | Landplane | Seaplane|\n')
fprintf('\n Takeoff | %g | %g |\n', mtoff,mtoffse)
fprintf('\n Climb | %g | %g |\n', mclimb,mclimbse)
fprintf('\n Cruising | %g | %g |\n', mcruise,mcruisese)
fprintf('\n Descent | %g | %g |\n', mdes,mdesse)
fprintf('\n Landing | %g | %g |\n', mland,mlandse)
fprintf('\n Total | %g | %g |\n', MF,MF)
fprintf('\n-----\n')

```